ABSTRACT

Title of Document: INVESTIGATION OF STRATEGIES FOR DRUG DELIVERY BY COMBINATION TARGETING OF NANOCARRIERS TO MULTIPLE EPITOPES OR RECEPTORS

Iason Titos Papademetriou, Doctor of Philosophy, 2013

Directed By: Associate Professor Silvia Muro,
Fischell Department of Bioengineering &
Institute for Bioscience and Biotechnology Research

Development of drug delivery systems (ie. nanocarriers) with controllable composition, architecture, and functionalities is heavily investigated in the field of drug delivery in order to improve clinical interventions. Designing drug nanocarriers which possess targeting properties is critical to enable them to reach the intended site of intervention in the body. To achieve this goal, the surface of drug nanocarriers can be modified with targeting moieties (antibodies, peptides, etc.) addressed to cell surface molecules expressed on the diseased tissues and cells. If these molecules are receptors capable of internalizing bound ligands via endocytosis, targeting can then enable drug transport into cells or across cellular barriers in the body. Yet, addressing

nanocarriers to single targets presents limited control over cellular interactions and biodistribution. Since most cell-surface markers are not exclusively expressed in a precise site in vivo, high affinity of targeted nanocarriers may lead to non-desired accumulation in regions of the body associated with low expression. Modification of nanocarriers to achieve combined-targeting (binding to more than one cell-surface receptor) may help modulate binding to cells and also endocytosis, since cell receptors possess distinct functions and features affecting these parameters, such as their expression, location on the plasmalemma, activation in disease, mechanism of endocytosis, etc. Further, targeting nanocarriers to multiple epitopes of the same receptor, a strategy which has never been tested, may also modulate these parameters since they are highly epitope specific. In this dissertation, we investigate the effect of targeting model polymer nanocarriers to: (1) multiple receptors of similar function (intercellular-, platelet-endothelial-, and/or vascular- cell adhesion molecules), (2) multiple receptors of different function (intercellular adhesion molecule 1 and transferrin receptor), or (3) multiple epitopes of the same receptor (transferrin receptor epitopes 8D3 and R17). Binding to cells, endocytosis within cells, and biodistribution in mice were tested. Results indicate that combination targeting enhanced performance of nanocarriers with regard to these three parameters as compared to non-targeted nanocarriers and modulated their outcome relative to single-targeted nanocarriers. This modulation was observed as enhanced, intermediate, or diminished interaction with cells, accumulation in particular organs, and specificity for diseased sites relative to single-targeted nanocarriers. These results were general to strategies 1-3 and were difficult to foresee *a priori* due to the

complex nature of said interactions. Importantly, outcomes depended on the multiplicity (dual- vs. triple-targeting) and/or combination of affinity moieties displayed on the nanocarrier surface, as well as the physiological/pathological state of cells and tissues. Modulation of the delivery of a model therapeutic cargo in mice relative to single-targeted nanocarriers demonstrated the potential of these strategies to control the biodistribution of therapeutic agents. Therefore, these findings illustrate that combination-targeting enables modulation over cellular interactions and biodistribution of nanocarriers, which may aid the development of nanocarriers tailored for particular therapeutic needs.

INVESTIGATION OF STRATEGIES FOR DRUG DELIVERY BY COMBINATION TARGETING OF NANOCARRIERS TO MULTIPLE EPITOPES OR RECEPTORS

By

Iason Titos Papademetriou

Dissertation submitted to the Faculty of the Graduate School of the
University of Maryland, College Park, in partial fulfillment
of the requirements for the degree of
Doctor of Philosophy
2013

Advisory Committee:

●Professor Silvia Muro, Fischell Dept. of Bioengineering &
Institute for Bioscience and Biotechnology Research, University of Maryland, Chair

●Professor Ioannis Bossis, Department of Veterinary Medicine, University of Maryland

●Professor Sheryl Ehrman, Dept. of Chemical and Biom. Engr., University of Maryland, Dean's representative

●Professor John Fisher, Fischell Dept. of Bioengineering, University of Maryland

●Professor Daniel Perez, Department of Veterinary Medicine, University of Maryland

Dedication

This dissertation is dedicated to Thiressia and Vasilis, my mother and father. Your love and caring mean so much to me, and you are an inspiration and a gift. Thank you for providing me with everything I needed and more to succeed. I love you and I treasure you.

Acknowledgements

I'd like to first acknowledge my advisor, Dr. Silvia Muro, for her outstanding guidance, support, and inspiration during my time in the lab. This has been an immensely rewarding and positive experience, and that is in large part the result of her efforts. It has been a pleasure and honor to work closely together, and I benefited greatly from her attention, feedback, and example. She challenged me consistently to do my best work, allowed flexibility to make adjustments when necessary, and also gave me a push when needed. Her humor made our discussions all the more enjoyable, and she acted with my best interests at heart... Thanks Silvia! I would also like to thank her for supporting my graduate studies over four years, and for funding trips to international conferences to present my research. Thank you as well to my committee members Drs. Ioannis Bossis, John Fisher, Daniel Perez, and Sheryl Ehrman for their time, effort, and constructive feedback.

I would like to acknowledge my fellow lab members Janet, Tridib, Maria, Zois, Rachel, Daniel, Rasa, and Viraj for their collegiality, advice, and scientific input. I would like to thank Janet in particular for being confined with me in a 10 x 15 foot room for the past four years. Much to your chagrin, there was only one exit available when I'd ask you to indulge my thoughts on science, life, and many other subjects which were much more trivial. A thank you to Tridib for our many discussions over coffee together which provided a much needed boost before an experiment. Thanks to Karen Carter for many pleasant discussions and time shared together in our office. Thanks also to Dr. Shyam Dube for scientific/philosophical

discussions at odd hours of the night and weekends in the interim periods of experiments. Thanks also to my previous mentor Dr. Nicholas Patronas and to Dr. Constantine Stratakis for helping to get me started in biomedical research. Thank you to Dr. Jeff Chyatte, Dr. Jack Chrikjian, and Dr. Mihael Polymeropoulos for taking an interest in me even earlier on.

A special thank you needs to go to my family and friends. Thank you Mom for your love and support always, and for having such an interest in me and my well being always. Thank you Dad for being my best friend always and for pushing me to push myself. Your fatherly and scientific advice, particularly during the research aptitude exam and my proposal, improved the quality of my work and your daily check-ins gave me energy to keep pushing and also keep things in perspective. Thank you to my sisters, Marianna and Elena, for your love and support over the years. Thank you to my girlfriend, Julie Rodriguez, for being there and for making the last year and a half so much fun. Thank you to my dear friends Kosmas Lois, Michael Konstantopoulos, Nick Bell, and Jon Shearin for their friendship over the years and for being there when I needed it... particularly over a pint of beer and some buffalo wings! Thanks to Nick also for his brotherly wisdom, comfortable couch and amazing parents who were always so kind to me. Thanks also for his unsolicited thoughts on foreign affairs and the economy... I know that you are really a covert CIA agent! Thanks to Tiffany Koons and Victoria Ungureanu Bell for their friendship and for being the better halves of my best friends. Thanks to Kos and Mike for your fantastic impressions of “old school” greek men, even though Kos probably is one already, and

for being great “hramaria.” Thanks to Jon for kicking my butt in basketball and golf, for kicking it out to me for three, for mispronouncing the battle of gaugamela, and for shaving my head after overdoing the dye job on my “frosted tips” in high school. Thanks also to my dear friends, Berj Bagdasarian, Eric Girard, Paul Merwin, Ted Harrington, Kostas Triantafillou, and William Buckingham, my god parents and brother Erato, George, and Panos Marcoullis, and my cousins Andreas, Chrystiana, and Paola Chrysostomou for their love and support over the years.

Table of Contents

Section 1: Introduction and Overview

1.1. Problem Description and Motivation

Drug delivery systems designed to target pharmaceutical agents to the intended site in the body can improve many current limitations of medical treatments by enhancing or optimizing accumulation at the intended site of activity and limiting accumulation in off-target areas.[1-3] A promising strategy to achieve targeting of drug delivery systems (i.e. nanocarriers) is to couple affinity moieties (e.g. antibodies or their fragments, peptides, aptamers, etc.) which recognize particular molecules present on the surface of cells.[1-3] This approach can enhance drug accumulation in specific organs, tissues, cells, subcellular compartments, or across cellular barriers, and is being heavily investigated for numerous diseases including cardiovascular, metabolic, pulmonary, neurological, and inherited disorders, as well as cancers, infectious diseases and many other applications.[1-3]

Despite these advantages, targeting nanocarriers to single cell-surface markers oftentimes results in suboptimal accumulation and lack of precise control of nanocarriers in the body. For example, although targeting can improve nanocarrier delivery at the target site, most targeted nanocarriers also accumulate in clearance organs, such as the spleen and liver, resulting in an improved (over non-targeted) but still suboptimal outcome.[4] Due to this, strategies which improve accumulation in other organs are highly beneficial,[5,6] and certain therapeutic approaches may require delivery to multiple cell types (e.g. angiogenic blood vessels and tumor cells for cancer therapy)[7] which may not all adequately express the target molecule. Further,

control of the biodistribution is limited in part because molecules used as targets are rarely expressed solely in a single cell type or tissue, making it difficult to maximize selectivity for precise niches *in vivo*.[3,4] Expression of a target within a population of cells is heterogeneous (i.e. spatially and temporally), which can limit the fraction of cells susceptible to targeting.[3,4] Accessibility of the selected target molecule may be restricted by its location on the plasmalemma, predominance of isoforms lacking the target epitope, or altered molecular conformation, and all of these characteristics may be affected by the physiology or pathophysiology of the local environment and severity of the disease state.[3,8] In addition, the factors affecting targeting are complex and intertwined, such that altering one parameter (e.g. increasing affinity for the target molecule) can produce several effects which may or may not be intended, e.g. increasing binding at the target site while simultaneously increasing binding at off-target sites, inducing endocytosis, etc.[3,9] Thus, although targeting to single cell-surface molecules can be beneficial, in many circumstances the result is not ideal and often cannot be corrected by optimizing nanocarrier design parameters (e.g. ligand valency, size, shape, etc.) due to the dynamic nature of the interaction. Strategies which improve control over targeting can help to optimize nanocarrier delivery for particular applications. From these points of view, targeting nanocarriers to multiple, rather than single, cell-surface molecules (namely combination targeting) may provide advantages for drug delivery applications.

1.2. Our approach

Combination targeting is an emerging approach which holds promise to enhance and/or more precisely control delivery of nanocarriers. It exists in nature with regard to infectious pathogens[10] and cells of the immune system[11] which interact with multiple receptors to adhere and/or induce transport into cells or across cellular barriers. Combination targeting strategies have recently arisen in targeted drug delivery,[7,12-14] providing new approaches to enhance and optimize specificity and selectivity of nanocarriers for the target site. For example, the overexpression of multiple molecules on the surface of cancer cells has been exploited to enhance tumor selectivity of liposomes by triggering internalization only in cells expressing both molecules.[14] In another study, multi-targeting enhanced accumulation of mesoporous silica nanoparticles in both angiogenic blood vessels and tumor cells by addressing multiple receptors in those cells.[7] Yet, such studies are limited to a particular scope or drug delivery system and in many cases the effects of targeting molecules of different or similar function have not been examined systematically in both cell cultures and *in vivo* models. In the case of polymer nanocarriers, combination targeting studies are mainly limited to cellular binding studies of receptors with similar function, leaving unknown the effects on endocytosis and biodistribution or the effects of targeting molecules with different functions. Targeting nanocarriers to multiple epitopes of the same molecule or receptor may also provide advantages with regard to enhancing and/or controlling accumulation. For example, binding at a certain epitope may alter the molecular conformation of the target to enhance accessibility of a second epitope[15] or it may enable targeting of

a greater or lesser number of molecular isoforms of the target present on a single cell type or in different tissues. However, such a strategy has never been explored in the context of nanocarriers.

The global hypothesis of this dissertation is that combination targeting can be utilized to modulate and control the binding, internalization, and/or the biodistribution of polymer nanocarriers addressed to three different categories of cell-surface targets: 1 multiple receptors with similar functions, 2 multiple receptors with different functions, and 3 multiple epitopes of the same receptor.

Investigation of these strategies in cell cultures and *in vivo* is necessary to develop general knowledge of combination targeting with respect to critical parameters of drug delivery, including binding to cells, accumulation on the cell surface versus intracellular compartments, performance in physiological versus diseased conditions, distribution of nanocarriers in the body, and the resultant impact on the delivery of the associated pharmaceutical "cargo." The reductionist environment of cell cultures provides a useful system for analyzing the effect of targeting on drug delivery parameters (e.g. binding, internalization, etc.). Yet, *in vivo* testing in laboratory animals is essential to affirm results in the context of the true physiology of the body, where structural features or regulation of the target receptors may vary in different tissues, and additional physiological factors (e.g. physiological shear stress from fluid flow,[16,17] clearance from the circulation by immune cells,[18] presence of cellular barriers,[19] etc.) add layers of complexity.[3,8,20]

In the next section (Section 2), background is provided on the many challenges which nanocarrier-based drug delivery systems aim to address, as well as targeting and transport of nanocarriers targeted to single cell-surface molecules and the nascent field of combination targeting. The methods used to conduct the studies are described (Section 3), followed by the results and discussion (Section 4), and the overall conclusions and potential future directions of the research in light of the presented findings (Section 5).

1.3. Significance and Novelty

The significance of the studies presented in this dissertation is that they expand current knowledge or provide the first data on combination targeting of polymer nanocarriers to multiple receptors or epitopes at the levels of binding and internalization in cells, distribution in the body, and delivery of associated therapeutic cargo. The receptors investigated are intercellular adhesion molecule-1 (ICAM-1),[21] platelet-endothelial cell adhesion molecule-1 (PECAM-1),[21] vascular cell adhesion molecule-1 (VCAM-1),[21] and the transferrin receptor (TfR).[6] These receptors are highly relevant for drug delivery due to their use in targeting numerous therapeutic and diagnostic agents in applications including cancer, atherosclerosis and other cardiovascular disorders, multiple sclerosis, inflammation, arthritis, stroke, graft rejection, thrombosis, genetic lysosomal storage disorders, or neurodegenative disorders.[22-47] In addition, most previous studies on combination targeting focused on binding of micro- rather than nano- carriers to cells with relatively few studies

examining internalization within cells, or biodistribution in vivo. This dissertation builds on this gap by evaluating nanocarrier internalization and biodistribution in addition to cell binding using nanoscale carriers which are relevant for most in vivo applications and for endocytic transport via most known mechanisms.

Existing knowledge of combination targeting of molecular receptors with functions which are related or similar (i.e. cell proliferation, adhesion, transmigration, pathogen detection, nutrient metabolism, etc.) is expanded to explore novel or scarcely examined aspects of multi-targeting cell adhesion molecules (CAMs), involved in cell adhesion and transmigration of leukocytes to sites of inflammation. In terms of targeting, combination targeting of nanocarriers to multiple Ig-like CAMs is examined for the first time using different combinations and multiplicity of affinity moieties (i.e. dual or triple-targeting) directed to intercellular-, platelet-endothelial-, and/or vascular- cell adhesion molecules (Section 4.1). Effects of this form of multi-CAM-targeting on the biodistribution and on delivery of biological therapeutics are also examined. In addition, we examine effects of multi-CAM-targeting on nanocarrier internalization using receptors associated with the same endocytic pathway (ICAM-1 and PECAM-1 associated with CAM-mediated endocytosis) versus receptors associated with different endocytic pathways (ICAM-1 and VCAM-1 associated with CAM- and clathrin-mediated endocytosis, respectively). In the next section (Section 4.2), knowledge of combination targeting of molecular receptors with different function is expanded to include ICAM-1 and transferrin receptor, which are involved in leukocyte adhesion

and transmigration versus iron transport, are upregulated or remain stable in response to disease, and are involved in CAM- versus clathrin-mediated endocytosis, respectively. These differences are unique from most prior combination targeting strategies which examined receptors involved in similar functions (cell adhesion) and endocytic pathways (clathrin-mediated endocytosis), and these factors can significantly affect nanocarrier targeting and internalization. In the final section, we examine the novel approach of targeting nanocarriers to multiple epitopes of the same receptor. Such a strategy can provide a new means to alter the avidity for the target receptor, and as a result modulate nanocarrier targeting performance. This approach may be particularly useful in circumstances where varying other targeting parameters (i.e. nanocarrier size, ligand valency, etc) leads to unwanted effects.

Overall the findings in this dissertation illustrate the promise of combination targeting as a strategy for drug delivery which enables control over cellular interactions and biodistribution of nanocarriers. Combination targeting, whether directed to multiple receptors of similar or different functions, or to multiple epitopes of the same receptor, allows modulation of drug delivery parameters including binding to cells, endocytosis, and biodistribution. Importantly, the resultant behavior can not be predicted *a priori* and requires experimental evaluation both in cell cultures and in vivo. Yet, combination targeting provides a useful approach for the development of nanomedicines because, rather than having to discover new targets, it allows the drug delivery system to be adapted to the needs of the therapy by combining properties of existing targets which can be optimized.

Section 2: Background

2.1. Drug Delivery: Purpose and Challenges

The overall purpose of drug delivery is to optimize the pharmacokinetics of agents administered into the body for an intended application. These agents can be used for prophylactic, therapeutic, or diagnostic applications, and are designed to prevent the occurrence of disease, determine whether disease is present, or treat disease, respectively. Therapeutic or prophylactic agents are biologically active substances. These can be small molecules, typically low molecular weight organic or inorganic molecules produced by chemical synthesis. In addition, the use of biologicals for prophylaxis or therapy has rapidly expanded. These are macromolecules derived from living systems, such as cell cultures, bioreactors, ascites animals, etc., and include proteins (antibodies,[48] enzymes,[49] etc.), nucleic acids (aptamers,[50] siRNA,[51] plasmids,[52] etc.), and carbohydrates (vaccines,[53] immunotherapies,[54] etc.). Additional types of agents are represented by metals,[55] radioisotopes,[56] fluorescent markers,[57,58] microbubbles,[59] etc., which are utilized to provide contrast for imaging modalities, such as computed X-ray tomography (CT), magnetic resonance imaging (MRI), optical coherence tomography, positron emission tomography (PET), ultrasound, etc. Yet, oftentimes the efficacy of all of these agents and their safety is impaired or suboptimal due to pharmacokinetic limitations. As a consequence, treatment of many diseases would be greatly improved by more effective drug delivery strategies.[6,60,61]

Drug delivery science is applied to most, if not all, aspects of pharmacokinetics. In general terms, pharmacokinetics is the study of the

accumulation and evolution of pharmaceutical agents the blood, tissues, and organs over time.[62] This typically involves the absorption of the agent into the bloodstream, circulation in the blood, distribution from the blood to tissues, metabolism of the agent in tissues, and excretion from the body.[62,63] Regarding absorption, a main goal of drug delivery is to improve the solubility of agents which are not soluble or poorly soluble in physiological fluids and, therefore, cannot be absorbed.[64] Agents which are absorbable should be stable in the presence of blood components, and also must remain in the circulation long enough to achieve an adequate concentration at the target site. This can be affected by interaction with blood components (e.g. opsonization)[65] and can result in premature clearance from the circulation, even in cases where delivery systems are endowed with "stealth" properties.[66] To improve the distribution of agents, which is another goal of paramount importance, drug delivery strategies aim to increase the agent concentration at the intended site of activity (enhancing its bioavailability) and to minimize distribution in areas of the body where the agent is not needed (reducing potential toxicity and waste of the agent).[1,2] Improving bioavailability can help create new treatments either by allowing agents to reach sites in the body which were previously inaccessible[67] or by increasing the bioavailability of an agent to the point where it is effective for a particular application.[1] For example, the vascular endothelial lining of blood vessels can allow a certain amount of transport into tumor areas,[68] but can also limit transport from the bloodstream to other tissues. This is most evident in the brain, where the blood-brain barrier restricts transport of most substances to the brain parenchyma.[67] Another major cellular barrier is the epithelial lining of the

gastrointestinal (GI) tract where free transport of substances is also restricted, limiting delivery of agents orally.[69] Biological barriers of drug delivery are also present in other organs including the skin,[70] lungs,[71] and mucosal linings throughout the body.[72] At the cellular level, the plasma membrane or the membranes of intracellular compartments represent additional barriers to drug penetration.[73] Consequently, targeting and internalization into cells can improve the distribution of agents to the site of activity. Reducing toxicity is also very important[74] as less or, ideally, no harm should result from administration of the agent, and/or allow the agent to be administered in greater amounts or for longer periods of time.

A good understanding of elimination (metabolism and excretion) of the agent is also necessary. Conversion of the agent to metabolites, known as biotransformation, occurs primarily via enzymatic reactions in the liver, although other tissues may also be involved, e.g., lungs, kidneys, or GI mucosa, etc.[75] Biotransformation can have several effects, including inactivation of the agent (the resulting metabolite(s) does not exert the intended effect), its activation (e.g. a pro-drug, where the metabolite exerts the intended effect), modification of activity (the resulting metabolite(s) exerts a secondary effect), or toxicity (the resulting metabolite(s) interrupts a normal cellular metabolic pathway which results in cell death).[76] Excretion from the body is also an important consideration. Excretion occurs primarily via the kidneys or also the liver, GI tract, and lungs, and this process lowers the concentration of agents in the body, which in turn can reduce both efficacy and toxicity.[75] Other efforts in drug delivery also hold promise to

improve multiple pharmacokinetic parameters, for example, controlling the rate of release of agents at the target site to maximize the therapeutic outcome.[77]

As mentioned, addressing these problems in drug delivery is critical to improving many medical treatments. Neurological, cancer, cardiovascular, infectious, immune, and genetic disorders are only a few examples of the many applications where drug delivery science can have a major impact by addressing challenges imposed by the physiology of the body, e.g., solubility of agents in physiological fluids, adequate and selective accumulation at the target tissue versus non-target tissues, passage from the bloodstream to the tissue compartment, accumulation in the appropriate cell type and subcellular compartment, reducing premature degradation, etc.

2.2. Drug Delivery Systems

The use of drug delivery systems to enhance the pharmacokinetics and effects of pharmaceutical agents has increased through advancements in nanotechnology known as nanocarriers. Nanocarriers of a diverse range of sizes (a few nanometers up to one micrometer), geometry, materials, and surface chemistries are now being developed to meet particular medical needs (Figure A).[78] For example, poorly soluble agents are being encapsulated in drug carriers to improve solubility in blood.[78] Therapeutics that are susceptible to pH or enzymatic degradation,[79] or which may be effluxed from cells by drug transport pumps,[80] can be loaded into nanocarriers as a means to address these issues. In addition to these advantages,

nanocarriers are being developed to have high loading capacity, increased biocompatibility and accumulation at the site of activity, enhanced functionality (i.e. adding surface coatings, targeting moieties, or therapeutic and imaging agents), and to enable controlled release of cargo.[2,78,81-83]

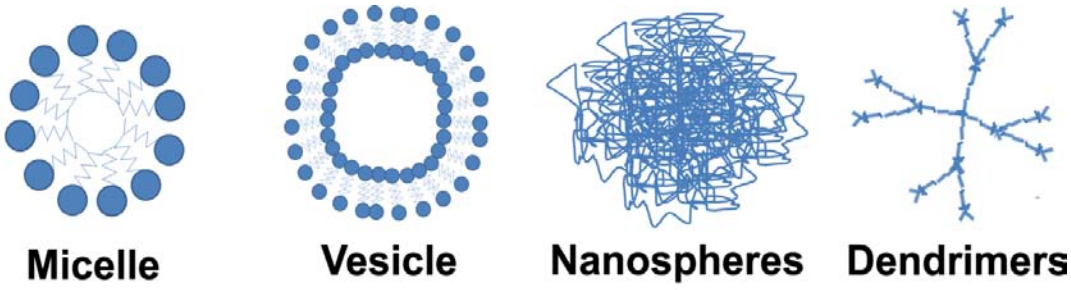

Figure A. Some structures of nanocarrier drug delivery systems

Liposomes were first reported in 1965, making them the oldest type of nanocarrier delivery system.[84] They are made by self-assembly of amphiphilic lipids in aqueous solution to form bilayered spherical vesicles with an aqueous lumen, and range in size from 50 nm to several microns.[85] The material composition of liposomes includes phospholipids found naturally in cell membranes as well as other membrane constituents such as cholesterol.[86] Due to this liposomes are generally biologically inert, which results in low toxicity.[87] In addition, they can be functionalized with targeting moieties and with polymer coatings (e.g. polyethylene glycol (PEG)) to provide selective targeting and/or imaging, and to limit clearance due to opsonization in the bloodstream.[85] Because they are amphiphilic, hydrophilic agents can be loaded in the interior lumen or surface while hydrophobic agents may

be loaded in the bilayer.[85] Liposomes also have some disadvantages, including a relatively low drug loading capacity, and the fact that the liposomal bilayer can become destabilized in the circulation by high density lipoproteins, resulting in premature release of cargo.[88] However, incorporation of certain lipids (e.g. phosphatidylcholine, sphingomyelin) or cholesterol in the liposomal membrane can increase stability.[87] Liposomes are also sensitive to destabilization by modification, e.g., can tolerate a relatively low number of targeting moieties before becoming destabilized.[89]

Polymeric nanocarriers are fabricated from synthetic, natural, or hybrid polymers which are defined as macromolecular entities created by covalent and repeated linkage of smaller structural units.[82] The main criteria for selection of polymeric materials are biocompatibility and degradability (properties which are important for limiting toxicity), controlled release, and excretion from the body. Poly(ethylene glycol) (PEG), poly(methyl methacrylate) (PMMA), and poly(lactide-co-glycolide) (PLGA) are commonly used synthetic polymers, with PEG also being widely utilized as a surface coating to reduce clearance from the circulation[87] and PLGA being FDA approved for use in drug delivery systems due to its biocompatibility.[90,91] Natural polymers made from gums, polysaccharides, and polypeptides (e.g. chitosan, sodium alginate, gelatin, albumin, etc.) are also utilized, offer lower batch-to-batch variability, and are potentially less toxic since they do not require use of chemicals during fabrication.[92-94] In addition to biocompatibility and degradability, polymeric materials are widely utilized because of their controllable

geometry. For example, polymeric nanocarriers can be fabricated in a wide variety of sizes (10 nm -1μm) and shapes (spheres, rods, disks, toroids, plugs, etc.)[95] with a hollow lumen or solid cores, and controllable porosity.[96] Functional agents (therapeutic, imaging, or targeting) can be added to the particle surface, core, or embedded throughout the polymer matrix.[97] Importantly, polymeric carriers are more tolerant of functionalization than liposomes without compromising carrier stability.[98] Controlled release can be achieved by diffusion, surface erosion, or bulk degradation of the nanoparticle over time.[77] Linear and branched polymers as well as polymerosomes, dendrimers, polymeric micelles, and niosomes can also be fabricated from polymeric materials.

Polymerosomes are considered the polymer analog of liposomes, with the difference that they are made from amphiphilic block copolymers instead of phospholipids.[99] Like liposomes, polymerosomes range in size from tens of nanometers to several microns, can be loaded with both hydrophilic and hydrophobic agents and are not very toxic, but in contrast are also more rigid and less permeable. This allows a greater number of functional moieties to be added and increases stability.

Dendrimers are named for their tree-like structure and are generated by adding layers of polymers sequentially around a central core either via convergent or divergent synthesis.[100,101] The result is a highly branched polymer network where functional agents may be entrapped within the layers or coupled to the dendrimer

surface.[102] The small size of dendrimers (only a few nanometers in diameter) is advantageous for oral delivery, allowing dendrimers to permeate through the epithelial cellular barrier of the GI tract.[103] As with other types of polymeric materials, dendrimer physical properties such as size, shape, and surface chemistry are controllable, which in this case is achieved by modifying the generation number.[101] A high surface-to-volume ratio allows for addition of a high number of functional groups, e.g., therapeutic, diagnostic, and targeting moieties.[101] Disadvantages of dendrimers include costly manufacturing, difficulties with quality control due to multi-step synthesis, and potential for toxicity in vivo.[74]

Polymeric micelles are also made from amphiphilic block copolymers which self-assemble to form a hydrophilic shell and a hydrophobic core.[104,105] Similar to dendrimers, polymer micelles are small in size (a few nanometers in diameter), yet in contrast have an inner hydrophobic core and an outer hydrophilic layer.[104] As with other polymeric carriers, micelles can be functionalized for targeting, formulated with low toxicity materials, designed to have a relatively high loading capacity for water-insoluble drugs, controlled release, prolonged blood circulation, and also self-assemble in aqueous solution resulting in simple formulation.[104]

Niosomes are vesicles formed using non-ionic surfactants, such as glycerol, glycerol esters, polysorbates, etc. Like liposomes, niosomes have both hydrophilic and hydrophobic domains, allowing for incorporation of agents with a range of solubilities. The niosome composition, fluidity, size, and lamellarity can be

controlled,[106] allowing for versatile nanocarrier design. In addition, surfactants are generally biodegradable, biocompatible, non-immunogenic, and relatively non-toxic due to their lack of charge.[106]

Inorganic nanoparticles are also being explored for drug delivery, including carbon nanostructures, quantum dots, metal particles, and mesoporous silica nanoparticles, and are used mainly for diagnostic applications. Carbon nanostructures are fabricated into various forms such as nanotubes.[107]They are stable and the structural conformation, charge, strength, flexibility can be varied, and can be functionalized with drugs and/or biomolecules for diagnostic and therapeutic purposes.[107]Quantum dots (QDs) are semiconductors fabricated from a combination of metals and non-metals.[108] These nanoparticles (~2-10 nm diameter) have greater fluorescence than traditional fluorophores, excitation and emission wavelengths can be tuned by the particle size, and are detected with a high level of sensitivity.[109] Metal nanoparticles such as iron oxide and gold are used as imaging agents due to their sensitive detection and stability.[110] Iron oxide and superparamagnetic iron oxide (SPIO) metal nanoparticles show potential for magnetic resonance imaging[111,112] and are also being exploited for targeting.[113] Gold is a biocompatible material which can be modified with numerous biomolecular agents for diagnostic and therapeutic applications.[114] Mesoporous silica nanoparticles are have been heavily investigated recently due to their controllable mesoporous structure (e.g. porosity diameter ~2-50 nm), high specific surface area, and large pore volume.[115] This has been advantageous for loading of therapeutic cargoes, including small

molecules, therapeutic proteins, and genes.[115] Ceramic materials in general are highly stable and, like PLGA, silica is considered a "Generally Recognized As Safe (GRAS)" material, making it promising for clinical studies.[115] These and many other nanocarrier-based drug delivery systems offer a means to optimize the pharmacokinetics of agents for particular medical needs. As mentioned above, most of these drug delivery systems can be functionalized to target sites of intervention in the body. In order to enhance delivery to the intended site, various targeting strategies may be utilized.

2.3. Targeting Strategies in Drug Delivery

In the broadest sense, to target a physiological system means to enable its interaction with a specific component of that system. Targeting occurs naturally as part of the normal physiological function of the body and also in pathophysiologal contexts. For example, at the subcellular level, components of the cell machinery such as microRNAs target specific genes in order to modulate their expression and, as a result, alter cell function, signaling, or sorting peptides of proteins for distribution to different compartments.[116] At the cellular and tissue/organ levels, infectious pathogens such as viruses or bacteria and cells of the immune system can gain access to specific cells, tissues, and/or organs by targeting molecules present on the cell surface.[117] Targeting also occurs at the level of organ systems, where ligands (e.g. metabolites, hormones, neurotransmitters, growth factors, etc.) travel from and to specific organs or tissues via the circulation.[118] Therefore, targeting occurs naturally and at several levels of organization/complexity as part of normal physiological function and also of pathophysiological processes.

Targeting for drug delivery was first theorized by Paul Ehrlich in the 1900's, who envisioned coupling a therapeutic cargo to an element which enabled specific binding to the target site.[1] Since then, targeting has been explored and expanded upon as a strategy to enhance delivery of agents to specific organs, tissues, cells, and more recently specific subcellular compartments.[3] Yet, targeting is a challenge which is intrinsically complex.[3] A targeted agent must first reach the target site at the organ level, whether via the systemic circulation or administration via other routes (e.g. inhalation/intratracheal installation for pulmonary delivery, intrathecal/intranasal/intracarotid for brain delivery, GI for oral delivery, etc.). Depending on the tissue of interest, the agent may have to traverse additional barriers to reach the tissue of interest (e.g. the blood-brain barrier, the intestinal epithelial barrier, mucus barriers of the lung airways, GI tract, eyes, etc.).[67,72] The agent must then reach the intended tissue and cell type via mass transport (e.g. diffusion, convection, etc.). If the site of activity is intracellular, the agent must further bind and enter the cell, traffic to the intended subcellular compartment, and interact with the molecular target.[3]

In current practice targeting strategies for drug delivery generally fall into four categories (Figure B). Passive targeting occurs when agents accumulate in certain locations of the body due to the physiological features and function of these sites.[3] Examples of passive targeting include accumulation in spleen and liver due to opsonization and subsequent clearance from the circulation by the

reticuloendothelial system at the organ level (or the monocyte-macrophage system at the cellular level),[18] or in sites afflicted by tumors where "leakiness" of the vasculature caused by the tumor microenvironment gives rise to the enhanced permeability and retention effect.[68] The converse of passive targeting is inverse targeting, where the goal is to block passive accumulation of the administered agent in order to enhance targeting to other sites.[3] For example, administration of empty liposomes prior to administration of adenoviral vectors enhanced gene transfer to hepatocytes by transiently saturating uptake via hepatic kupferr cells.[119] In contrast to passive or inverse targeting, active targeting involves adding targeting properties on the agent either intrinsically or extrinsically. Intrinsic active targeting refers to selecting or modifying the therapeutic agent itself to improve targeting specificity.[120] On the other hand, extrinsic active targeting involves coupling the agent to a component which possesses targeting features. This can be accomplished by physical means (e.g. pH,[121] temperature,[122,123] etc.) where the agent is coupled to a component which enables activation or release at the target site due to features of the target environment or via an external stimulus.[122] In addition, the modifying component can be a ligand which displays affinity for particular determinants (e.g. cell-surface molecules) present at the site of disease.[3] The targeting ligand can be coupled directly to the agent or to the surface of a nanocarrier delivery system.[3] Finally combined targeting refers to using a combination of the other targeting approaches.[3] For example, carriers can been designed using a pH-sensitive polymeric material and also a targeting ligand to enable targeting via both intrinsic and extrinsic active-targeting for cancer therapy.[124]

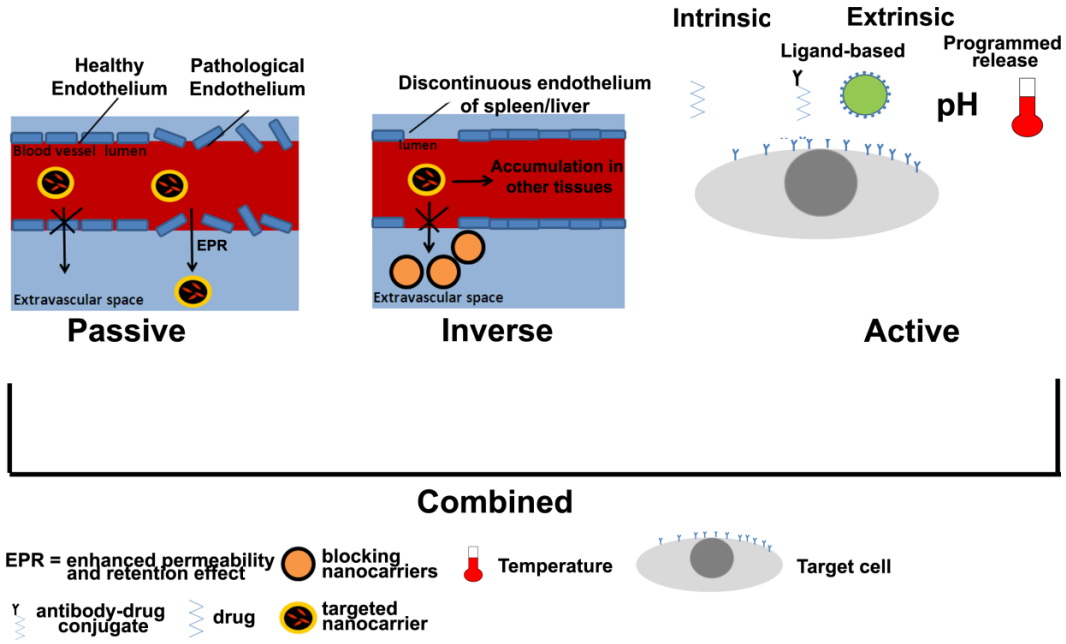

Figure B. Drug targeting strategies.

2.4. Targeting to Cells and Subcellular Compartments

Active targeting with ligands is a heavily investigated form of targeting which has been utilized to improve specificity of nanomedicines under development.[3] This targeting allows agents to associate to, for instance, cells of interest, resulting in increased specificity for the target site. This association can be either "promiscuous" or selective depending on the strategy which is utilized. In the case of non-selective targeting, an agent is functionalized with a polycationic or amphipathic targeting peptide (e.g. Tat, octa-arginine, Penetratin, etc.) that enables adhesion to cells in a broad manner.[125-128] These peptides are termed cell-penetrating peptides because they also enable transport into cells.[128] A promiscuous targeting strategy is advantageous for treatment of diseases affecting multiple organs (e.g. the lysosomal storage disorders and other monogenic diseases, oxidative stress, etc.),[96] in cases

where accumulation of the agent in off-target sites will not produce significant side effects, or for prophylactic applications.[3] However, for many applications non-selective targeting is considered a disadvantage, such as delivery of cytotoxic agents in cancer therapy.

In contrast to non-selective targeting, specific targeting enables association to cells by binding specific molecules (e.g. receptors, enzymes, mucins, etc.) present on the surface of cells.[3] Binding is an equilibrium between the ligand and the target, and therefore is affected by both the target and ligand concentrations as well as the accessibility of both of these components. Expression of the target is, therefore, an important factor which can be modulated by cell activation (e.g. increased expression of certain adhesion molecules[28] is observed in response to inflammatory stimuli, while expression of other molecules is decreased due to cleavage by proteases).[3] On the other hand, the concentration of available ligands can be adjusted according to the administered dose, by adjusting the number of ligands coupled directly to the agent or indirectly to a nanocarrier delivery system.[129,130]

In terms of accessibility, the target must be displayed on the cell surface rather than intracellularly. Yet, access to the target molecule may be hindered if the molecule is part of a complex or interacts with other molecules on the cell surface.[3] The precise location of the target epitope is also critical. For example, targeted agents may compete with endogenous ligands for binding at certain receptor epitopes. Also, binding certain domains of a receptor can modulate its own

expression. For example, binding of angiotensin converting enzyme (ACE) at certain epitopes induces shedding from the plasma membrane.[131] Masking of the binding epitope may occur in certain cell types or tissues due to post-translational modifications, or it may be less accessible or eliminated in certain receptor isoforms.[3] Epitope dependent targeting is also observed with regard to *in vivo* biodistribution, where targeting different epitopes of the transferrin receptor (TfR) affects selectivity for the brain versus other organs.[132] Finally, if the target site is intra- or transcellular, an epitope that triggers transport into the cell via membrane-bound vesicles (endocytosis) into or across the cell must be selected.[3]

Importantly, therapeutic targets are present on the plasma membrane or in intracellular compartments and, therefore, targeting strategies enabling delivery at the subcellular level is necessary.[2] Anchoring therapeutics to the plasma membrane can be utilized, as an example, for prophylaxis of thrombosis or inflammation, and can be accomplished by targeting cell-surface molecules which are poorly internalized (e.g. antibodies targeting intercellular adhesion molecule 1 (ICAM-1)).[28] Lysosomal targeting is essential for many enzyme replacement therapies of lysosomal diseases, and can be achieved by targeting many different cell-surface molecules including ICAM-1,[133,134] mannose-6-phosphate receptor,[135] insulin growth factor II,[136] the low density lipoprotein receptor family,[137] insulin receptor, transferrin receptor,[138,139] and many others.[3] Mitochondrial dysfunction is associated with many diseases including cancer, diabetes, as well as cardiovascular and neurological conditions.[140] Delivery to the mitochondria can be achieved by using

targeting peptides containing mitochondrial localization sequences,[141,142] cytochrome oxidase subunits,[143] or retinoic-inteferon-induced mortality proteins.[143] Nuclear delivery is needed for gene therapy and for therapeutics with nuclear targets (e.g. cytotoxic agents), and may be accomplished using nuclear localization sequences which target import proteins present on the nuclear envelope.[144] Targeting is necessary for most agents intended for the nucleus as the size cutoff for passive diffusion across nuclear envelope pores is 30-40kDa. Targeting the Golgi apparatus and endoplasmic reticulum is less well defined, yet has been utilized for certain cytotoxic cancer agents via conjugation to shiga or cholera toxins which target these organelles by binding to molecules on the cell surface and subsequent endocytic transport.[145]

2.5. Transport Into or Across Cells

Transport from the surface to the interior of cells can occur either directly from the extracellular space to the cytosol or by vesicular uptake resulting from endocytosis.[3] Direct transport can occur via passive diffusion, although this is restricted to small, hydrophobic molecules such as small alkanes, benzene, diethyl urea, etc.[146] Active direct transport can occur for ions and various small molecules to move against their concentration gradients as substrates of transporter pumps.[147,148] Approaches involving disruption of the plasma membrane with a transiently applied physical stimulus (e.g. electroporation, ultrasound, hydroporation, magnetofection, ballistic) have also been utilized to enable transport into the cytosol.[149-154] However these approaches are damaging and are only used locally. Positively-charged cell

penetrating peptides or toxins can also provide direct transport to the cytosol by transiently forming pores in the plasma membrane.[155-157] In contrast, agents targeted to surface molecules can be transported intracellularly by endocytosis.[3] Endocytosis is preferable for nanocarriers because their size restricts passive diffusion across the plasma membrane or transport via transporter pumps.

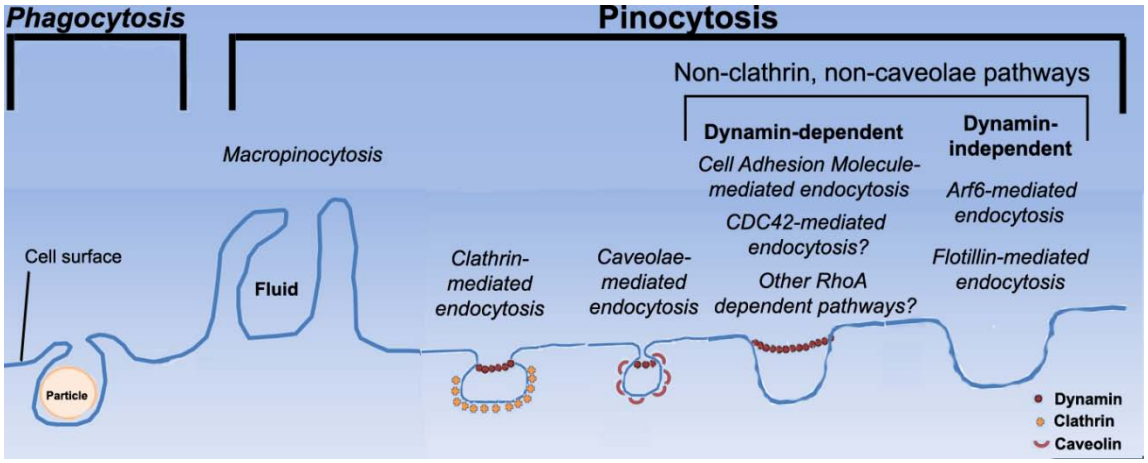

Figure C. Mechanisms of endocytosis.

Several different mechanisms of endocytosis have been elucidated, and multiple are involved in uptake and intracellular transport of nanocarriers (Figure C). Phagocytosis involves the uptake of relatively large (up to several micrometers in size) amounts of extracellular particulate matter into the cell.[20] Phagocytosis can be induced by cross-linking of certain cell receptors and results in uptake into a vesicular compartment termed the phagosome, with subsequent transport to lysosomes which function as a degradative compartment in the cell.[158] Targeting of the mannose receptor or of integrins CD11b/CD18, binding of the Fc class of receptors via the constant region of antibodies, or targeting of other receptors can

enable uptake into cells by phagocytosis.[158] The ability to take in large material represents an advantage from the standpoint of drug delivery, because nanocarrier size may be used to control the rate of clearance from the circulation, amount of drug loading, etc. In addition, phagocytosis can be controlled by nanocarrier shape, where a high degree of surface curvature at the ends of rod-like structures increase induction of phagocytosis relative to more spherical structures.[159] On the other hand, although lysosomal delivery is needed in certain contexts (e.g. therapy of lysosomal storage disease), it represents a relative disadvantage in most contexts.[3] In addition, phagocytosis occurs primarily on cells which are professional phagocytes (e.g. macrophages), limiting targeting to cells of the reticuloendothelial system (RES).[20] Although this may be advantageous in certain cases, RES-mediated clearance is largely undesired in most contexts, as it hinders delivery to other areas of the body.

In contrast to phagocytosis, macropinocytosis involves uptake of extracellular fluid (e.g. pinocytosis) into cells (Figure C). Macropinocytosis is induced by binding of growth factors which stimulate receptor tyrosine kinases and subsequent intracellular signaling produces ruffling of the plasma membrane and reorganization of the actin cytoskeleton to accommodate engulfment of fluid and nutrients from the extracellular milieu.[160] Since vesicles of 0.5μm to 5μm form as a result, this pathway can also potentially take up carriers of large sizes and it's involvement in uptake of various nanocarriers has been demonstrated.[161] On the other hand, the uptake of nanocarriers via macropinocytosis is more difficult to control for drug delivery purposes, as it is often non-specific, and the intracellular

fate is variable but often involves acidification and shrinkage of the compartment, eventual delivery to lysosomes, or recycling to the cell surface.[162]

Clathrin-mediated endocytosis is perhaps the best characterized mechanism of endocytic transport and is also pinocytic (Figure C). It can be accessed with or without ligands targeted to molecules such as transferrin receptor (TfR), vascular cell adhesion molecule 1 (VCAM-1), $\alpha_v\beta_3$ integrin, LDL receptor, selectins, and many others.[3] Binding of the target receptors on the cell surface induces uptake by forming invaginations on the plasma membrane with the aid of a clathrin coat, and endocytosed material is delivered initially to endosomes with subsequent recycling to the cell surface, delivery to lysosomes, or transcytosis.[20,163] Clathrin-mediated endocytosis is ubiquitous to most cells which can be useful in applications where endocytic transport in multiple cell types may be necessary (e.g. sequential transport across the blood-brain barrier, followed by endocytosis in parenchymal cells).[164] However, a disadvantage is that the size of internalizable ligands via clathrin-mediated endocytosis is limited to ~100-150 nm, restricting internalization to monovalent drug conjugates and carriers below this size.[162]

Caveolae-mediated endocytosis is pinocytic and can be accessed with or without the use of targeting ligands. Endocytosis via caveolae can be triggered as result of binding to molecules such as aminopeptidase N and P, gp60, and others.[3] Caveolae are distinctive, flask-shaped invaginations on the plasma membrane and are prevalent in endothelial cells.[165,166] Endocytosis via caveolae presents an

advantage primarily because it results in transport to a sorting compartment known as the caveosome with subsequent transcytosis to the basolateral surface.[167] This along with the observation that transcytosis is more common to caveolae- than clathrin-mediated endocytosis,[3] make this pathway advantageous for crossing cellular barriers. Similar to clathrin-mediated endocytosis, however, the size of internalizable ligands is restricted by lack of accessibility of target receptors due to their location deep within caveolar invaginations, or because the size of caveolar vesicles is limited to ~70 nanometers.[3]

Non-classical pathways such as flotillin-, cdc42-, RhoA, and Arf6-dependent pathways can also be utilized.[161] These pathways are involved in transport of cargoes such as simian virus 40, cholera toxin, glycosylphosphatidylinositol (GPI)-linked proteins, interleukin-2, and growth hormones.[161] Nanomaterials utilizing these mechanisms have been documented in rare cases, such as macromolecules modified to target folate.[161]

In certain cases, endocytic pathways which have not been described to be constitutive can be induced by binding of receptors even when these are not commonly associated with endocytic transport. This is the case for intercellular adhesion molecule-1 (ICAM-1) or platelet-endothelial cell adhesion molecule-1 (PECAM-1), where binding of targeted nanocarriers or conjugates to multiple copies of the receptor induces endocytosis via an uncommon pathway termed cell adhesion molecule-mediated endocytosis (CAM)-mediated endocytosis.[168] Polymer

nanocarriers targeted ICAM-1 or PECAM-1 have been observed to use this mechanism of endocytic transport.[168-173] The advantages of CAM-mediated endocytosis include presence in several cell types, including endothelial, epithelial, macrophages, fibroblasts, neurons, etc.[3] Endocytosis via the CAM pathway can accommodate uptake of carriers up to 5 microns in size and, enables slow transport to lysosomes, which can be exploited to prolong activity of therapeutics before degradation,[169] or enables transcytosis.[19] The disadvantages of CAM-mediated endocytosis include relatively little knowledge of the precise mechanics of endocytic transport and fate in subcellular compartments, and also that targeting ICAM-1 or PECAM-1 may result in broad distribution in tissues which is unwanted for certain applications (e.g. delivery of cytotoxic agents).

As mentioned above, several endocytic pathways allow transcytosis which enables vesicular transport across cell barriers (e.g. the blood-brain barrier) to reach target sites in the tissue parenchyma.[174] Transcytosis can occur as a result of uptake via the fluid phase, or can be receptor-mediated where the target molecule is bound at the apical cell surface, endocytosed, and transported across the cell to the basolateral cell surface via vesicular trafficking.[174] An advantage of transcytosis is that it can allow transport without disrupting cell junctions. Opening of cell junctions can induce toxicity due to concomitant transport of substances in the extracellular milieu. Certain molecules associated with clathrin-mediated endocytosis, such as TfR, LDLR, and insulin receptor are known to enable transcytosis,[3,174] but transcytosis via caveolae also occurs via ligand binding and is more common.[3] As

with intracellular delivery, a significant drawback of these routes is that uptake is restricted by size which limits the potential transport of nanocarriers. Transcytosis via CAM-mediated endocytosis may provide a preferable alternative as intracellular uptake of relatively larger carriers is accomodated.[175]

Transport via paracellular routes (i.e. between cells) is also possible, but requires disruption of tight junctions linking adjacent cells (Figure D). This can be done transiently with certain nanocarriers (e.g. dendrimers) or by using hyperosmotic solutions, vasoactive agents, ultrasound, solvents, or stabilizers.[5] However, these strategies are transient and local, and can be invasive or damaging due to toxic effects associated with induction of barrier permeability. Finally, carrier-mediated transport and passive diffusion are other potential routes of transport across cells, but are limited to small molecules.

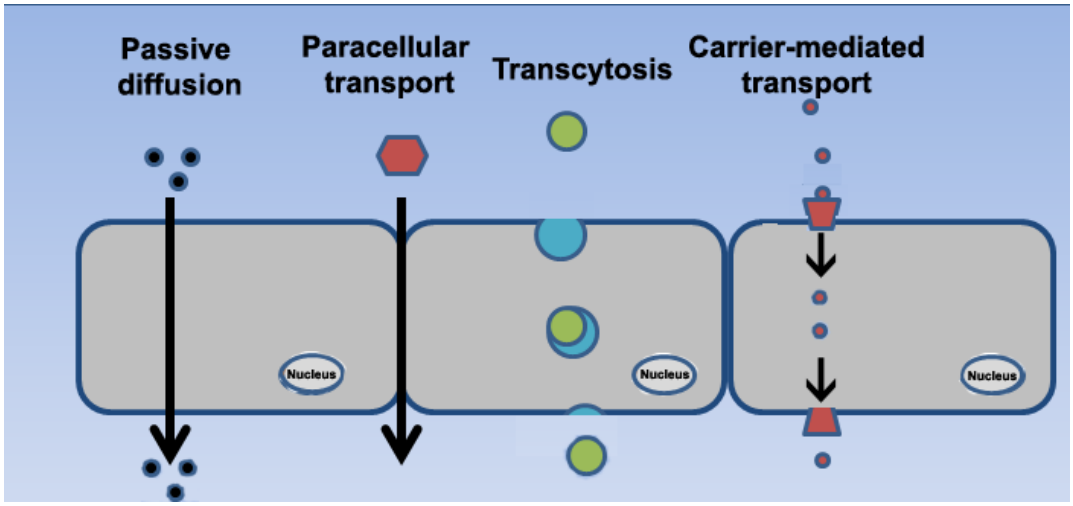

Figure D. Transport across cellular barriers.

2.6. Targeting and Endocytosis of Nanocarriers: Role of Size and Valency

With regard to targeting and transport of agents, the targeting valency (number of ligands utilized) and size of nanocarriers have an impact on most aspects of pharmacokinetics. One clear advantage of targeted nanocarriers over simple conjugation of an agent to an affinity moiety is that the design is amenable to modifications which add functionality or improve the pharmacokinetic profile (e.g. nanocarriers shape, structure, surface coatings, etc). Multivalent display of targeting ligands on the nanocarrier surface can also affect drug delivery on several levels. For example, multivalency can accelerate clearance from the circulation by increasing recognition by cells of the reticuloendothelial system.[176] This is very apparent in the case where antibodies, recognizable by their Fc region, are used as targeting ligands.[176] Avidity for the target receptor is enhanced by ligand multivalency which can, in turn, enhance binding.[3] This is particularly important *in vivo*, where physiological factors such as shear stress from the flow of blood, or competition for the target epitope with endogenous ligands can work against effective targeting.[3] Yet, multivalency may also enhance binding to off-target sites, which, despite lower expression of the target, may be amplified by higher avidity for the target receptor than monovalent drug conjugates.[3] Regarding internalization, binding multiple target molecules on the cell surface may enhance nanocarrier internalization. For example, in the case of ICAM-1 targeting, only multivalent binding with ICAM-1-targeted-nanocarriers, but not free anti-ICAM, enables endocytosis.[168] Multivalency can also affect subcellular transport as has been observed for the slow trafficking to lysosomes of multivalent transferrin oligomers versus monomeric transferrin.[177]

Multivalency may also enhance adhesion to components of the extracellular matrix within tissues, but this has not been examined. Therefore, the behavior of a targeting moiety when coupled to a nanocarrier may be completely different from that observed from the naked targeting moiety.

The size of the nanocarrier also affects delivery on many levels. Size is inversely correlated with the rate of clearance from the circulation, due to increased adsorption of opsonins and subsequent recognition by macrophages in the spleen and liver.[18] Steric hindrance can lower the ability of nanocarriers to bind the target receptor which may also depend on the expression level and location of the the target receptor on the plasma membrane.[3,129,178] This is particularly apparent when the target epitope is proximal to the plasma membrane, affecting binding of nanocarriers to the target receptor.[179] Intracellular transport of targeted nanocarriers also seems to be affected by size, e.g. in the case of targeting to ICAM-1, micron-sized spheres reach the lysosomes at a slower rate than submicron-sized counterparts.[175] In addition, size may restrict internalization via certain pathways altogether.[180] Larger size also lowers the ability of nanocarriers to diffuse to the target site, yet lymphatic drainage may also be lower.[3] Therefore, nanocarrier size effects may be offset by comparatively greater retention in tissues than smaller drug conjugates.

Overall, size and valency have advantages and disadvantages which cannot be predicted *a priori*, and therefore must be evaluated empirically according to the particular target, cell type, carrier, pathological status, and therapeutic intervention.[3]

2.7. Combination Targeting

Apart from valency and size described above, targeting can also be modulated by combination targeting of nanocarriers. Combination targeting is an emerging approach for drug delivery to enhance or improve control over the distribution of nanomaterials in the body. It is seen in nature with infectious pathogens and cells of the immune system which interact with multiple cell-surface receptors to adhere to and induce transport into cells or across cellular barriers.[10,21] Combination targeting strategies have also arisen in targeted drug delivery, providing new approaches to enhance and optimize delivery of therapeutics and imaging agents for a number of applications.

One of the most studied examples of combination-targeting is that of targeting multiple CAMs expressed on the vascular endothelium.[12,23,30,181-187] Endothelial CAMs consist of selectins (E- or P- selectin) and immunoglobulin-like CAMs (ICAM-1, PECAM-1, and vascular cell adhesion molecule-1, VCAM-1) which are involved in the adhesion and transmigration of leukocytes to sites of inflammation.[21] Selectins mediate the initial tethering and rolling interactions of leukocytes on the endothelial surface by forming relatively weak, catch-slip bond interactions, while Ig-like CAMs mediate firm adhesion and transmigration of leukocytes across the endothelial border by engaging in stronger binding interactions.[21] An important application of targeting CAMs is delivery of pharmaceutical agents to the vascular endothelium which is involved in the pathogenesis of many diseases.[188] Nanocarriers have been targeted to particular

CAMs in order to enhance delivery of imaging and therapeutic agents in many contexts, including treatment of inflammation, cancer, atherosclerosis, arthritis, thrombosis, and lysosomal storage disorders.[21] CAMs provide endocytosis into endothelial cells via clathrin-mediated (E- or P- selectin, VCAM-1)[189-192] or CAM-mediated (ICAM-1 and PECAM-1)[168] endocytosis, respectively. The endothelium is also a critical barrier restricting transport from the circulation to the organ parenchyma. ICAM-1 and VCAM-1 have been shown to enable transport of nanocarriers across endothelial or epithelial cells via transcytosis which may provide a useful means to deliver nanocarrier cargo from the bloodstream to extravascular tissues.[19,193]

Although a relatively nascent strategy, combination targeting of CAMs has been explored in several contexts. For example, microparticles carrying iron oxide[12] or fluorescent probes,[182] perfluorocarbon-filled microbubbles,[23,30] or gold nanorods[187] have been used in imaging, and polymerosomes,[186] immunoliposomes,[184,185] or PLGA microspheres[181] have been developed for drug delivery applications. These examples emulate adhesive properties of leukocytes by combining targeting to an endothelial selectin and an Ig-like CAM.[12,23,30,181-187] Simultaneous targeting to these molecules is beneficial, as demonstrated for microspheres functionalized with sialyl Lewis(X) and anti-ICAM, for which certain ligand-receptor ratios and flow shear rates allowed binding only through interaction with both receptors, enhancing selectivity.[181] Targeting polymerosomes to P-selectin and ICAM-1 also enhanced binding over single-targeted counterparts and improved

selectivity toward inflammation,[186] and combined P-selectin/VCAM-1 targeting seemed to improve binding of microbubbles in receptor-coated flow chambers.[23] These "leukomimetic" approaches are being explored for treatment and/or diagnosis of inflammation, atherosclerosis, and cancer. Combination-targeting to molecules with different function has also been examined in particular contexts, and has been shown to enhance transport to tumor areas,[13,194,195] improve site selectivity,[14] and enhance delivery to multiple cell types within the tumor environment.[7]

On the other hand, targeting nanocarriers to multiple epitopes of the same receptor is completely unexplored. Epitope dependent targeting has been observed for nanocarriers targeted to single receptors. Binding, endocytosis, and lysosomal transport of PECAM-1-targeted nanocarriers were shown to depend on the epitope targeted.[179] Epitope selection is important for lung accumulation and induced cleavage of anti-ACE,[131,196] and brain selectivity of anti-TfR.[132] In addition, stimulation *in vivo* of PECAM-1 with an antibody subsequently enhanced lung accumulation of a second antibody or fusion conjugate.[15]

Interestingly, newer generations of nanocarriers are being developed to have spatially-segregated display of ligands on the nanocarrier surface.[197,198] These "patchy" or janus nanoparticles may enable more precise control of ligand-receptor interactions which could be utilized to optimize combination targeting strategies in a more rational manner. For example, ligands could be diplayed at varying distances

from one another, or in different patterns on the nanocarrier surface to develop control over targeting.

Translation of these strategies requires a good understanding of their impact on cellular binding, internalization and biodistribution *in vivo*. Yet, much remains to be done with regard to these areas. Targeting nanocarriers to multiple epitopes of the same receptor has never been examined in these contexts, and only a few examples have been published in the case of targeting receptors with similar or different function. Consequently, the behavior of nanocarriers with regard to these parameters and targeting strategies remains largely an open question.

The results presented in this dissertation provide insight into the performance of model polymer nanocarriers designed for combination targeting. Nanocarriers targeted to multiple receptors with similar function is investigated in the context of multi-CAM-targeting (Section 4.1). Nanocarriers are targeted to multiple Ig-like CAMs in single, dual- or triple-targeted combinations, and binding, internalization within cells, and biodistribution *in vivo* are evaluated. Combination targeting of polymer nanocarriers to different receptors is investigated next (Section 4.2) using ICAM-1 and TfR which are involved in leukocyte adhesion vs. iron transport. Finally, a novel approach for combination targeting is presented (Section 4.3) where polymer nanocarriers are targeted to multiple epitopes of the same receptor (e.g. TfR epitopes).

Section 3: Methods

3.1. Materials

Monoclonal antibodies used in the study were: mouse anti-human TfR clone T56/14 from EMD Millipore (Billerica, MA), rat anti-mouse TfR clone R17217 (hereafter referred to as R17) from Biolegend (San Diego, CA),[132] rat anti-mouse TfR clone 8D3 from Novus Biologicals (Littleton, CO),[199] mouse anti-human ICAM-1 clone R6.5[200] and rat anti-mouse ICAM-1 clone YN1 from ATCC (Manassas, VA),[201] rat anti-mouse PECAM-1 clone MEC13 (BD Biosciences; San Jose, CA), and rat anti-mouse VCAM-1 clone MK2 (Santa Cruz Biotechnology; Dallas, TX). ICAM-1-targeting peptide, γ3 (NNQKIVNIKEKVAQIEA [37,202]), was synthesized by United Biochemical Research (Seattle, WA). Transferrin (Tf) and secondary antibodies were from Molecular Probes (Eugene, OR). Recombinant human acid sphingomyelinase (ASM) was produced by our collaborator Dr. Schuchman (Mt. Sinai Hospital, NY) in chinese hamster ovary cells and purified as described.[203] Control rat and mouse IgG were from Jackson Immunoresearch (Pike West Grove, PA). Polystyrene particles were from Polysciences (Warrington, PA). Unless otherwise stated, all other reagents were from Sigma aldrich (St. Louis, MO).

3.2. Iodination of Proteins

Antibodies used to determine coating efficiency of antibodies on carriers or for *in vivo* studies in mice were labeled with ^{125}I by adding ~20 μCi of ^{125}I to 1 μg/μl of antibody and 2-3 iodination beads from Fisher Scientific (Waltham, MA) in a total volume of 100 μl of PBS for 3-5 min at room temperature. Iodogen pre-coated tubes

from Fischer Scientific (Waltham, MA) were also used in lieu of iodination beads for this procedure. Unincorporated ^{125}I was removed by centrifugation at 1000g for 4 min in a gel size exclusion column with 6,000 MW cutoff from Biorad (Hercules, CA). This column was prepared by inverting 2-3 times to homogenize the gel suspension, adding 2 ml of PBS to pack the column, and centrifuging at 1000g for 1 min to remove PBS prior to adding the iodinated antibody. The concentration and activity of iodinated protein were determined by Bradford assay and measurement in a gamma counter, respectively. The percentage of free iodine remaining in solution was estimated by adding the ^{125}I-antibody to 3% BSA and trichloroacetic acid (1 part in 6 v/v) which drives precipitation of the ^{125}I-antibody but leaves free ^{125}I in the supernatant fraction. Measurement of the activity of the supernatant relative to the total activity of the sample was used to determine the percentage of free iodine in solution.

3.3. Preparation and Characterization of Antibody-coated Nanocarriers

Model targeted polymer nanocarriers were prepared by coating ligands (Tf or γ3 peptide) or antibodies onto the nanoparticle surface by adsorption. This results in a surface coating of antibodies which are randomly oriented on the nanocarrier surface, yet for all formulations tested this method resulted in specific binding relative to a control formulaton coated with non-specific IgG. As in our previous studies,[134,175,204] and in order to avoid potential confounding results of concomitant nanoparticle degradation, we used model polystyrene nanoparticles which, after targeting with antibodies, have shown similar biodistribution than biodegradable

poly(lactic-co-glycolic acid) counterparts.[205] This was done by incubating 0.7 mg antibody/mL with 9 x 10^{12} nanoparticles/mL for 1 h at room temperature, as described.[206] Single-targeted nanocarriers contained only targeting moiety on the coat, i.e. control IgG (mouse or rat), Tf or anti-TfR (R17, 8D3, or T56/14), γ3 or anti-ICAM (YN1 or R6.5), anti-PECAM-MEC13, anti-VCAM-MK2, or a 1:1 mass ratio of control IgG and one of the targeting antibodies with valency of ~185-300 antibodies per nanocarrier. Dual-targeted nanocarriers were coated by adding a 1:1 mass ratio of anti-ICAM-YN1/TfR-R17, anti-TfR-R17/anti-TfR-8D3, anti-PECAM-MEC13/anti-VCAM-MK2, or anti-ICAM-YN1/anti-PECAM-MEC13 which resulted in each antibody having a valency of ~99-154 antibodies per nanocarrier for a total of ~221-290 antibodies per nanocarrier. Triple-targeted nanocarriers were coated by adding a 1:1:1 mass ratio of anti-ICAM-YN1/PECAM-MEC13/VCAM-MK2 with each antibody having a valency of ~67-92 antibodies per nanocarrier for a total of ~236 antibodies per nanocarrier. Nanocarriers carrying a therapeutic enzyme contained a 1:1 mass ratio of ASM and total antibody component (single, dual, or triple) mix. For experiments in mice, nanocarriers contained ^{125}I-IgG or ^{125}I-ASM as tracers the enzymatic cargo. Uncoated counterparts were removed by centrifugation at 13,800 g for 3 min. Nanocarriers were then resuspended to a final concentration of ~6.8 x 10^{11} nanocarriers/mL (cell cultures) or ~5.8x10^{12} nanocarriers/mL (mouse studies) in phosphate-buffered saline (PBS) containing 1% bovine serum albumin (BSA) (cell cultures) or 0.3% BSA (mouse studies). These solutions were sonicated with 15-30 short pulses (i.e < 1 second/pulse) using a probe sonicator to avoid aggregation. The final size, polydispersity, and zeta potential of nanocarrier

formulations were estimated by dynamic light scattering or laser doppler velocimetry of electrophoretic mobility, respectively (Malvern Zetasizer, Worcestershire, UK). The coating density was assessed by preparing nanocarriers with ^{125}I-labeled antibody and measuring the ^{125}I content of the coated nanocarrier suspension in a gamma counter (PerkinElmer Wizard^2, Waltham, MA). For dual or triple targeted formulations, only one of the antibodies was labeled per preparation to detect the valency of each antibody individually. The number of antibodies per nanocarrier were calculated as follows:

$$\text{antibodies coated per nanocarrier} = \frac{\left[\frac{^{125}\text{I-antibody coated to NCs (CPM)} \times 1\ \text{dalton} \times 1\ \text{IgG antibody} \times 6.02 \times 10^{17}\ \text{molecules}/\mu\text{mol}}{^{125}\text{I-antibody (CPM}/\mu\text{g)} \times (1\ \mu\text{g}/\mu\text{mol}) \times 150{,}000\ \text{daltons}}\right]}{\text{Volume NCs } (\mu\text{l}) \times \text{NC concentration (NCs}/\mu\text{l)}}$$

Where NC = nanocarriers and CPM = counts per minute.

3.4. Cell Culture

Pooled human umbilical vein endothelial cells (HUVECs) from Lonza (Walkersville, MD) were seeded onto gelatin-coated coverslips and cultured at 37°C, 5% CO_2, and 95% relative humidity. Cells (3-4 passages) were grown in M-199 medium supplemented with 15% fetal bovine serum (FBS), 2 mM glutamine, 15 μg/ml endothelial cell growth supplement, 100 μg/ml heparin, 100 μ/ml penicillin, and 100 μg/ml streptomycin. Murine heart ECs (H5V)[207] were seeded onto gelatin-coated coverslips at 37°C, 5% CO_2, and 95% relative humidity in DMEM medium supplemented with 10% FBS, 2 mM glutamine, 100 μg/ml penicillin, and 100 μg/ml streptomycin. When indicated, pathological activation of

ECs was mimicked by 16-20 h incubation at 37°C with 10 ng/ml tumor necrosis factor alpha (TNFα).

3.5. Binding Studies

Cells were washed with basal cell medium (pre-warmed to 37°C, all washing steps involved 3 washes and 1 mL volume) before the nanocarrier incubation period to remove cellular debris. Control or TNFα-activated ECs were incubated with naked antibodies (~16.7 μg/ml) or antibody-coated carriers (~5 μg antibody/ml and 6.8 x 10^{10} particles/ml) in cell medium at 37°C. The particular incubation times are specified in each figure legend. Following this incubation, cells were washed three times with 1 mL basal cell medium to remove unbound nanocarriers and fixed with cold 2% paraformaldehyde (PFA) for 15 min at room temperature. Where indicated, cells were fixed prior to incubation at room temperature with naked antibodies or antibody-coated nanocarriers, in order to examine binding in the absence of cellular activity (and consequently endocytosis).

Binding of naked antibodies on cells was detected by immunostaining with FITC-labeled secondary antibodies (goat anti-mouse or goat anti-rat IgGs). To detect antibodies both bound to the cell surface and internalized, cells were first washed to remove excess PFA, permeabilized with 0.2% Triton X-100 for 15 min at room temperature, washed, and subsequently stained with FITC-labeled goat anti-rat IgG. No additional staining was required to detect antibody-coated carriers since FITC is contained within the polymer matrix. Cell nuclei were stained with 4',6-diamidino-2-

phenylindole (DAPI) for 5 min at room temperature prior to mounting onto slides with MOWIOL.

Fluorescence microscopy images were taken using an Olympus IX81 microscope (Olympus, Inc., Center Valley, PA), ORCA-ER camera (Hamamatsu, Bridgewater, New Jersey), 60x objective (Olympus Uplan Apo F LN; Olympus) and FITC-optimized filter from Semrock (Rochester, NY, excitation BP460-490 nm, dichroic DM505 nm, emission BA515-550 nm). Images were acquired with SlideBook 4.2 (Intelligent Imaging Innovations, Denver, Colorado) and analyzed using Image-Pro 6.3 (Media Cybernetics, Inc., Bethesda, MD) to estimate antibody binding (mean fluorescence intensity),[208] carriers bound per cell[168] (number of 100–200 nm fluorescent objects), or specificity index (e.g. targeting of antibody over control IgG or targeting of antibody-coated carriers over control IgG-coated carriers). Phase-contrast images were used to delimit the cell borders.

3.6. Imaging of Endothelial Engulfment Structures

To examine initial stages of carrier engulfment, HUVECs were incubated for 15 min at 37^{o}C with anti-ICAM carriers or anti-TfR carriers, where carrier particles were 4.5 μm to allow detailed visualization of engulfment structures.[173] After washing unbound carriers, cells were fixed, permeabilized with 0.2% Triton X-100, and immunolabeled to detect enrichment of sodium proton exchanger 1 (NHE1) or clathrin heavy chain (which are partners associated to CAM vs. clathrin pathways)[173] at sites of carrier binding.

3.7. Endocytosis Studies

Control or TNFα-activated ECs were incubated with antibodies (~16.7 μg/ml) or antibody-coated carriers (~5 μg antibody/ml and 6.8 x 10^{10} particles/ml) ub cell medium as specified above. Iincubation times and temperatures are specified in figure legends. Cellular internalization was tested at 37^{o}C, which is physiological temperature for eukaryotic cells. Following the incubation period, cells were fixed with PFA for 15 min at room temperature.

To detect targeting antibodies on the cell surface, cells were stained for 30 min at room temperature with 6 μg/ml Texas-Red-labeled goat anti-mouse or goat anti-rat IgGs (which can bind to the Fc region of the targeting antibody), in PBS containing 1% BSA to block non-specific binding. Cells were then permeabilized with 0.2% Triton X-100 for 15 min at room temperature and subsequently incubated with 15 μg/ml FITC-labeled goat anti-mouse or goat anti-rat IgGs in 1% BSA PBS for 30 min at room temperature to stain both surface + internalized targeting antibody. In the case of antibody-coated nanocarriers, cells were stained with Texas-Red-labeled goat anti-rat or goat anti-mouse IgGs to label nanocarriers present on the cell surface,[168] while all cell associated nanocarriers (surface + internalized) had intrinsic green signal due to FITC-fluorophore embedded within the polymer matrix. Cell nuclei were stained with DAPI for 5 min at room temperature prior to mounting onto slides with MOWIOL.

Fluorescent microscopy was used to distinguish internalized materials as FITC single-labeled antibodies or carriers from surface-bound materials appearing yellow due to Texas-Red + FITC double-labeling. Images from each fluorescence channel were acquired (Texas-Red filter from Semrock (Rochester, NY), excitation BP360-370 nm, dichroic DM570 nm, emission BA590-800+ nm), merged, and analyzed using Image-Pro 6.3 to estimate the percentage of nanocarriers internalized per cell (% internalization) and the total number of nanocarriers internalized per cell.[168] Percent internalization was calculated as the number of internalized materials divided by the signal for total cell-associated counterparts. Phase-contrast images were used to delimit cell borders.

3.8. Biodistribution Studies in Mice

Anesthetized C57BL/6J male mice (aged ~2-5 months and weighing ~20 – 30 g) were injected intravenously (28 G) via the jugular vein with ^{125}I-labeled antibodies or antibody-coated nanocarrier counterparts (~1.3 mg total antibody/kg body weight, ~1.8 x 10^{13} particles/kg). Antibodies were directly labeled with ^{125}I, while trace amounts of ^{125}I-IgG (i.e. 0.03-0.24 μCI, ≤ 5% of total antibody) were used on the particle coat to enable detection in a gamma counter. This is particular useful for monitoring particle targeting upon administration because the distribution of non-specific IgG is clearly distinguishable from nanocarriers coated with targeting antibodies. For experiments involving a therapeutic cargo, mice were injected with ^{125}I-labeled ASM as a naked counterpart or coated on ~250 nm antibody-coated particles (~0.7 mg ASM/kg body weight, ~1.8 x 10^{13} particles/kg). Blood samples

were collected by penetrating the retro-orbital sinus with a capillary tube (~50-100 μl collected per sample) at 1, 15, and 30 min after injection, and organs (kidneys, spleen, heart, lungs, liver, and brain) were harvested at 30 min following euthanasia by cervical dislocation under anesthetic. ^{125}I content and weight of samples were determined to estimate the localization ratio (LR) and specificity index (SI). LR represents the percent of injected dose accumulated per gram of tissue (%ID/g) divided by the %ID/g in blood, to account for differences in organ size and circulating nanocarriers.[134] The SI is calculated as the LR of targeted formulations divided by the LR of non-targeted counterparts (IgG NCs or naked ASM) and represents specific targeting.[134] These studies complied with IACUC (protocols R-13-15, R-10-22, R-09-54), University of Maryland regulations, and the Guide for Care and Use of Laboratory Animals of the U.S National Institutes of Health.

3.9. Statistics

Data were calculated as mean ± S.E.M, where statistical significance was determined as $p \leq 0.05$ by Student's *t*-test (2-tailed distribution designed for two samples of equal variance (i.e. homoscedastic)). Animal experiments were performed using replicates of ≥3 mice per experiment (except for injection of anti-PECAM in control mice or anti-ICAM/ASM NCs, anti- TfR/ASM NCs, or free ASM in mice pre-treated with LPS where n = 2). Cell culture experiments were performed by using ≥ 10^5 cells/well, duplicate wells per condition, and at least 2 repeats. Images were randomly taken through the entire coverslip, from which ≥ 15 cells per sample were selected randomly and analyzed.

Section 4: Results and Discussion

4.1. Combination Targeting to Multiple Receptors with Similar Functions

4.1.1. Introduction

Similar to the interactions of infectious pathogens or leukocytes with multiple cell-surface markers in nature, combination targeting may enhance accumulation and/or precise control of nanocarriers. Targeting nanocarriers to multiple receptors with similar function (e.g. involved in a common process or event) was examined in a few previous studies mainly in the context of cellular binding of carriers addressed to multiple CAMs (see Background: combination targeting).[12,23,30,181-187] These examples aimed at emulating the adhesive properties of leukocytes by targeting a selectin and an Ig-like CAM, which mediate leukocyte rolling and firm adhesion, respectively.[12,23,30,181-187] Future translation of these strategies, however, requires a good understanding of their impact *in vivo*, where the data are scarce, yet promising. For example, targeting iron oxide microparticles to P-selectin/VCAM-1 enhances adhesion to aortic root endothelium in a mouse model of atherosclerosis.[12] Targeting fluorescent microspheres to P-selectin/ICAM-1 enhances adhesion and detection of ocular inflammatory disease in the choroidal or retinal microvasculature.[182] However, to our knowledge the in vivo performance of nanocarriers targeted to multiple CAMs has not been examined for submicrometer carriers, a size more amenable for intracellular drug delivery applications.[3] In addition, combination targeting to CAMs involved solely in leukocyte firm adhesion (vs. those encompassing rolling and firm adhesion) has never been tested. In addition, the impact of this combination targeting strategy in terms of its potential for intracellular transport is unknown and critical, as

many therapeutics require delivery to intracellular compartments. For example, the effects of targeting multiple CAMs associated to the same versus different endocytic pathways or located in different regions of the plasma membrane have not been examined. Finally, the comparative impact of dual vs. triple combination-targeting to CAMs is an open question which holds relevance since it better reflects the multiplicity of interactions between leukocytes and the endothelium.

We selected ICAM-1, PECAM-1, and VCAM-1 to test the hypothesis that targeting polymer nanocarriers to multiple Ig-like CAMs with similar function (namely, firm adhesion and extravasation of leukocytes) modifies nanocarrier delivery in terms of binding to cells, endocytosis, and biodistribution. These three receptors differ in expression level, cell-surface location, pathological stimulation, and/or cell uptake pathway, all of which can affect greatly these parameters. For instance, ICAM-1 and VCAM-1 are predominantly located on the luminal surface of endothelial cells, while PECAM-1 is enriched at the cell borders.[21] In control conditions VCAM-1 expression is very low, followed by ICAM-1, and much higher expression of PECAM-1.[21] VCAM-1 and ICAM-1 expression are enhanced by cytokines and other pathological stimuli, while PECAM-1 remains relatively stable.[21] ICAM-1 and PECAM-1 mediate endocytosis of both nano- and micron-sized carriers via non-classical CAM-mediated endocytosis,[168] whereas VCAM-1 enables uptake by clathrin-mediated endocytosis,[189] which is more size-restrictive (≤200-nm).[162,208] The effects of these differences are described in the next section.

4.1.2. Binding and endocytosis of antibody-coated nanocarriers single-targeted to ICAM-1, PECAM-1, or VCAM-1

We first tested binding and endocytosis of nanocarriers single-targeted to ICAM-1, PECAM-1, or VCAM-1. Polysytyrene nanospheres were utilized as model polymer nanocarriers due to their stability which avoids confounding results of concomitant nanocarrier degradation (see Methods). Nanocarriers coated with non-specific IgG or with antibodies targeted to PECAM-1 (anti-PECAM NCs), VCAM-1 (anti-VCAM NCs), or ICAM-1 (anti-ICAM NCs) displayed similar valency (~240-270 antibodies/NC), size ~220-330-nm diameter, polydispersity ~0.2-0.3, and zeta potential of ~-27 - -33 mV, with anti-PECAM NCs somewhat larger in size (Table 1). The literature values reported for the affinity of antibodies directed to ICAM-1 or PECAM-1 ranged from 0.5-8.5 nm,[15,205] while the affinity of the antibody directed to VCAM-1 is to our knowledge unpublished.

Table 1. Characterization of CAM-targeted nanocarriers

Nanocarrier coating	Size (nm)	PDI	ZP (mv)	Coating valency (Ab/NC)		
Uncoated NCs	143±18	0.05±0.05	-37.6±1.8			
Single:						
IgG NCs	238±8.3	0.17±0.02	-27.2±17	240±25		
Anti-ICAM NCs	217±3.5	0.14±0.01	-33.0±3.3	273±37		
Anti-PECAM NCs	333±26	0.26±0.04	-31.0±2.3	250±4.5		
Anti-VCAM NCs	226±10	0.17±0.02	-30.3±0.1	239±22		
Dual:						
Anti-ICAM/ PECAM NCs	268±22	0.17±0.04	-33.0±1.6	ICAM: 132±6.7	PECAM: 123±6.4	
Anti-PECAM/ VCAM NCs	251±10	0.19±0.01	-32.2±1.4	PECAM: 101±26	VCAM: 120±0.3	
Triple:						
Anti-ICAM/PECAM/ VCAM NCs	257±16	0.19±0.03	-32.6±4.9	ICAM: 92±0.2	PECAM: 67±20.9	VCAM: 77±18.2

Data are Mean±S.E.M. Ab = antibody; NC = nanocarrier; PDI = polydispersity; ZP = zeta potential. Antibody clones were YN1 (ICAM-1), MEC13 (PECAM-1), MK2 (VCAM-1).

Binding of anti-ICAM NCs was efficient in control ECs (38-fold over control IgG NCs), and increased significantly (85-fold over control IgG NCs) in activated ECs (Figure 1). This parallels activation of ICAM-1 expression in disease conditions where, for example, endothelial expression is on the order ~10^5-10^6 receptors per cell in comparison to 10^4 receptors per cell in physiological conditions.[21] Anti-PECAM NCs displayed higher binding than anti-ICAM NCs in control cells (93-fold over IgG NCs) and similar binding to anti-ICAM NCs in activated ECs (110-fold over IgG NCs) which paralleled relative expression levels of ICAM-1 and PECAM-1 in disease conditions.[155] In control conditions PECAM-1 expression on endothelium is on the order of 10^6 molecules per cell, which remains fairly stable under pathological activation of the endothelium.[21] On the other hand, anti-VCAM NCs displayed the lowest binding in both control and activated ECs, in agreement with comparatively lower expression of VCAM-1 in control vs. inflammatory conditions (10^3 vs. 10^{4-5} receptors per cell, respectively).[21,209]

Nanocarriers targeted to ICAM-1, PECAM-1, or VCAM-1 were efficiently endocytosed by ECs (Figure 1c-d). The fraction of nanocarriers endocytosed by cells relative to the total number of cell-associated nanocarriers (which reflects endocytosis efficiency or rate) was ~75-85% at 1 h in control cells (Figure 1c).

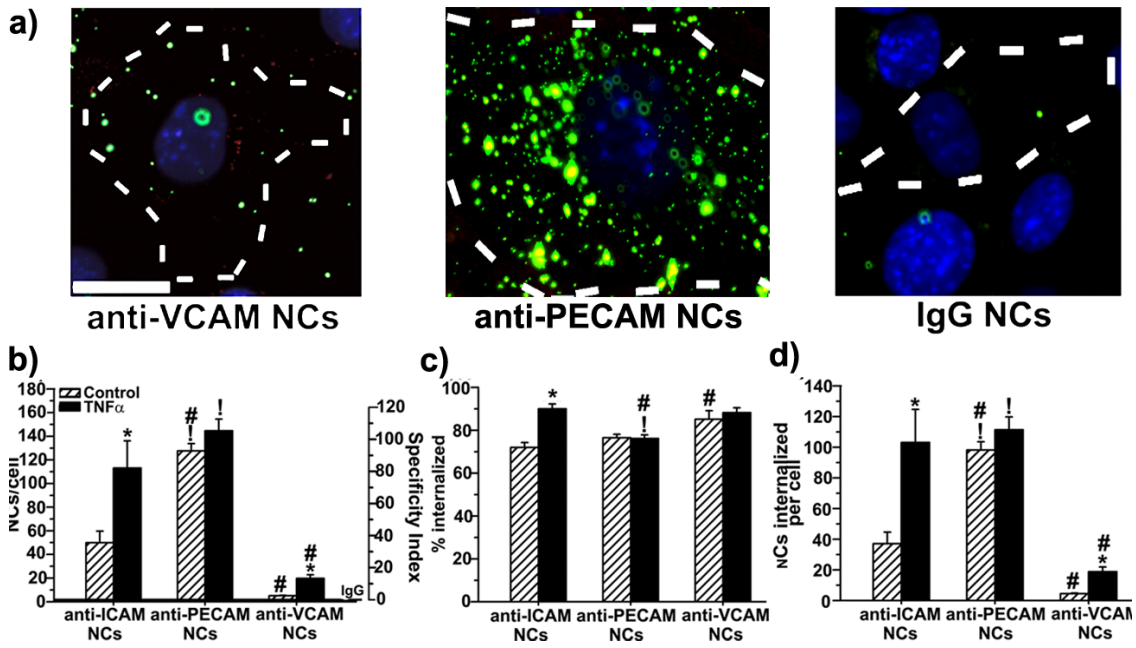

Figure 1. Binding and internalization of nanocarriers targeted to ICAM-1, PECAM-1, or VCAM-1. (a) Fluorescent images of nanocarrier binding and internalization tested after incubation for 1 h at 37 °C in TNFα-activated H5V cells, and analyzed by fluorescence microscopy to assess the: (b) number of nanocarriers per cell (NCs/cell) and specificity index (SI), (c) percent of internalized nanocarriers per cell, and (d) total nanocarriers internalized per cell for each formulation. Internalized carriers appeared green due to single-labeling with FITC, while surface-bound carriers appeared yellow due to FITC + Texas-Red double-labeling. Phase-contrast images were used to delimit cell borders (dashed lines).Scale bar is ~ 10 μm. Control IgG NCs are shown as a line in (b). Data are mean ± S.E.M. * Compares control vs. TNFα for each formulation, ! compares anti-PECAM NCs to anti-VCAM NCs, # compares to anti-ICAM NCs. *,# represents $p < 0.05$ by Student's *t*-test.

The rate of endocytosis in control condition was similar for anti-ICAM NCs and anti-PECAM NCs with both displaying modestly lower rate than anti-VCAM NCs. Yet, in terms of total nanocarrier internalization (Figure 1d), targeting PECAM-1 or ICAM-1 was similarly more efficient than targeting VCAM-1 in control or activated cells. In activated ECs, the internalization rate was similar for anti-ICAM NCs and anti-VCAM NCs which was higher than for anti-PECAM NCs. This may reflect differences in receptor location where receptor-mediated endocytosis is somewhat slower via receptors present at cell borders versus receptors present on the cell surface. As with modulation of ICAM-1, VCAM-1, and PECAM-1 expression levels in disease, the bulk number of internalized nanocarriers increased significantly in activated ECs for anti-ICAM NCs and anti-VCAM NCs, but not anti-PECAM NCs.

4.1.3. Binding and endocytosis of antibody-coated nanocarriers dual-targeted to PECAM-1 and VCAM-1

We next examined combination-targeting to PECAM-1 and VCAM-1, which differ the most with regard to expression level, location, and response to pathology.[21] Anti-PECAM/VCAM NCs had equal amount of anti-PECAM and anti-VCAM on the carrier surface (Table 1), with a total added valency similar to that of parent single-targeted NCs. The size, polydispersity, and zeta potential of anti-PECAM/VCAM NCs was also within the range of that observed for parent counterparts and control IgG NCs (Table 1).

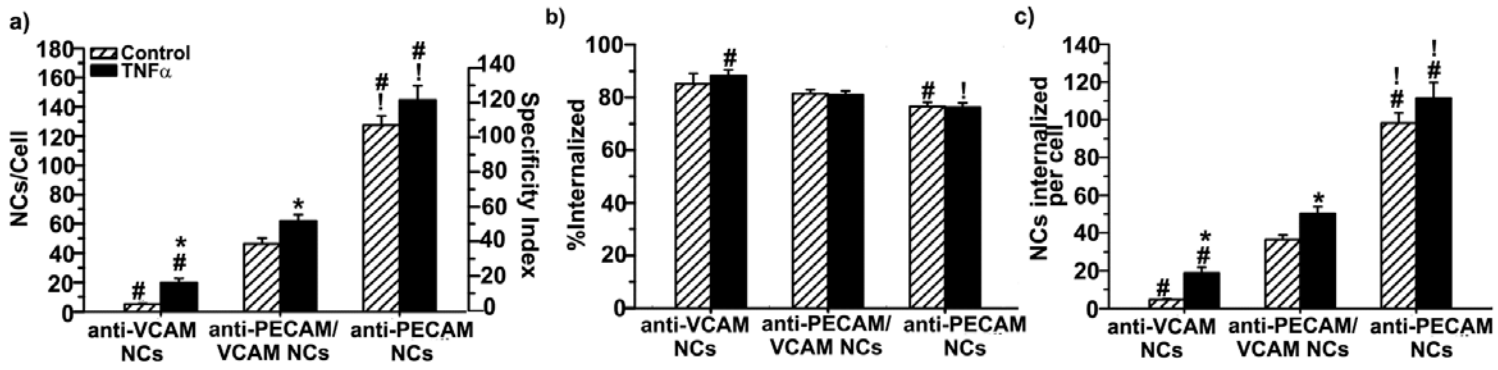

Figure 2. Binding and internalization of nanocarriers targeted to PECAM-1 and/or VCAM-1 in ECs. FITC-labeled nanocarriers were incubated for 1 h at 37°C with control or TNFα-activated H5V cells. Cells were then washed, fixed, and surface-bound nanocarriers where immunostained with a Texas-Red secondary antibody. Internalized carriers appeared green due to single-labeling with FITC, while surface-bound carriers appeared yellow due to FITC + Texas-Red double-labeling. Images were quantified by fluorescence microscopy to determine: (a) the number of nanocarriers per cell and specificity index, (b) the percentage of internalized nanocarriers, and (c) total internalized nanocarriers per cell. Data are mean ± S.E.M. * Compares control vs. TNFα for each formulation, ! compares anti-PECAM NCs to anti-VCAM NCs, # compares single-targeted formulation to dual-targeted counterparts. *, #, ! represents $p < 0.05$; by Student's *t*-test.

Binding of anti-PECAM/VCAM NCs to control ECs was intermediate compared to single-targeted anti-PECAM NCs or anti-VCAM NCs, and this was also the case for activated ECs (Figure 2a). Intermediate binding of anti-PECAM/VCAM NCs differs from the behavior previously reported relative to carriers dual-targeted to selectins and Ig-like CAMs, which synergistically enhanced binding relative to the single-targeted counterparts.[23,181,186] It is difficult to compare these strategies because most particles used in those studies were in the micrometer-size range versus the submicrometer counterparts used here. Yet, in another study E-selectin/ICAM-1 targeting was also shown to synergistically enhance binding of submicrometer liposomes.[184] The intermediate level of binding of anti-PECAM/VCAM NCs could imply attachment only through PECAM-1, since dual-targeted nanocarriers have 50% valency towards the receptor compared to single-targeted nanocarriers. However, binding of anti-PECAM/VCAM NCs increased by ~34% in challenged cells vs. control conditions (Figure 2a). This suggests that dual-targeted nanocarriers attach to both PECAM-1 and VCAM-1 on the cell surface, since only VCAM-1-targeting had shown increased binding of single-targeted nanocarriers to activated cells (Figure 2a). Hence, combination-targeting to PECAM-1/VCAM-1 may offer advantages over single-targeted formulations: it improves binding compared to VCAM-1-targeting and provides reduced attachment to control cells with enhanced binding toward diseased ones, compared to PECAM-1-targeting.

Regarding internalization, anti-PECAM/anti-VCAM NCS were internalized efficiently and the internalization rate was not significantly changed under

pathological stimulation (Figure 2b). Since PECAM-1 and VCAM-1 are associated with CAM-mediated and clathrin-mediated endocytosis, respectively, anti-PECAM/VCAM NCs may be internalized via both pathways and result in intermediate rate of endocytosis compared to single-targeted counterparts. Yet, this remains to be determined. In addition, dual targeting modulated total nanocarrier uptake as the total number of internalized anti-PECAM/VCAM NCs was intermediate with respect to anti-PECAM NCs and anti-VCAM NCs in both control and activated conditions. The high endocytosis rates observed for these formulations implies that, binding (not rate of endocytosis) affects the capacity of anti-PECAM/VCAM NCs to modulate intracellular delivery, and, therefore, tuning targeting plays a key role in optimizing these drug delivery systems.

4.1.4. Binding and endocytosis of antibody-coated nanocarriers dual-targeted to ICAM-1 and PECAM-1

We next tested combination-targeting to ICAM-1 and PECAM-1. These molecules have less different levels of expression compared to the previous combination (still higher for PECAM-1 but less different in control condition and on the same order of magnitude under pathology),[21] and they both utilize the same endocytic pathway (CAM-mediated endocytosis) for nanocarrier uptake.[168] Yet, as in the case of VCAM-1 vs. PECAM-1, these molecules are also located on the cell lumen vs. border, respectively, and are overexpressed vs. unchanged in disease.[21] Anti-ICAM/PECAM NCs had size, polydispersity, zeta-potential, and total valency within the range of all other formulations (Table 1).

Binding of anti-ICAM/PECAM NCs was first compared to anti-ICAM NCs and anti-PECAM NCs and as with the PECAM-1/VCAM-1 combination was found to be intermediate of single-targeted, parental formulations (Figure 3a). However, pathological stimulation with TNFα did not enhance binding of anti-ICAM/PECAM NCs to cells and, as a result, binding was lower than parental formulations which was a different behavior than observed with the PECAM-1/VCAM-1 combination. This is in agreement with previous studies which have described that, although the level of expression and binding of naked anti-ICAM to ECs is markedly increased (~50-100-fold) by pathological activation, the level of binding of anti-ICAM NCs changes only minimally (~2-4-fold). This is believed to be due to the fact that, although naked antibody can potentially interact with every ICAM-1 molecule on the cell surface, steric hindrances posed by bulkier nanocarriers may not allow binding to all available receptors.[205] An analogous result was observed in the case of polymerosomes targeting ICAM-1, which showed similar binding in control versus TNFα conditions.[186] If this is the case, then binding of anti-ICAM/PECAM NCs is expected to respond to activation even less than anti-ICAM NCs, since PECAM-1-targeting contributes to binding of anti-ICAM/PECAM NCs and this counterpart is not responsive to such stimulation.

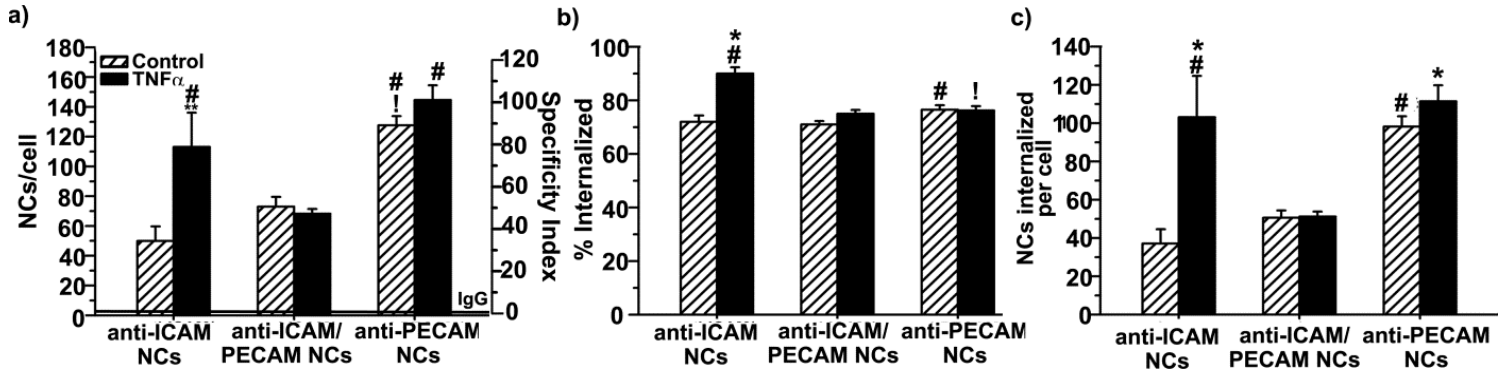

Figure 3. Binding and internalization of nanocarriers targeted to ICAM-1 and/or PECAM-1 in ECs. FITC-labeled nanocarriers were incubated for 1 h at 37°C with control or TNFα-activated H5V cells. Cells were then washed, fixed, and surface-bound nanocarriers where immunostained with a Texas-Red secondary antibody. Internalized carriers appeared green due to single-labeling with FITC, while surface-bound carriers appeared yellow due to FITC + Texas-Red double-labeling. Images were quantified by fluorescence microscopy to determine: (a) the number of nanocarriers per cell and specificity index, (b) the percentage of internalized nanocarriers, and (c) total internalized nanocarriers per cell. Data are mean ± S.E.M. * Compares control vs. TNFα for each formulation, ! compares anti-PECAM NCs to anti-VCAM NCs, # compares single-targeted formulations to dual-targeted counterparts. *,!,# represents $p < 0.05$ by Student's *t*-test.

Contrary to anti-PECAM/VCAM NCs, anti-ICAM/PECAM NCs target two receptors associated to the same endocytic pathway, CAM-endocytosis. In control and TNFα-activated cells anti-ICAM/PECAM NCs maintained high internalization of nanocarriers, as observed for nanocarriers single-targeted to ICAM-1 or PECAM-1 (Figure 3b). Dual binding to ICAM-1 and PECAM-1 did not appear to alter the rate of endocytosis in control condition. However, unlike anti-ICAM NCs the internalization rate of anti-ICAM/PECAM NCs did not change in TNFα-activated ECs (Figure 3b). The total uptake of anti-ICAM/PECAM NCs was intermediate of anti-ICAM NCs and anti-PECAM NCs in control conditions and lower than both parents in TNFα-activated conditions (Figure 3c). This was expected because of the similarly high internalization rate of anti-ICAM/PECAM NCs compared with parental formulations. As a result and in common with anti-PECAM/VCAM NCs, the binding level primarily affected intracellular accumulation rather than differences in induction of endocytosis.

4.1.5. Binding and endocytosis of antibody-coated nanocarriers dual or triple-targeted to ICAM-1, PECAM-1, and/or VCAM-1

We next compared dual targeted formulations with respect to one another and to nanocarriers triple-targeted to ICAM-1, PECAM-1, and VCAM-1 (anti-ICAM/PECAM/VCAM NCs). Binding of anti-ICAM/PECAM NCs was significantly higher than anti-PECAM/VCAM NCs in control ECs (1.6-fold, Figure 4a) and similar in TNFα-activated ECs (0.93-fold, Figure 4a). This result pairs well with greater basal expression of ICAM-1 over VCAM-1[21] and also with greater binding of

anti-ICAM NCs over anti-VCAM NCs as shown in Figure 1a. Therefore, the ICAM-1/PECAM-1 combination displays better targeting to cells, while the PECAM-1/VCAM-1 combination displays somewhat greater selectivity for diseased cells.

For both anti-PECAM/VCAM NCs and anti-ICAM/PECAM NCs, internalization was highly efficient and unaffected by activation of cells with TNFα (Figure 4b). Yet, the rate of endocytosis of anti-ICAM/PECAM NCs was somewhat lower than anti-PECAM/VCAM NCs (statistically significant). This is counterintuitive since both ICAM-1 and PECAM-1 mediate uptake of carriers by the same mechanism, while VCAM-1 and PECAM-1 associate to distinct routes.[168,189] However, it is plausible that simultaneous engagement of two receptors that use the same cell machinery for intracellular transport may result in a competition phenomenon, leading to decreased endocytosis. Germane to this speculation is that sequential stimulation with antibodies to ICAM-1 followed by PECAM-1 has been shown to inhibit ICAM-1-induced signaling in ECs, including RhoA activation and actin cytoskeletal rearrangement.[168,210] The total number of internalized anti-ICAM/PECAM NCs was greater than anti-PECAM/VCAM NCs in control and similar in TNFα-activated ECs (Figure 4c). Therefore, the ICAM-1/PECAM-1 combination performs better in control conditions where expression of ICAM-1 exceeds VCAM-1, but in pathophysiologically activated conditions the difference is diminished due to activation of VCAM-1 expression. Despite these interesting differences the endocytosis rates were high, hence, potential for intracellular delivery rather depended on the level of carrier binding.

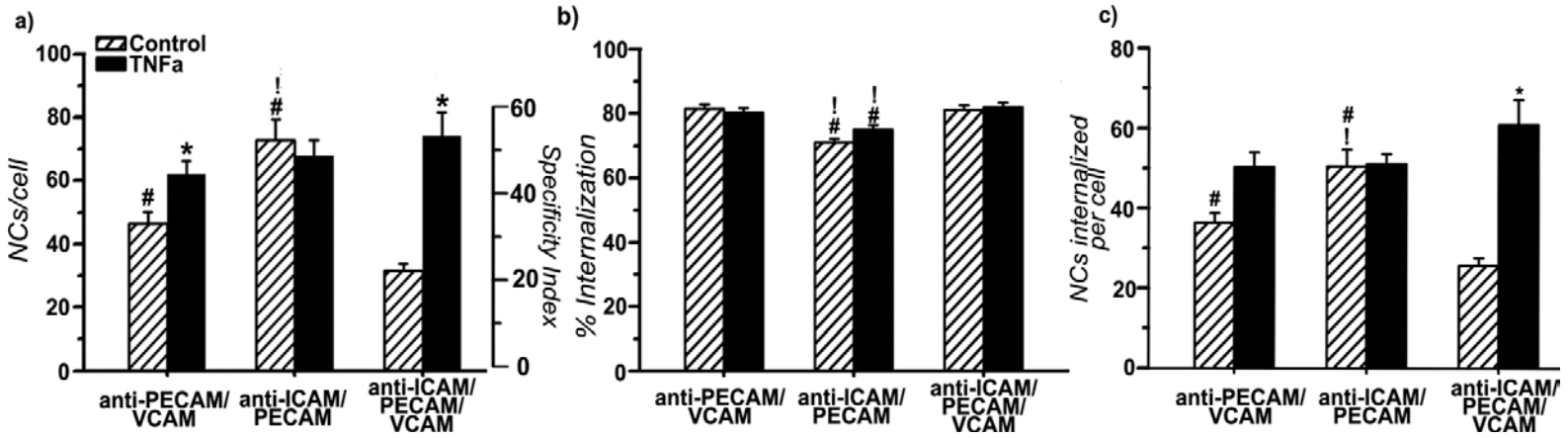

Figure 4. Binding and internalization of nanocarriers dual- or triple-targeted to ICAM-1, PECAM-1, and/or VCAM-1 in ECs. FITC-labeled nanocarriers were incubated for 1 h at 37°C with control or TNFα-activated H5V cells. Cells were then washed, fixed, and surface-bound nanocarriers where immunostained with a Texas-Red secondary antibody. Internalized carriers appeared green due to single-labeling with FITC, while surface-bound carriers appeared yellow due to FITC + Texas-Red double-labeling. Images were quantified by fluorescence microscopy to determine: (a) the number of nanocarriers per cell and specificity index, (b) the percentage of internalized nanocarriers, and (c) total internalized nanocarriers per cell. Data are mean ± S.E.M. * Compares control vs. TNFα for each formulation, ! compares anti-PECAM NCs to anti-VCAM NCs, # compares single-targeted formulation to dual-targeted counterparts. *,#,! represents $p < 0.05$ by Student's *t*-test.

We next tested nanocarriers triple-targeted to ICAM-1, PECAM-1, and VCAM-1 (anti-ICAM/PECAM/VCAM NCs). This is, to the best of our knowledge, the first time that triple-CAM targeting is examined. The size, polydispersity, zeta potential, and total valency of these carriers were similar to that of all other formulations, with equal split of valency between anti-ICAM, anti-PECAM, and anti-VCAM (Table 1).

Under control conditions, binding of triple-CAM targeted nanocarriers to ECs was significantly lower compared to either dual-targeted counterpart, including anti-ICAM/PECAM NCs and anti-PECAM/VCAM NCs (2.3-fold and 1.5-fold lower, respectively; Figure 4a). This is desirable for delivery of therapeutics where it is beneficial to selectively target sites of inflammation. It is possible that lowering the valency of targeting to ICAM-1 and/or PECAM-1 past a certain threshold (as occurred for the valency of triple- vs. dual-targeted counterparts) reduced the binding ability of this formulation, just as the binding capacity provided by anti-VCAM NCs was reduced in control conditions (in accord with expression). Binding of anti-ICAM/PECAM/VCAM NCs markedly increased under pathological stimulation, reaching a comparable level to anti-ICAM/PECAM NCs and beyond anti-PECAM/VCAM NCs (Figure 4a). This suggests that increased expression of ICAM-1 and/or VCAM-1 in TNFα-activated ECs can compensate for the reduced valency of the triple-targeted formulations. Importantly, triple-targeted nanocarriers showed the greatest difference in binding between control and TNFα-activated conditions (2.3-fold, vs. 1.3-fold for anti-PECAM/VCAM NCs or 0.9-fold for anti-ICAM/PECAM

NCs), hence, providing the best selectivity toward disease sites without affecting the total number of bound nanocarriers per cell (Figure 4a). This finding pairs well with selectivity of natural combination-targeting of leukocyte integrins to multiple endothelial CAMs during inflammation.[211]

Furthermore, endocytosis of anti-ICAM/PECAM/VCAM NCs was comparable to anti-PECAM/VCAM NCs and slightly greater than anti-ICAM/PECAM NCs in both control and TNFα-activated ECs (Figure 4b). As in the case of dual-targeted formulations, no change in the endocytic rate of anti-ICAM/PECAM/VCAM NCs was observed when comparing control to disease conditions. This emphasizes the fact that endocytic potential of these formulations does not change regardless of absolute binding, at least for the valency ranges used here. This also suggests that concomitant attachment to VCAM-1 provided by the triple-targeted formulation modestly enhances endocytosis. This is in accord with our previous observation comparing dual-targeted carriers indicating that binding to CAMs associated to different vs. same endocytic route may be beneficial by relaxing the competition for the same cell signaling/machinery involved.

Overall, these results demonstrate that cell binding of nanocarriers functionalized to target multiple CAMs is dependent on the combination of targeted receptors utilized, physiological state of the cells, and dual- vs triple- targeted surface coating of nanocarriers. As per intracellular transport, this is highly efficient regardless of multiplicity of targeting or patho-physiological conditions, and

somewhat endocytic pathway, with only slightly better results when targeting different endocytic mechanisms. Hence, the potential for intracellular delivery of these formulations is mostly controlled by the level of binding of the functionalized carriers.

4.1.6. Biodistribution of antibodies vs. antibody-coated nanocarriers single-targeted to ICAM-1, PECAM-1, or VCAM-1

Differential accumulation of multi-CAM-targeted nanocarriers to cells in culture suggests that this surface functionalization strategy may also modify accumulation in organs *in vivo*. Yet, no previous *in vivo* studies have focused on combination-targeting to multiple Ig-like CAMs (vs. selectins with Ig-like CAMs) involving nanocarriers (vs. micro-scale counterparts). Multi-CAM-targeted materials previously examined *in vivo* include microbubbles targeted to $\alpha_v\beta_3$-integrin/P-selectin/vascular endothelial growth factor receptor 2, which enhanced imaging intensity of MDA-MB-231 tumors in mice.[212] Also, P-selectin/ICAM-1 targeting enhanced adhesion of iron-oxide microparticles to aortic endothelium in atherosclerosis model mice,[12] or fluorescent microparticles to retinal and choroidal vessels in rats exposed to lipopolysaccharide.[182] In addition, one cannot extrapolate the *in vivo* outcome based on results obtained in cell culture.[206]

To confirm and comparatively assess targeting of anti-ICAM, anti-PECAM, and anti-VCAM *in vivo*, we first injected these antibodies as naked targeting moieties. We focused on brain, lungs, and liver (Figure 5) as examples of central nervous

system, peripheral, and clearance organs, respectively, and comprehensive data on the biodistribution of these formulations in all organs examined are presented in Table 2. Of the three targeting antibodies, anti-PECAM displayed highest accumulation and specificity (over IgG) in brain, lungs, liver, and other organs (Figure 5 a,b and Table 2), which was expected because of much higher levels of PECAM-1 (highest) vs. ICAM-1 (intermediate) or VCAM-1 (lowest) expression in endothelium.[21] Also in agreement with relative levels of expression, anti-ICAM and anti-PECAM displayed higher accumulation and specificity than anti-VCAM in the lungs and liver (Figure 5 a,b), as well as other organs (Table 2). Only PECAM-1-targeting showed specificity in the brain (Figure 5 a,b), as anti-ICAM and anti-VCAM both had SI values near to 1. Higher brain specificity of anti-PECAM vs anti-ICAM appears affected by factors beyond expression, as expression levels of PECAM-1 vs. ICAM-1 in brain has been reported to be fairly comparable (~0.05 vs 0.06 mg antibody/g tissue in [213]).

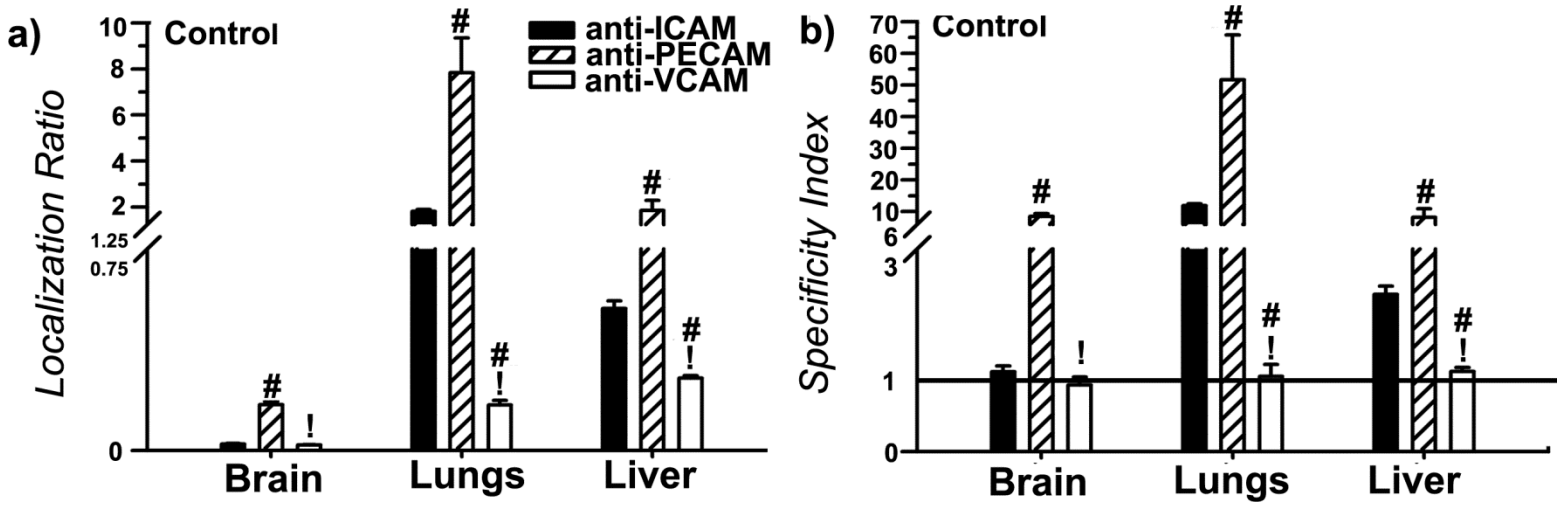

Figure 5. Biodistribution of antibodies targeted to ICAM-1, PECAM-1, or VCAM-1 in control mice. Mice were injected intravenously with ^{125}I-labeled anti-ICAM, anti-PECAM, or anti-VCAM, and blood and organs were harvested at 30 min after injection. (a) The organ-to-blood localization ratio (LR) and (b) the targeted-to-untargeted specificity index (SI) over control IgG are shown for the brain, lungs, and liver (see Methods for details). Data are mean ± S.E.M. ! Compares anti-PECAM to anti-VCAM; # compares each these formulation to anti-ICAM. #,! represents $p < 0.05$ by Student's *t*-test.

We next compared the biodistribution of nanocarriers single-targeted to ICAM-1, PECAM-1, or VCAM-1 after intravenous injection in control mice (Figure 6, Table 2). The greatest accumulation of anti-ICAM NCs was in the lungs (LR ~33), followed by the spleen (LR ~20), and the liver (LR ~11). Anti-PECAM NCs accumulated preferentially in the spleen (LR ~25), followed by the lungs (LR ~16), and the liver (LR ~7). Finally, anti-VCAM NCs were highest in the spleen (LR ~40), followed by the liver (LR ~24) and the lungs (LR ~4). Hence, the biodistribution of all three carriers differed (Figure 6a, Table 2).

Accumulation of anti-ICAM NCs was highly specific in lungs and brain, as evidenced by 17.8-fold and 3.2-fold higher LR of anti-ICAM NCs relative to IgG NCs, respectively (SI, Figure 6b), while less specificity was observed in other organs (Figure 6b, Table 2). Anti-PECAM NCs had the greatest specificity in the lungs (SI ~8.8), followed by heart (~2.5), brain and kidney (SI ~2.1), and lower specificity for other organs (Figure 6b, Table 2). In contrast, anti-VCAM NCs had greatest specificity in brain (~4.6), followed by kidney (3.0), and spleen (2.6) with lower specificity in other organs (Figure 6b, Table 2).

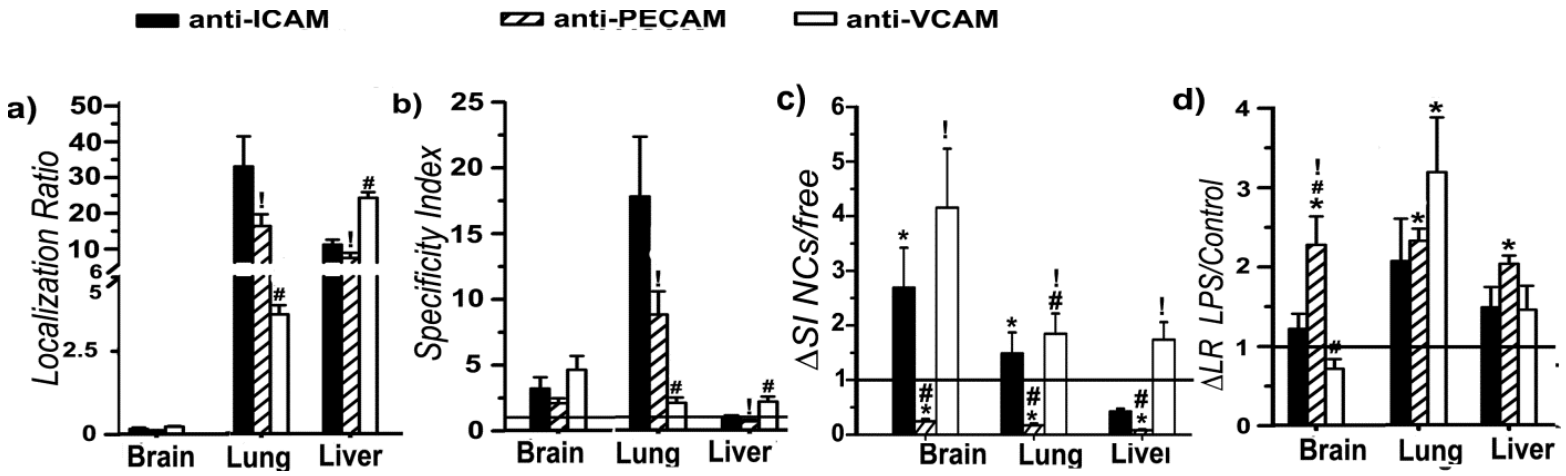

Figure 6. Biodistribution of nanocarriers single-targeted to ICAM-1, PECAM-1, or VCAM-1 in control mice versus lipolysaccharide (LPS)-treated mice. Mice were injected intravenously with ^{125}I-labeled anti-ICAM NCs, anti-PECAM NCs, or anti-VCAM NCs, and blood and organs were harvested at 30 min after injection. LR (a) and SI (b) are shown for the brain, lungs, and liver. (c) shows the fold-change in SI when utilizing a targeting antibody versus antibody-coated nanocarriers (ΔSI). (d) Shows the fold-change in LR as a result of LPS challenge (ΔLR). Data are mean ± S.E.M. ! Compares anti-PECAM NCs to anti-VCAM NCs; # compares each these formulation to anti-ICAM NCs; * compares each formulation in control versus mice treated with LPS. *,#,! represents $p < 0.05$ by Student's *t*-test.

These results are partially in agreement with cell culture data. For instance, a good example reflective of endothelial targeting *in vivo* is the lungs. This is because the pulmonary vasculature constitutes approximately 20-30% of the total endothelial surface area in the body, is exposed to relatively low shear stress, and receives the full cardiac output.[8] In agreement with binding data in cell cultures (Figure 1b), LR and SI of anti-VCAM NCs were lower in this organ compared to anti-ICAM NCs and anti-PECAM NCs. Yet, in contrast to cell culture, pulmonary accumulation and specificity of anti-ICAM NCs were higher compared to anti-PECAM NCs, whereas anti-PECAM counterparts displayed greater binding to cells (2.6-fold; Figure 1b). It is possible that higher ICAM-1 expression *in vivo* versus in cell cultures and/or reduced access to PECAM-1 located in the cell-cell borders[21] due to a tighter endothelium *in vivo* may account for this difference. Indeed, PECAM-1 expression is more restricted to the cell-cell border region in ECs exposed to flow conditions (reflective of the *in vivo* situation) than in static cultures.[16]

Targeting each molecule with antibodies versus antibody-coated nanocarriers greatly and differentially affected organ specificity. Targeting ICAM-1 or VCAM-1 in nanocarrier format enhanced specificity in all organs with the greatest improvement observed in brain (Figure 6c, Table 2). Relatively greater improvement in nanocarrier format was observed for anti-VCAM NCs over anti-ICAM NCs, perhaps because anti-ICAM targeted organs better than anti-VCAM (Figure 5b). On the other hand, specificity declined in all organs for targeted nanocarriers versus free antibody addressed to PECAM-1 (Figure 6c, Table 2). This was somewhat expected

due to high magnitude of targeting observed for anti-PECAM, likely because of much higher PECAM-1 expression, and perhaps also due to steric hindrance effects associated with targeting PECAM-1 at cell borders with relatively bulkier nanocarriers.

With regard to mice challenged to mimic a pathological situation (LPS-treated mice), we observed enhanced accumulation over control mice although at different extent and patterns comparing anti-ICAM NCs, anti-PECAM NCs, and anti-VCAM NCs (Figure 6d). Accumulation of anti-ICAM NCs was enhanced in all organs except the brain, with similar improvement in the spleen, heart, and lungs (ΔLR ~2.4, 2.2, 2.1, respectively; Figure 6c, Table 2). For anti-PECAM NCs, all organs displayed enhanced accumulation except for the spleen, with greatest improvement in the lungs, brain, and kidneys (ΔLR ~2.3, 2.3, 2.0). The only enhancement in accumulation observed for anti-VCAM NCs was in the lungs (ΔLR ~3.2). This result was somewhat unexpected, e.g., PECAM-1 expression is rather unaffected by inflammatory mediators, while ICAM-1 and VCAM-1 are markedly enhanced.[21] The biodistribution pattern of anti-ICAM NCs reflected this, but this was not the case for anti-VCAM NCs, except for the lungs. It is possible that the greater accumulation differences observed in control lungs between anti-VCAM NCs vs. ICAM-1- or PECAM-1-targeted counterparts allowed detection of the corresponding enhancement under the inflammatory condition. In the case of anti-PECAM NCs, possible redistribution of PECAM-1 from intercellular junctions to the luminal surface in diseased mice (as shown in other models)[214] may have increased accessibility of PECAM-1 relative to control mice.

Table 2. Biodistribution of anti-CAM-targeted antibodies and single-targeted nanocarriers

Ab or NC	Blood	Kidney		Heart		Spleen		Lungs		Liver		Brain	
	%ID	LR	SI	LR	SI	LR	SI	LR	SI	LR	SI	LR	SI
Antibody:													
Anti-ICAM	47±2.7	0.6±0.02	2.2±0.1	0.2±0.02	2.0±0.2	0.6±0.04	4.3±0.3	1.8±0.1	12±0.6	0.5±0.03	2.3±0.1	0.02±0.002	1.2±0.1
Anti-PECAM	11±1.1	2.5±0.3	9.5±1.6	1.9±0.2	18±2.5	3.8±0.1	25±0.9	7.8±1.5	52±14	1.9±0.43	8.2±2.7	0.17±0.01	8.5±0.9
Anti-VCAM	61±0.4	0.3±0.01	1.3±0.04	0.1±0.01	1.2±0.1	0.7±0.02	4.5±0.2	0.2±0.02	1.1±0.2	0.3±0.01	1.2±0.1	0.02±0.002	1.0±0.1
Nanocarrier:													
Anti-ICAM NCs	6.1±1.3	1.3±0.2	2.7±0.5	0.8±0.2	2.1±0.4	20±4.5	1.3±0.3	32±8.4	18±4.6	11±1.38	1.0±0.1	0.16±0.04	3.2±0.9
Anti-ICAM NCs (LPS+)	3.3±0.6	1.9±0.5	2.3±0.6	1.7±0.4	3.5±0.8	48±11	1.4±0.3	68±17	15±3.9	16±2.80	0.7±0.1	0.20±0.03	1.4±0.2
Anti-PECAM NCs	6.6±0.7	1.0±0.1	2.1±0.2	0.9±0.2	2.5±0.6	25±5.4	1.6±0.4	16±3.3	88±1.8	7.3±1.42	0.7±0.1	0.10±0.02	2.1±0.4
Anti-PECAM NCs (LPS+)	3.5±0.3	2.0±0.3	2.4±0.4	1.5±0.3	3.1±0.6	29±9.6	0.9±0.2	38±3.5	8.4±0.6	15±1.05	0.7±0.03	0.24±0.05	1.7±0.3
Anti-VCAM NCs	3.5±0.6	1.4±0.3	3.0±0.5	0.7±0.1	2.0±0.4	40±2.2	2.6±0.3	3.8±0.3	2.1±0.4	24±1.61	2.2±0.4	0.23±0.02	4.6±1.1
Anti-VCAM NCs (LPS+)	2.0±0.2	1.7±0.3	2.0±0.3	1.1±0.2	2.0±0.3	71±12	2.4±0.5	11±2.6	3.1±0.6	48±7.24	2.9±0.6	0.20±0.03	1.4±0.2

Data are Mean ± S.E.M. %ID = perentage of injected dose; Ab = antibody; NC = nanocarrier; LPS = lipopolysaccharide; LR = localization ratio; SI = specificity index. Anti-ICAM was clone YN1, anti-PECAM was clone MEC13, and anti-VCAM was clone MK2.

4.1.7. Biodistribution of antibody-coated nanocarriers dual- or triple-targeted to ICAM-1, PECAM-1, and/or VCAM-1

We next tested *in vivo* biodistribution and specificity of nanocarriers displaying surface coatings for dual- or triple-CAM targeting (Figure 7). In the spleen and liver, the level of accumulation (LR ~16-21 and 9-10, respectively; Figure 7a and Table 3) and lack of specificity over control IgG NCs (SI ~1; Figure 7b and Table 3) for all three combinations tested (anti-ICAM/PECAM NCs, anti-PECAM/VCAM NCs, and anti-ICAM/PECAM/VCAM NCs) was similar to that of parent anti-ICAM NCs and anti-PECAM NCs, and markedly reduced compared to anti-VCAM NCs. Hence, multi-targeting nanocarriers to ICAM-1 and/or PECAM-1 ruled accumulation and resulted in avoidance of these organs relative to VCAM-1, which likely occurred primarily via RES-mediated clearance (not targeting the endothelium in these tissues) as compared to control IgG NCs.

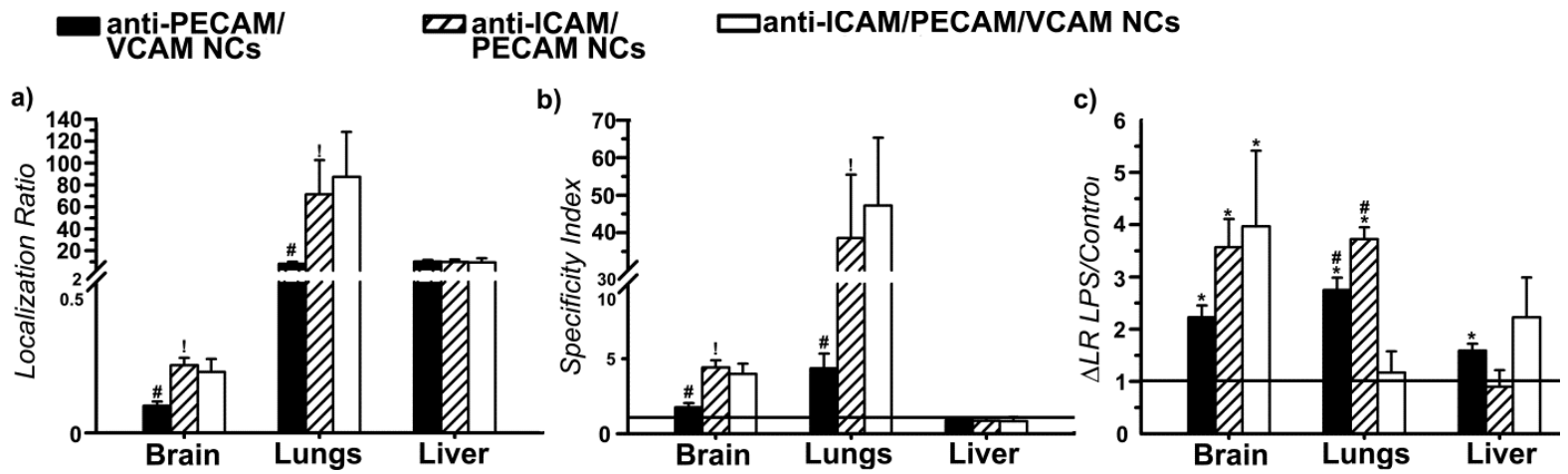

Figure 7. Biodistribution of nanocarriers dual- or triple-targeted to ICAM-1, PECAM-1, and/or VCAM-1 in control mice versus LPS-treated mice. Mice were injected intravenously with ^{125}I-labeled anti-PECAM/VCAM NCs, anti-ICAM/PECAM NCs, or anti-ICAM/PECAM/VCAM NCs, and blood and organs were harvested at 30 min after injection. (a) The organ-to-blood localization ratio (LR) and (b) specificity index (SI) over control IgG NCs are shown for the brain, lungs, and liver. (c) Effect of LPS challenge on the biodistribution expressed as the fold-change in LR (ΔLR). Data are mean ± S.E.M. ! compares anti-ICAM/PECAM NCs to anti-PECAM/VCAM NCs; # compares dual-targeted formulations to the triple-targeted counterpart. * Compares each formulation in control versus mice treated with LPS. #,! represents $p < 0.05$ by Student's *t*-test.

Table 3. Biodistribution of multi-CAM-targeted nanocarriers

Nanocarrier	Blood	Kidney		Heart		Spleen		Lungs		Liver		Brain	
Dual:	%ID	LR	SI	LR	SI	LR	SI	LR	SI	LR	SI	LR	SI
Anti-PECAM/ VCAM NCs	6.2±0.5	0.8±0.1	1.7±0.2	0.5±0.1	1.4±0.3	21±4.5	1.4±0.3	8.1±1.8	4.4±1.0	10±1.4	0.9±0.1	0.1±0.0	1.8±0.3
Anti-PECAM/ VCAM (+LPS)	3.6±0.1	1.2±0.1	1.5±0.1	0.8±0.0	1.8±0.1	26±3.1	0.8±0.1	22±1.9	4.9±0.4	16±1.3	0.7±0.1	0.2±0.0	1.4±0.1
Anti-ICAM/ PECAM NCs	5.2±1.0	1.3±0.2	2.7±0.5	1.8±0.3	4.9±0.7	16±4.9	1.1±0.3	71±32	39±17.0	9.7±2.4	0.9±0.2	0.2±0.0	4.4±0.5
Anti-ICAM/PECAM NCs (+LPS)	2.2±0.3	4.0±0.8	4.8±1.0	4.5±0.2	9.4±0.4	16±1.8	0.5±0.1	266±16	59±3.6	8.7±3.0	0.4±0.1	0.8±0.1	5.6±0.9
Triple:													
Anti-ICAM/PECAM/ VCAM NCs	4.5±0.8	1.6±0.5	3.3±1.0	1.8±0.2	4.8±0.4	19±3.9	1.2±0.2	87±34	47±18	9.3±3.2	0.8±0.3	0.2±0.0	4.0±0.7
Anti-ICAM/PECAM/ VCAM NCs (+LPS)	2.4±0.8	3.7±1.4	4.4±1.7	4.1±1.8	8.6±3.7	73±34	2.2±1.0	102±36	23±7.9	21±7.1	0.9±0.3	0.8±0.3	5.6±2.1
Anti-ICAM/PECAM/ VCAM/ASM NCs	5.1±0.4	1.5±0.3	3.6±0.9	1.1±0.0	6.4±0.2	23±3.8	50±10	10±2.0	31±7.6	15±2.4	13±2.4	0.2±0.1	6.4±1.6
Anti-ICAM/PECAM/ VCAM/ASM NCs (+LPS)	2.0±0.2	4.2±0.3	10±0.8	2.7±0.7	15±3.9	81±31	242±93	30±3.3	115±12	36±3.0	64±5.4	0.5±0.0	9.5±0.7

Data are Mean±S.E.M.. %ID = percentage of injected dose; LR = Localization Ratio; SI = Specificity Index; NCs= Nanocarriers.

Anti-ICAM was clone YN1, anti-PECAM was clone MEC13, and anti-VCAM was clone MK2.

In the lungs of control mice, the accumulation and specificity of dual-targeted anti-ICAM/PECAM NCs was significantly increased with respect to single-targeted counterparts: LR (and SI as well) was enhanced ~2.2-fold compared to anti-ICAM NCs and 4.4-fold compared to anti-PECAM NCs. This was also the case for triple-targeted nanocarriers, which had slightly higher (22.4%, not significant by *t*-test) accumulation and specificity than anti-ICAM/PECAM formulations. Anti-PECAM/VCAM NCs showed intermediate pulmonary accumulation and specificity compared to single-targeted counterparts. Intermediate targeting by anti-PECAM/VCAM NCs as compared to parent counterparts and enhanced targeting of anti-ICAM/PECAM NCs over anti-PECAM/VCAM NCs closely matched observations made in cell culture under control conditions. Yet, enhanced lung targeting of the triple-targeted formulation is opposite to cell culture results. As discussed above, this outcome is possibly due to higher expression of pulmonary ICAM-1 *in vivo*.[8,204]

With regard to other organs, the biodistribution and specificity patterns also varied. In general, targeting to VCAM-1 lowered performance of the dual-targeted combination, but not that of triple-targeted nanocarriers (Figure 7a-b, Table 3). In the heart, anti-ICAM/PECAM NCs displayed synergy in that accumulation in this organ was considerably better than its single-targeted counterparts, and with similar values to triple-targeted formulations (Figure 7 a-b, Table 2-3). In comparison, anti-PECAM/VCAM NCs showed reduced heart accumulation and specificity, which was similar to anti-VCAM NC results and lower than anti-PECAM NCs. In the kidneys,

anti-ICAM/PECAM NCs acted similarly to its single-targeted counterparts, anti-PECAM/VCAM NCs showed decreased performance, and triple-targeted nanocarriers improved accumulation and specificity over PECAM-1/VCAM-1, but only slightly (not statistically significant) over ICAM-1/PECAM-1-targeted formulations. In the brain, anti-ICAM/PECAM NCs outperformed PECAM-1 and was similar to ICAM-1 single-targeted counterparts. Triple-targeted nanocarriers did not further improve this enhancement, and anti-PECAM/VCAM formulations behaved similarly to anti-PECAM NCs and anti-VCAM NCs. Hence, overall, anti-ICAM/PECAM NCs performed better than anti-PECAM/VCAM NCs, as with binding in cell cultures. Triple-targeted formulations performed closely but somewhat better than anti-ICAM/PECAM NCs, which seems to reflect the advantage of engaging multiple CAMs used by leukocytes.[211]

In LPS-challenged mice, all dual- or triple-targeted combinations enabled specific targeting to the kidneys, heart, lung, and brain, as compared to IgG NCs, while showing similar accumulation to this control in liver and spleen (Figure 7c and Table 3). On top of the already high accumulation in control mice, anti-ICAM/PECAM NCs displayed even greater accumulation in LPS-treated mice in the kidneys, heart, lungs, and brain, with the greatest improvements shown for the last two organs (3.7-fold and 3.6-fold enhancement, respectively; Figure 7c and Table 3). Anti-PECAM/VCAM NCs showed enhanced accumulation in LPS-activated vs. control mice for the kidneys, heart, lungs, liver, and brain, with most acute improvements also in the lungs and brain (2.7-fold and 2.2-fold increase,

respectively). In general, these results complement well the observation that single-targeted nanocarriers seemed to respond to inflammatory stimulation *in vivo*, except for the case of anti-VCAM NCs which only showed enhancement by LPS in the lungs. Combining targeting to VCAM-1 with targeting to other CAMs seems to overcome this caveat and provides for enhanced accumulation in other organs.

Triple-targeted nanocarriers also showed enhanced accumulation in all organs under pathological stimulation except for the lungs, with greatest enhancement in the brain and spleen (4.0-fold and 3.9-fold increase), followed by the kidneys and heart (2.3-fold and 2.3-fold increase). This result was unexpected, since the lungs represent the major targeting organ for single-targeted ICAM-1 or PECAM-1 and considerable specific accumulation also occurs with single-targeted VCAM-1 formulations (Figure 6a,b and Table 2). Also, enhancement under LPS-treatment was observed in this organ for both dual-targeted carriers (Figure 7c). However, triple-targeted nanocarriers had shown the highest targeting in the lungs of control mice (Fig. 7a). Hence, it is possible that this is already a saturating level of targeting and no further enhancement can be achieved with carriers displaying this valency and concentration.

4.1.8. Biodistribution of a therapeutic cargo by triple-CAM-targeted nanocarriers

Overall our data show that, with certain differences with regard of organ distribution, dual- and triple-targeted formulations enhanced accumulation and specificity of nanocarriers in the body under both physiological and pathophysiological contexts. Under disease-like conditions, triple-targeted formulations performed closely but

somewhat better than anti-ICAM/PECAM NCs and clearly superior than anti-PECAM/VCAM counterparts. Hence, we selected the triple-targeted formulation to investigate its potential to improve the biodistribution of a therapeutic cargo in the body.

As an example, we aimed at delivering recombinant acid sphingomyelinase (ASM) using the triple-targeted formulation. ASM is a lysosomal enzyme deficient in genetic Niemann-Pick disease type A-B (Type A OMIM # 257200, Type B OMIM # 607616), which is being explored for enzyme replacement therapy via i.v. injection of the naked recombinant enzyme.[203,215] ASM delivery is necessary throughout the body and predominantly in the lungs, brain, and reticulo-endothelial system (liver and spleen), which are most severely affected in this disease.[5,215] This syndrome also associates with inflammation, making CAMs adequate targets for this intervention.[215]

We labeled ASM with ^{125}I to track the biodistribution of this cargo coupled to anti-ICAM/PECAM/VCAM NCs vs. a similar dose of naked ASM intravenously injected in mice (Figure 8 and Table 3). Triple-targeted nanocarriers drove accumulation of ASM in all organs tested, with greatest LR in the spleen and liver, and lowest LR in the brain (Figure 8a and Table 3). Still, this represented a very marked enhancement in ASM delivery by nanocarriers over the naked enzyme (SI) for all organs tested, including those where LR was relatively low such as the brain, where nanocarriers outperformed the naked enzyme by 6.4-fold (Figure 8b and Table 3). Specific, enhanced delivery by nanocarriers in other organs included 3.6-fold for

kidney, 49.9-fold for spleen, 6.4-fold for heart, 30.9-fold for lungs, and 12.7 for liver (Figure 8b and Table 3). ASM delivery by anti-ICAM/PECAM/VCAM/ASM NCs improved considerably in all organs of LPS-challenged mice, although improvement in spleen was not statistically significant (Figure 8a and Table 3). As a result, delivery specificity of ASM by nanocarriers over naked enzyme improved by 10.2-fold in kidneys, 242-fold in spleen, 15.3-fold in heart, 115-fold in lungs, 63.8-fold in liver, and 9.5-fold in brain (Figure 8b and Table 3). Therefore, this strategy seems beneficial to improve ASM biodistribution in the body, particularly under pathological conditions (as intended for therapeutic intervention).

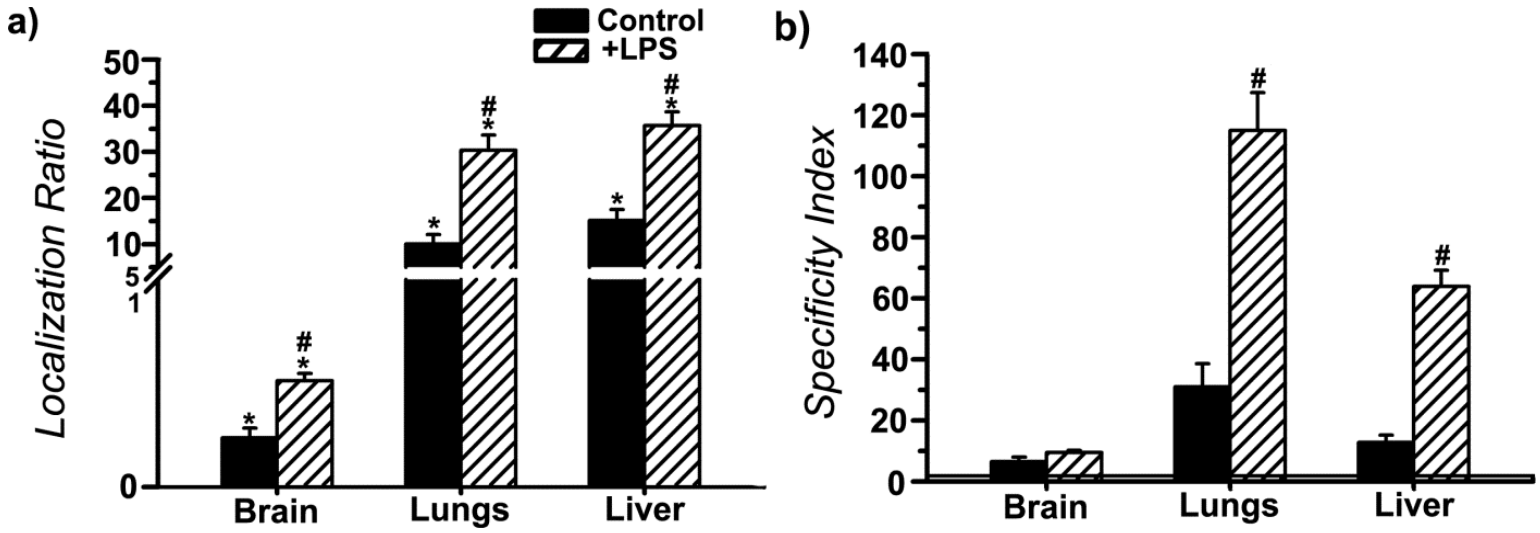

Figure 8. ASM delivery by nanocarriers triple-targeted to ICAM-1, PECAM-1, and VCAM-1 in control versus LPS-treated mice. Mice were injected intravenously with anti-ICAM/PECAM/VCAM/^{125}I- ASM NCs, and blood and organs were harvested at 30 min after injection. (a) The organ-to-blood localization ratio (LR) and (b) specificity index (SI) over non-targeted naked ASM are shown for the brain, lungs, and liver. Data are mean ± S.E.M. * Compares naked enzyme vs. enzyme coupled to anti-ICAM/PECAM/VCAM NCs; # compares control vs. LPS-challenged mice. *,# represents $p < 0.05$ by Student's *t*-test.

Enhanced delivery of ASM by nanocarriers triple-targeted to ICAM-1, PECAM-1, and VCAM-1 emphasizes the potential of combination-targeting in drug delivery and pairs well with other studies reported in the literature. For instance, triple-targeting has been explored in the context of cancer, where microbubbles targeted to $\alpha_v\beta_3$-integrin, P-selectin, and vascular endothelial growth factor receptor 2 showed enhanced cellular binding *in vitro* and imaging intensity of tumors *in vivo*.[212] In addition, triple-targeting of tumor endothelial marker 7, folate receptor, and PECAM-1 has been investigated as a strategy to enhance uptake of mesoporous nanoparticles in both cancer cells and angiogenic blood vessels.[7]

4.1.9. Conclusions

Targeting nanocarriers to multiple receptors with similar function (e.g. leukocyte adhesion and extravasation) can provide advantages for drug delivery, such as synergistically enhancing cell binding of nanocarriers targeted to a selectin and an Ig-like CAM as shown in the literature.[12,23,30] In addition, our findings demonstrate that targeting nanocarriers to multiple Ig-like CAMs modulates delivery performance relative to single-targeted counterparts in a manner which depended on the combination and multiplicity of affinity moieties functionalized on the surface of nanocarriers, and the physiological state of cells and tissues. PECAM-1/VCAM-1 targeting improved cellular binding compared to VCAM-1-targeting and slightly increased the selectivity toward diseased vs. control cells compared to PECAM-1-targeting. Anti-ICAM/PECAM NCs provided greater binding than anti-PECAM/VCAM counterparts, yet were less selective for diseased vs. control cells. Triple-targeted nanocarriers appeared promising as they bound activated ECs

similarly to anti-ICAM/PECAM NCs, yet displayed superior selectivity over either dual-targeted combination. Targeting receptors associated with different endocytosis pathways (VCAM-1/PECAM-1) appeared to enhance nanocarrier internalization over targeting receptors associated with the same endocytic pathway (ICAM-1//PECAM-1). Nevertheless, intracellular transport was highly efficient for all conditions tested. Hence, the potential for intracellular delivery of these formulations is mostly controlled by the level of binding of the functionalized carriers. As in cell culture, enhanced targeting of anti-ICAM/PECAM NCs vs. anti-PECAM/VCAM NCs was also observed *in vivo*. Specific targeting of both dual-targeted combinations improved further in diseased conditions, suggesting that they can be utilized to enhance delivery to sites of disease. Triple-targeted nanocarriers outperformed both double-targeted counterparts, greatly enhanced delivery of therapeutic cargo, and showed selectivity in certain organs for disease vs. control conditions *in vivo*, which pairs well with natural selectivity of leukocyte integrins engaged in endothelial binding through multi-CAM interactions during inflammation.[211] Multi-CAM-targeting is a promising example of the potential that combination-targeting strategies hold in the context of development of functionalized nanocarriers for prophylactic, diagnostic or therapeutic applications.

4.2. Combination targeting to multiple receptors with different functions

4.2.1. Introduction

Targeting nanocarriers to multiple receptors with different roles in cellular processes (e.g. cell functions) may modulate targeting performance in a distinct manner than targeting multiple receptors with similar functions. As discussed in the background, this approach is an emerging strategy for drug delivery. However, most prior strategies aimed at targeting receptors involved in similar endocytic transport pathways, particularly regulated via clathrin-coated pits.[13,194,195,216] For example, binding to cancer cells of liposomes loaded with the anti-cancer drug doxorubicin was enhanced by combination targeting of transferrin receptor and glucose transporter.[194] In addition, pegylated liposomes targeted to transferrin receptor and insulin receptor were shown to enable sequential targeting and transport across the blood-brain and blood-tumor barriers.[13] Only in a couple of examples, the receptors targeted were associated with different endocytic mechanisms, yet these studies did not assess targeting *in vivo* and also involved dual targeting of receptors of similar function (e.g. cell growth: folate receptor/glucose transporter and folate receptor/epidermal growth factor receptor).[14,217]

We selected TfR and ICAM-1 to test the hypothesis that targeting multiple receptors of unrelated function, regulation, and endocytic mechanism can modify the binding, internalization, or biodistribution of polymer nanocarriers. TfR is a transmembrane glycoprotein expressed on the surface of many cells, including endothelium, and its expression remains relatively stable in disease conditions.[6,218]

TfR enables iron transport across cellular barriers via transcytosis (e.g. in the BBB) and into cells by clathrin-mediated endocytosis.[219-221] ICAM-1 is also a transmembrane glycoprotein expressed on the cell surface of ECs and most other cell types, has inducible expression upon activation by inflammatory mediators, and is associated with CAM-mediated endocytic transport which enables transport into cells and across cell barriers.[200,222] Importantly, combination targeting of ICAM-1 and TfR may be affected by different valency and size requirements of these receptors for binding and endocytosis. However, the targeting performance of these receptors has not been assessed comparatively.

4.2.2. Binding of antibodies vs. antibody-coated nanocarriers or micron-sized carriers targeted to ICAM-1 or TfR

To test the impact of the different characteristics of ICAM-1 and TfR on their drug targeting performances, we first compared binding of antibodies targeted to ICAM-1 versus TfR in cell cultures. This was assessed using HUVECs in control or disease conditions (TNFα-activation). Fluorescence microscopy analysis showed similar antibody binding under control conditions (Figure 9a). However, in agreement with ICAM-1 overexpression in disease,[200,223] binding increased markedly in ECs pre-treated with TNFα (15-fold), whereas TfR-binding increased very modestly (1.6-fold). Consequently, bound anti-ICAM greatly exceeded (by 9.6-fold) anti-TfR under pathological stimulation, suggesting that addressing ICAM-1 enhances binding of antibodies to sites of disease.

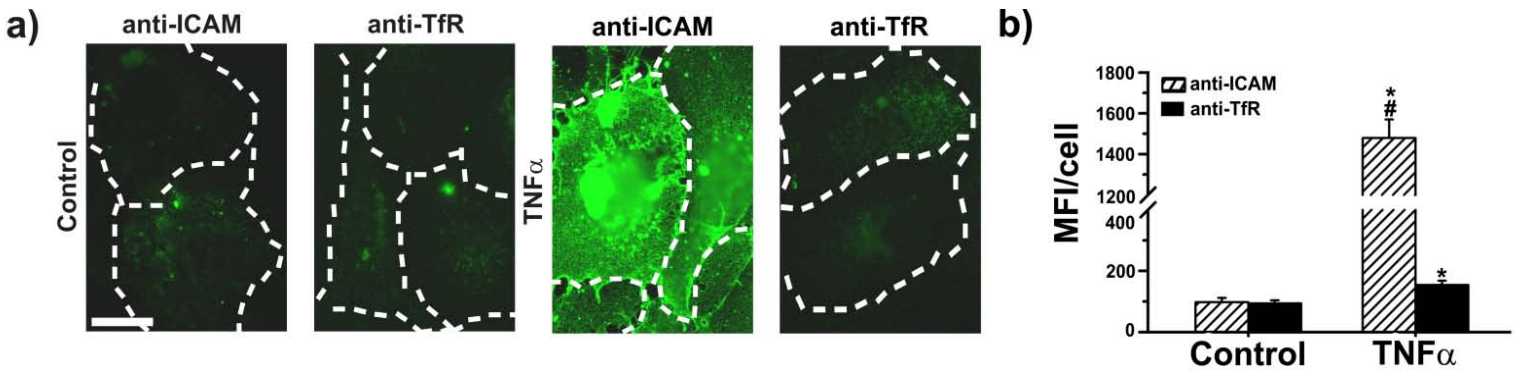

Figure 9. Fluorescence microscopy of antibody binding to ICAM-1 vs. TfR on ECs. **(**a-b) Control or TNFα-activated HUVECs were incubated with anti-ICAM or anti-TfR for 15 min at 37^{o}C. Cells were washed to remove unbound antibody, fixed, stained with FITC-conjugated goat anti-mouse IgG, and analyzed by fluorescent microscopy to determine the mean fluorescent intensity per cell. Phase-contrast images were used to delimit cell borders (dashed lines). Scale bar is ~10 μm. Data are mean±S.E.M. * compares control vs. TNFα for each target and # compares ICAM-1 vs. TfR for each condition. *,# represents $p < 0.05$ by Student's *t*-test.

We next compared binding of antibody-coated carriers targeting ICAM-1 versus TfR (Table 4). Anti-ICAM NCs and anti-TfR NCs displayed similar size (~250 nm), polydispersity (~0.180), zeta potential (~−9 mV), and valency (~275–300 antibodies/carrier particle).

Table 4. Characterization of single-targeted nanocarriers directed to ICAM-1 and TfR

Nanocarrier coating	Size (nm)	PDI	Zeta potential (mv)	Coating valency (Ab/NC)
Anti-ICAM NCs	262±8.6	0.18±0.01	-9.7±0.7	273±37
Anti-TfR NCs	242±7.1	0.18±0.01	-8.7±0.8	300±31

Data are mean ± S.E.M. Ab = antibodies; NC = nanocarrier; PDI = polydispersity; Anti-ICAM was clone R6.5 and anti-TfR was clone T56/14.

Despite similar antibody binding under control conditions, anti-ICAM carriers displayed two-fold enhanced binding to ECs compared with anti-TfR carriers (Figure 10). For activated ECs, binding of anti-ICAM carriers was enhanced further compared to anti-TfR carriers (17.4-fold, Figure 10). Hence, ICAM-1-targeted carriers enhanced binding by eight-fold in TNFα-activated conditions, whereas binding of TfR-targeted carriers was unchanged compared to control conditions, suggesting that targeting nanocarriers to ICAM-1 enhances the binding over TfR in both control and disease conditions.

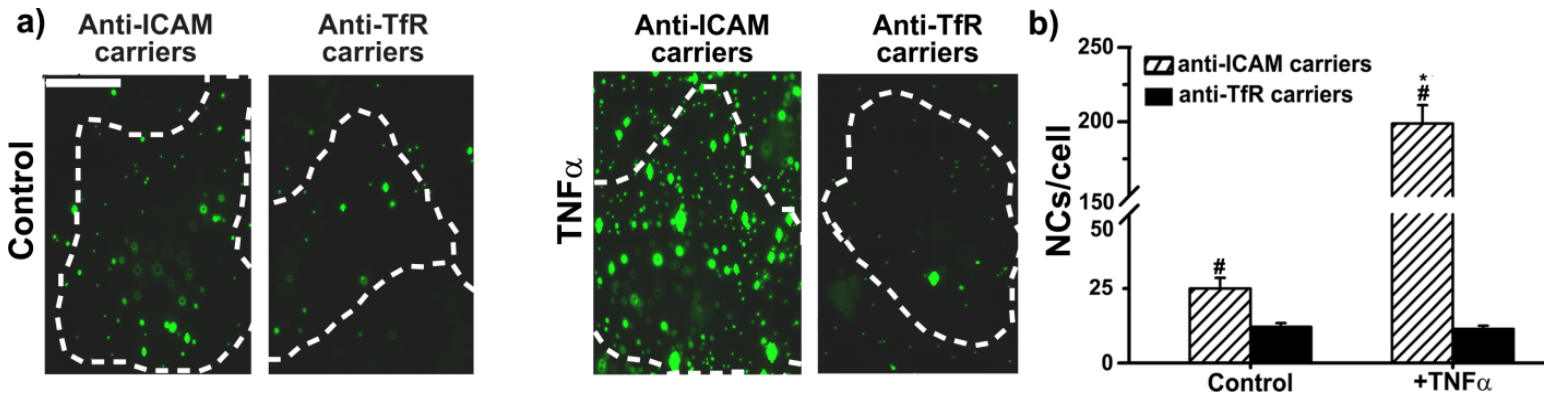

Figure 10. Binding of antibody-coated nanocarriers targeted to ICAM-1 or TfR. (a) Fluorescence microscopy of FITC-labeled ~250 nm anti-ICAM vs. anti-TfR nanocarriers to control or TNFα-activated HUVECs after 1 h incubation at 37°C. Cells were subsequently washed to remove unbound carriers. Phase-contrast images were used to delimit cell borders (dashed lines). Scale bar is ~10 μm. (b) Binding was determined as the number of nanocarriers per cell. Data are mean ± S.E.M. * compares control vs. TNFα for each target, and # compares ICAM-1 vs. TfR for each condition. *,# represents $p < 0.05$ by Student's *t*-test.

Since only nanocarriers appeared to bind more efficiently when targeted to ICAM-1 as opposed to TfR, we reasoned that steric hindrance effects may influence the targeting. Hence, we examined the effect of ligand size and of nanocarrier size on the binding of ICAM-1- vs. TfR-targeted nanocarriers. To examine the effect of ligand size, ~250 nm carriers were coated antibodies or with smaller affinity moieties, namely the ICAM-targeting γ3 peptide or TfR-targeting transferrin (Tf). Binding was additionally assessed for carriers of sizes 1μm and 4.5μm to also examine the effect of nanocarrier size. We selected the incubation period to be shorter in this case (e.g. 15 min in Figure 11 versus 1 h in Figure 10), to minimize endocytosis and thus avoid confounding effects.

In control ECs, the binding difference between ICAM-1 and TfR-targeted carriers was more pronounced using coatings with affinity moieties smaller than in the case of antibodies (9.3-fold vs. 0.8-fold, Figure 11b). For larger sized carriers, binding of ICAM-1-targeted carriers was greater than TfR-targeted carriers when carrier size increased to 1 μm (Figure 11a,c), but similar for even larger, 4.5 μm carriers (Figure 11c). In TNFα-activated ECs, binding of ICAM-1 targeted carriers remained enhanced vs. TfR-targeted carriers at 1μm size (Figure 11a,c). At 4.5 μm carrier size, ICAM-1 targeting also improved binding, although by a smaller margin, perhaps due to greater steric hindrance effects (Figure 11c).

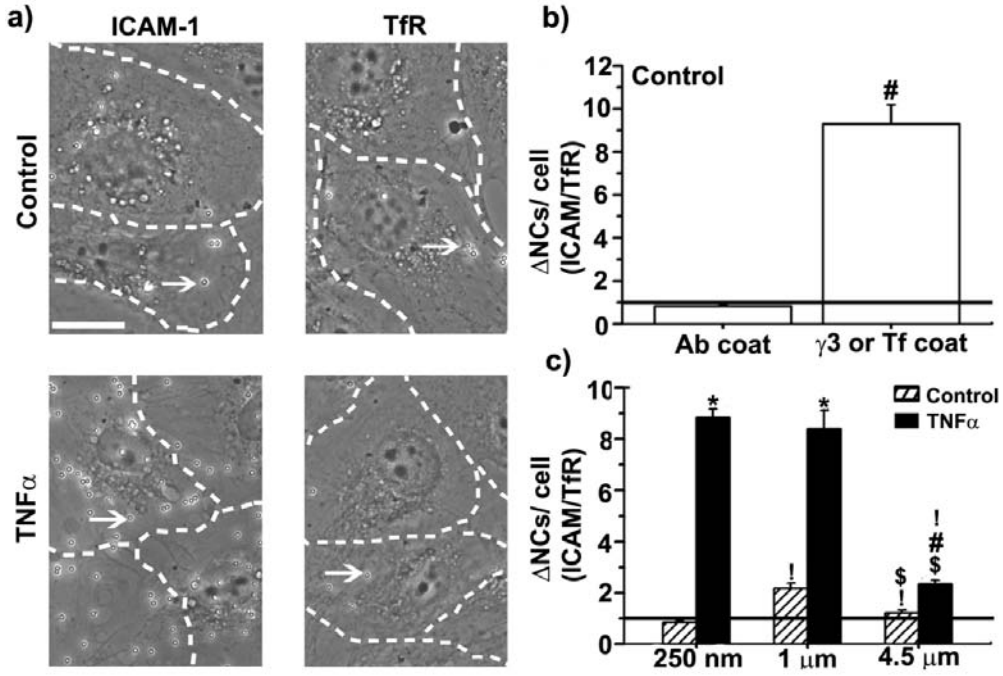

Figure 11. Binding of ICAM-1 or TfR-targeted nanocarriers using ligands and carriers of different size. Binding was assessed by fluorescence (~250 nm carriers) or phase contrast (1μm, 4.5μm carriers) microscopy to determine the number of nanocarriers bound per cell in control HUVECs after 15 min incubation at 37°C. (a) Phase contrast micrographs of binding of 1 μm anti-ICAM or anti-TfR coated carriers (arrows). (b) Binding of FITC-labeled, ~250 nm carriers coated with anti-ICAM or anti-TfR (Ab coat) vs. ICAM-1 targeting γ3 peptide or TfR-targeting Tf. (c) Binding of anti-ICAM or anti-TfR coated carriers of size ~250 nm, 1 μm, and 4.5 μm in control (dashed bars) or TNFα-activated (black bars). Scale bar is ~ 10 μm. Dashed white lines delimit cell borders. Data are mean ± S.E.M. * compares control vs. TNFα for each target, # compares ICAM-1-targeted vs. TfR-targeted carriers, ! compares 1μm or 4.5μm sized carriers to ~250 nm sized carriers, $ compares 1μm vs. 4.5μm sized carriers. *,#,! represents $p < 0.05$ by Student's *t*-test.

These data suggest a dependency on both proximity of the targeting ligands to the nanocarrier surface and a dependency on the size of the carriers due to the effects of steric hindrance on binding. ICAM-1 targeting generally appears to enhance EC binding over TfR-targeting and this effect became more pronounced in the presence of increased steric hindrance. Such an effect may depend on the molecular location of the particular epitope targeted by the antibodies used. Anti-ICAM antibodies used in this study bind to the two most membrane-distal domains on ICAM-1.[200,201] Unfortunately, this information is not available for anti-TfR antibodies used, yet inferring from homology between human and mouse TfR, the antibody used in mice may bind a membrane-distal domain of TfR.[199] As an example of this concept, it has been previously shown that similar carriers directed to a membrane-proximal epitope of a related molecule (PECAM-1) lacked binding to cultured ECs vs. carriers targeted to membrane-distal epitopes, despite similar binding when presented as free counterparts.[179] In another study the efficiency of ACE binding to endothelium *in vivo* varied greatly depending on the epitope targeted.[196]

Also related to potential steric hindrance for carrier binding, intrinsic features of the examined receptors, such as their length and location on the plasmalemma, can impact targeting. For example, ICAM-1 extends further from the endothelial lumen than TfR (<19 nm vs <9 nm, respectively)[224,225] and appears to reside in luminal microvilli-like projections[226,227] which may be more amenable for engagement by targeted carriers. A similar effect was reported for targeting ganglioside GM1 on intestinal cells using cholera toxin B as a ligand. While FITC-labeled cholera toxin B

(<6 nm) bound cells, conjugation to particles (<29 nm) reduced targeting, and binding was totally abolished by increasing particle size (<1.1 μm).[228]

ICAM-1 targeting with antibodies or antibody-coated carriers was superior to TfR in ECs activated with TNFα. This is likely because ICAM-1 is overexpressed in pathological conditions including inflammation, thrombosis, atherosclerosis, oxidative stress, and metabolic imbalance.[5,229,230] Alternatively, TfR expression increases relatively modestly or responds neutrally to different inflammatory mediators.[231,232] Hence, selecting between these molecules for therapeutic or prophylactic interventions depends somewhat on overall and local physiological–pathological balance.

4.2.3. Endocytosis of antibodies vs. antibody-coated nanocarriers targeted to ICAM-1 or TfR

Since varying the valency of combined-targeting nanocarriers may provide a means to optimize nanocarrier internalization, we next compared endocytosis of bivalent antibodies and multivalent antibody-coated nanocarriers. Confirming previously described (yet not comparative) observations, we found anti-ICAM was poorly internalized by ECs compared with anti-TfR (35.6±8.7% vs. 97.7±0.9% uptake; Figure 12), even under TNFα-activation where anti-ICAM binding greatly exceeded anti-TfR.

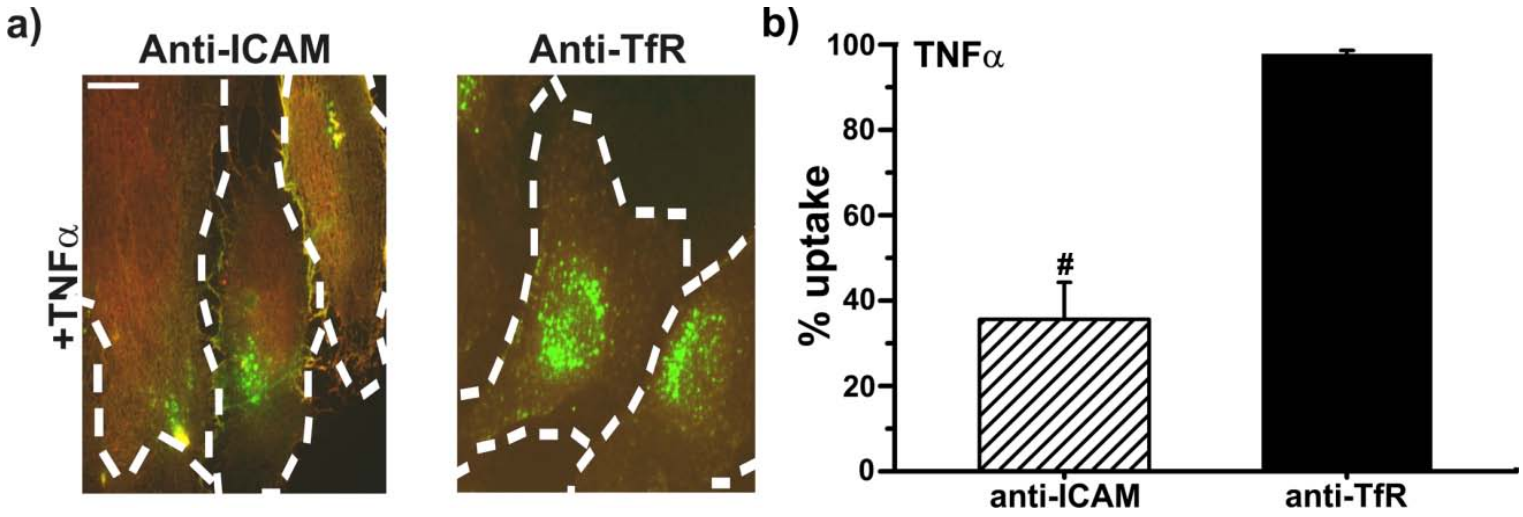

Figure 12. Endothelial endocytosis of antibodies targeted to ICAM-1 vs. TfR. (a) Fluorescence microscopy of endocytosis of antibodies targeted to endothelial ICAM-1 vs. TfR. Unbound carriers were removed and surface-bound carriers were stained with a Texas-Red secondary IgG. Internalized carriers appear as FITC single-labeled in green, while surface-bound carriers display FITC + Texas-Red double-labeled yellow color. Phase-contrast images were used to delimit cell borders (dashed lines). Scale bar is ~10 μm. (b) Quantification of uptake of naked anti-ICAM vs. anti-TfR antibodies, assessed after 1 h incubation at 37^{o}C with TNFα-activated HUVECs. Data are mean ± S.E.M. # Compares anti-ICAM vs. anti-TfR. # represents $p < 0.05$ by Student's *t*-test.

Contrarily, internalization of ICAM-1-targeted carriers exceeded TfR-targeted carriers (Figure 13) in control (83.8±1.7% vs 57.7±2.0% internalization) and disease conditions (68.6±0.1% vs. 59.1±0.2% internalization), suggesting more efficient carrier uptake by CAM-mediated vs. clathrin-mediated endocytosis. Due to this enhanced binding and uptake, the absolute amount of internalized carriers was ~2.6-fold greater when targeting ICAM-1 vs. TfR: 61.4±3.3 vs. 23.8±1.6 carriers/cell in control cells, and 147.0±1.0 vs. 56.1±0.5 carriers/cell in TNFα-activated cells. Consequently, although both markers have been shown to support endocytosis and also transcytosis,[19,168,233] ICAM-1- vs. TfR-mediated vesicular uptake exhibits marked differences in that TfR supports better uptake of antibodies and ICAM-1 is more amenable for nanocarriers.

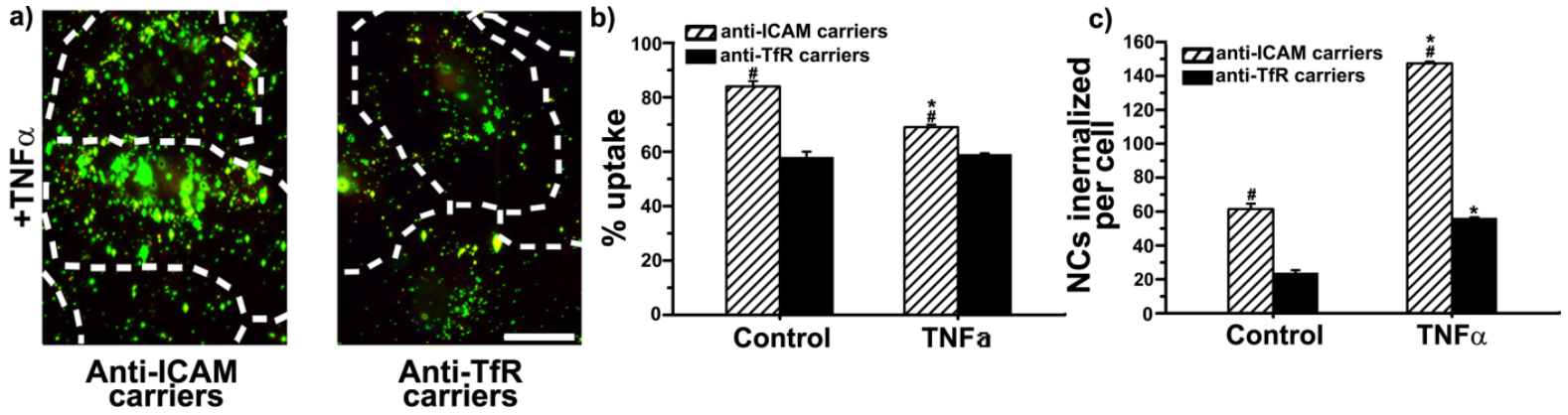

Figure 13. Endothelial endocytosis of nanocarriers targeted to ICAM-1 vs. TfR. (a) Fluorescence microscopy of endocytosis of carriers targeted to endothelial ICAM-1 vs. TfR. Uptake of ~250 nm FITC-labeled anti-ICAM vs. anti-TfR carriers, assessed after 1 h incubation at 37°C in TNFα-activated HUVECs. Unbound carriers were removed and surface-bound carriers were stained with a Texas-Red secondary IgG. Internalized carriers appear as FITC single-labeled in green, while surface-bound carriers display FITC + Texas-Red, double-labeled yellow color. Phase-contrast images were used to delimit cell borders (dashed lines). Scale bar is ~10 μm. (b-c) Internalization was quantified by fluorescence microscopy and expressed as percentage of uptake compared to total cell-associated carriers (b) or absolute number of carriers internalized per cell (c). Data are mean ± S.E.M. * compares control vs. TNFα for each target, and # compares anti-ICAM vs. anti-TfR carriers. *,# represents $p < 0.05$ by Student's *t*-test.

To further validate this hypothesis, we then visualized formation of membrane engulfment structures around carriers bound to ECs and recruitment of molecular partners associated to CAM vs. clathrin pathway. Large 4.5 µm carriers were used to facilitate immunofluorescence imaging of NHE1 or clathrin heavy chain enrichment at binding sites of anti-ICAM or anti-TfR carriers, respectively. As shown in Figure 14, ICAM-1 binding lead to rapid (within 15 min) formation of NHE1-enriched engulfment structures at the plasmalemma (68.8±3.3% carriers displayed full-ring NHE1 clusters around carriers), while engulfment structures enriched in clathrin heavy chain were much less apparent for anti-TfR carriers (17.8±3.7% carriers displayed full-ring clathrin clusters). This result pairs well with greater vesicular endocytosis observed for anti-ICAM carriers.

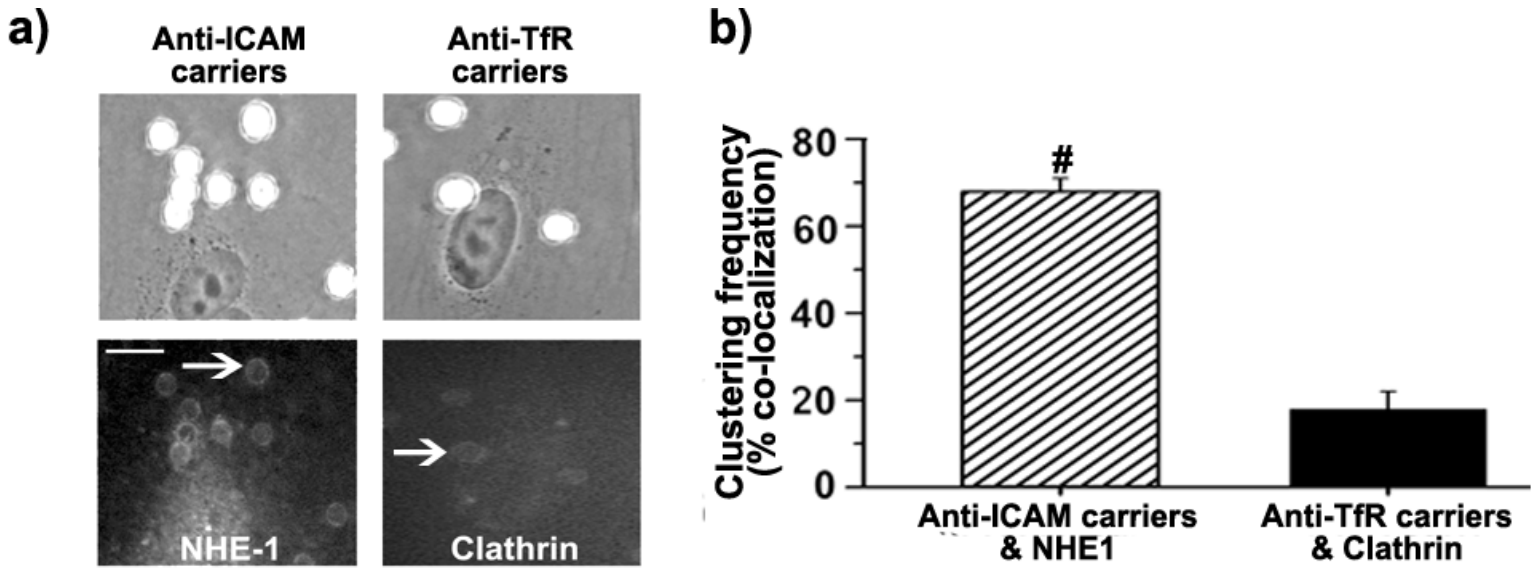

Figure 14. Imaging endothelial engulfment of anti-ICAM vs anti-TfR carriers. (a) Microscopy micrographs showing phase contrast images (top panels) of ~4.5 μm anti-ICAM vs. anti-TfR carriers after binding for 15 min at 37°C to HUVECs, and fluorescence immunostaining (bottom panels) of NHE1 vs. clathrin heavy chain clustering at sites of carrier binding and engulfment (ring-like structures indicated with an arrow). Scale bar is ~10 μm. (b) Quantification of the percent of bound carriers showing full ring-like engulfment structures enriched in NHE1 or clathrin heavy chain. Data are mean ± S.E.M. # compares anti-ICAM vs. anti-TfR carriers. # represents $p < 0.05$ by Student's *t*-test.

4.2.4. Binding and endocytosis of nanocarriers dual-targeted to ICAM-1 and TfR

We next tested the behavior of nanocarriers dually-targeted to ICAM-1 and TfR. As shown in Table 5, nanocarriers coated with both anti-ICAM (clone YN1) and anti-TfR (clone R17) (anti-ICAM/TfR) displayed size, zeta potential, and total antibody surface-coating similar to their single-targeted counterparts, with a 1:1 coating-ratio of anti-ICAM to anti-TfR. Literature values of the affinity of antibodies directed to ICAM-1 or TfR ranged from 0.5-8.5 nm.[205,234]

Table 5. Characterization of single- vs. dual-targeted nanocarriers directed to ICAM and TfR

Nanocarrier coating	Size (nm)	PDI	Zeta potential (mv)	Coating valency (Ab/NC)	
Single:					
Anti-ICAM NCs	228±2.8	0.16±0.03	-9.4±0.5	273±37	
Anti-TfR NCs	217±5.5	0.16±0.03	-16±1.6	220±6.3	
Anti-TfR/IgG NCs	240±5.0	0.19±0.01	-9.5±0.3	Anti-TfR: 154±0.9	IgG: 136±0.3
Anti-ICAM/IgG NCs	225±6.6	0.13±0.02	-9.0±0.3	Anti-ICAM:: 124±25	IgG: 139±2.4
Dual:					
Anti-ICAM/TfR NCs	204±11	0.13±0.003	-12±0.1	Anti-ICAM: 132±12	Anti-TfR: 145±9.7

Data are Mean±S.E.M. Ab = antibody; NC = nanocarrier; PDI = polydispersity. Antibody clones were YN1 for anti-ICAM and R17217 for anti-TfR.

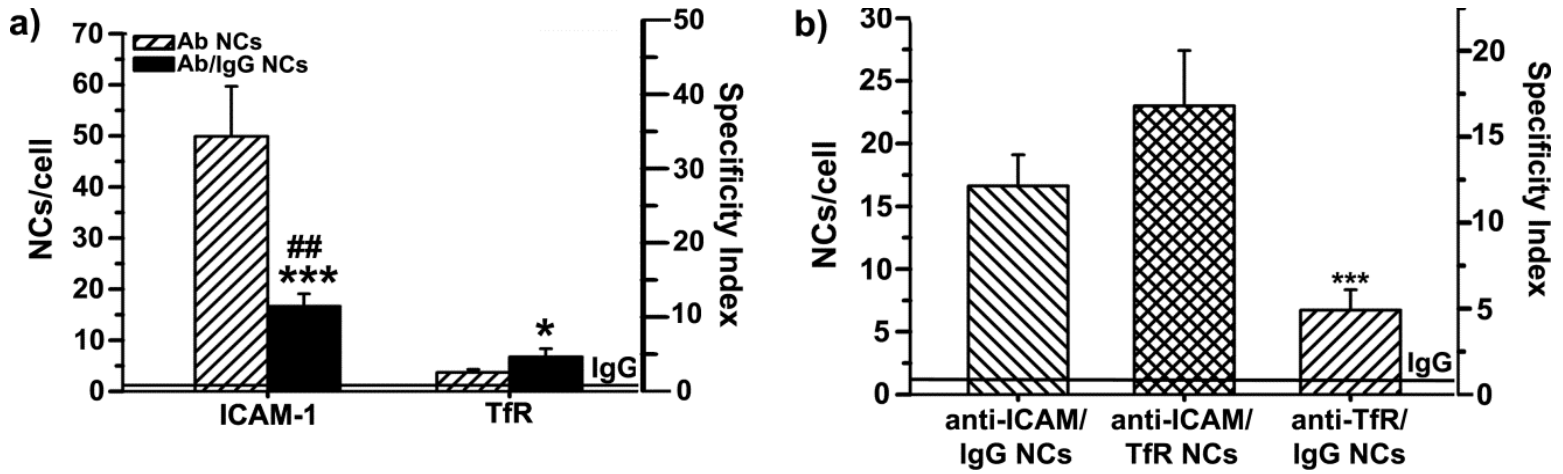

Figure 15. Binding of nanocarriers single-targeted or dual-targeted to ICAM-1 and/or TfR. (a-b) Binding was tested after incubation for 1 h at 37°C in control H5V cells and analyzed by fluorescence microscopy to assess the mean nanocarriers per cell (NCs/cell) and specificity index (SI) for each formulation. Control IgG NCs are represented as a line. Data are mean ± S.E.M. *Compares fully-coated anti-TfR NCs to nanocarriers with a 1:1 coating of anti-TfR and control IgG. *,# represents $p < 0.05$ by Student's *t*-test.

Lowering valency of anti-ICAM NCs towards ICAM-1 by half reduced binding by 3-fold (Compare anti-ICAM NCs to anti-ICAM/IgG NCs, Figure 15a), while binding via TfR improved 1.8-fold as a result of lowered valency. This indicated that adjusting the valency of nanocarriers directed to ICAM-1 vs. TfR could result in different effects. Varying effects of ligand valency have been observed with different receptors previously. For example, multivalency increases binding to cells and targeting in vivo in the case of ICAM-1-targeted nanocarriers,[205] yet nanocarriers targeted to VCAM-1 displayed greater binding to cells using intermediate ligand valencies.[130] Hence, the valency of targeted nanocarrier formulations needs to be evaluated empirically.

Although binding of nanocarriers via ICAM-1 targeting was significantly lowered by reduced valency of anti-ICAM/IgG NCs, binding still remained significantly higher than anti-TfR/IgG NCs, indicating that binding at these intermediate valency levels was favored by targeting ICAM-1 over TfR (Figure 15a). As per the dual-targeted formulation, binding of anti-ICAM/TfR NCs was similar to nanocarriers targeting ICAM-1 and higher than nanocarriers targeting TfR, when compared to nanocarriers with similar valency of either antibody (anti-ICAM/IgG NCs and anti-TfR/IgG NCs, Figure 15b).

Binding of anti-ICAM/TfR NCs was slightly enhanced (although not statistically different) relative to anti-ICAM/IgG NCs and higher than anti-TfR/IgG NCs (Figure 15b) which would suggest that a contribution from TfR-targeting may

also have occurred. Binding of anti-ICAM/TfR NCs was intermediate relative to anti-ICAM NCs and anti-TfR NCs which was similar to the pattern observed for nanocarriers dual-targeted to CAMs described in the previous section.

Following binding, we examined the endocytosis of anti-ICAM/TfR NCs. Lowering valency of anti-ICAM/NCs resulted in less efficient internalization than the full-coated formulation (Figure 16a), suggesting that lower anti-ICAM valency of the formulation reduced induction of CAM-endocytosis. On the other hand, endocytosis of TfR-targeted carriers remained low independent of valency change (Figure 16a). The internalization rate of anti-ICAM/TfR NCs was slightly higher (although not significant) than anti-ICAM/IgG NCs and significantly higher than anti-TfR/IgG NCs (Figure 16b). Indeed, the total number of nanocarriers internalized was significantly greater for anti-ICAM/TfR NCs than anti-ICAM/IgG NCs, suggesting that TfR-targeting enhanced internalization (Figure 16c). This may be due to greater binding as a result of dual ICAM-1- and TfR-targeting, perhaps because of internalization by endocytic receptors associated with different pathways. Interestingly, the behavior of anti-ICAM/TfR NCs was similar to the behavior of anti-PECAM/VCAM NCs from the previous section, suggesting that this effect may be general to receptors associated with CAM- and clathrin-mediated endocytosis.

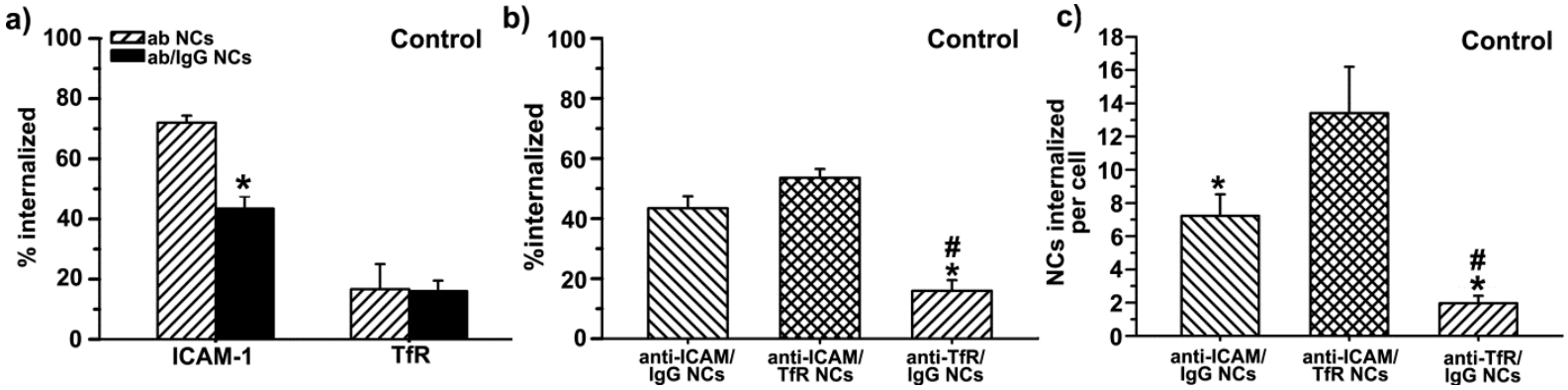

Figure 16. Internalization of nanocarriers targeted to ICAM-1 and TfR. Internalization was assessed after 1 h incubation at 37C with H5V cells. (a) Effect of valency on internalization of ICAM-1 or TfR-targeted nanocarriers, (b) the percent of internalized nanocarriers, and (c) total number of internalized nanocarriers (b) were analyzed by fluorescence microscopy. Data are mean ± S.E.M. * compares to anti-ICAM/TfR NCs, # compares anti-ICAM/IgG NCs and anti-TfR/IgG NCs *,# represents $p < 0.05$ by Student's *t*-test.

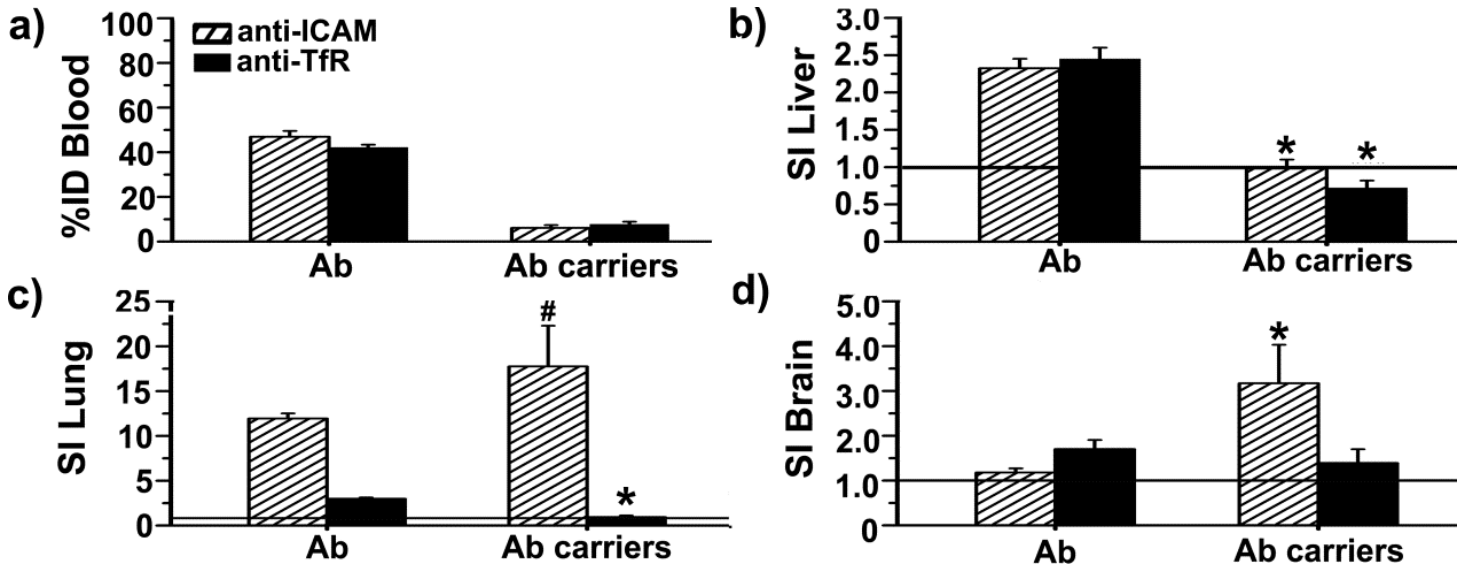

Figure 17. Biodistribution of anti-ICAM versus anti-TfR antibodies and antibody-coated carriers in mice. (a) Blood levels of ^{125}I-labeled anti-ICAM vs. anti-TfR or their ~250 nm carrier counterparts measured at 30 min after i.v. injection in mice, expressed as the percentage of the injected dose (%ID). (b-d) Specific tissue accumulation of these formulations compared to control IgG counterparts, calculated as the specificity index (SI, see Methods). Data are mean ± S.E.M. * Compares antibodies vs carriers for each target and # compares targeting to ICAM-1 vs. TfR for each formulation. * represents $p < 0.05$ by Student's *t*-test.

4.2.5. Biodistribution of antibodies vs. antibody-coated nanocarriers targeted to ICAM-1 or TfR

As mentioned above, effective targeting and vesicular transport are crucial elements impacting biodistribution of therapeutics. Using radioisotope tracing, we tested antibodies and antibody-coated carriers targeted to ICAM-1 vs. TfR (Figure 17 and Table 6). As shown in Figure 17a, the circulating blood level of anti-ICAM was comparable to anti-TfR at 30 min after injection (46.9±2.7% and 42.1±1.3% of injected dose (% ID), and appreciably lower than control IgG (75.5±3.7% ID; data not shown), suggesting enhanced accumulation in tissues. Both anti-ICAM and anti-TfR displayed increase accumulation over control IgG (SI > 1) in all organs with similar targeting specificity in liver (SI 2.3±0.1 and 2.4±0.2, respectively; Fig. 17b), higher for anti-ICAM vs. anti-TfR in lungs (SI 11.9±0.6 vs. 3.0±0.1; Fig. 17c), while anti-TfR showed higher accumulation than anti-ICAM in brain (SI 1.2±0.1 vs. 1.7±0.2; Figure 17d).

A different behavior was observed for antibody-coated carriers (Table 6). Blood levels of anti-ICAM NCs or anti-TfR NCs were considerably lower than naked counterparts (Figure 17a). This suggested increased removal from blood and/or accumulation in organs, likely due to carrier multivalency. For example, anti-ICAM NCs displayed increased accumulation but reduced specificity in RES organs, likely resulting from greater non-specific uptake (liver SI decreased from 2.3±0.1 for antibodies to 1.0±0.1 for nanocarriers; Figure 17b) and enhanced accumulation in peripheral organs and brain: lung SI increased from 11.9±0.6 for antibodies to

17.8±4.6 for carriers (Figure 17c) and brain SI increased from 1.2±0.1 to 3.2±0.9 (Figure 17d). Contrarily, specific tissue accumulation decreased for anti-TfR NCs compared to naked antibody counterpart: e.g. liver SI decreased from 2.5±0.2 for antibodies to 0.7±0.1 for carriers (Figure 17b), lung SI decreased from 3.0±0.1 to 0.9±1.2 (Figure 17c), and brain SI decreased from 1.7±0.2 to 1.4±0.3 (Figure 17d). Anti-TfR NCs exceeded accumulation over control IgG NCs in brain but not lungs, while anti-ICAM NCs displayed specificity in both lungs and brain, with even better performance than anti-TfR in brain (1.9-fold improvement). Hence, results *in vivo* correlate well with cell culture observations of reduced binding and endocytosis of anti-TfR NCs compared to naked anti-TfR, and an opposite effect for targeting ICAM-1.

Table 6. Biodistribution of nanocarriers targeted to ICAM-1 or TfR

Ab or NC	Blood	Kidney		Heart		Spleen		Lungs		Liver		Brain	
	%ID	LR	SI	LR	SI	LR	SI	LR	SI	LR	SI	LR	SI
Antibodies:													
Anti-ICAM	47±2.7	0.6±0.02	2.2±0.09	0.2±0.02	2.0±0.2	0.6±0.04	4.3±0.3	1.8±0.09	12±0.58	0.5±0.03	2.3±0.1	0.02±0.002	1.2±0.1
Anti-TfR-8D3	42±1.3	0.6±0.05	2.3±0.14	0.1±0.01	1.2±0.1	0.6±0.06	4.2±0.4	0.5±0.02	3.0±0.13	0.6±0.04	2.5±0.2	0.03±0.004	1.7±0.2
Single:													
Anti-TfR-8D3 NCs	7.8±1.2	0.3±0.04	0.7±0.09	0.3±0.02	0.8±0.1	38±6.40	2.5±0.4	1.7±0.32	0.9±0.18	8.1±1.1	0.7±0.1	0.07±0.02	1.4±0.3
Anti-TfR-R17 NCs	6.8±0.7	0.5±0.03	1.1±0.05	0.5±0.06	1.2±0.2	23±3.91	1.5±0.3	2.4±0.33	1.3±0.18	12±1.6	1.1±0.1	0.09±0.02	1.8±0.3
Anti-TfR-R17/IgG NCs	5.3±0.4	0.5±0.08	1.0±0.16	0.4±0.04	1.0±0.1	18±1.09	1.2±0.1	1.6±0.36	0.9±0.19	13±2.6	1.2±0.2	0.08±0.02	1.7±0.4
Anti-TfR/ASM NCs	9.8±0.5	0.8±0.10	1.8±0.31	0.5±0.07	2.8±0.5	12±1.85	25±4.9	0.8±0.03	2.4±0.12	5.7±0.4	4.8±0.4	0.11±0.02	2.9±0.5
Anti-ICAM NCs	6.1±1.3	1.3±0.23	2.7±0.47	0.8±0.16	2.1±0.4	20±4.47	1.3±0.3	33±8.42	18±4.55	11±1.4	1.0±0.1	0.16±0.04	3.2±0.9
Anti-ICAM/IgG NCs	4.5±0.7	1.0±0.21	2.0±0.44	0.4±0.15	1.2±0.4	38±2.09	2.5±0.1	14±1.99	7.5±1.08	16±2.0	1.5±0.2	0.14±0.05	2.9±1.0
Anti-ICAM/ASM NCs	4.1±0.4	2.1±0.19	5.1±0.48	1.6±0.24	9.3±1.4	23±3.83	50±8.5	64±11.4	195±36	17±2.4	15±2.1	0.27±0.11	7.2±3.1
Dual:													
Anti-ICAM/TfR NCs	4.5±0.7	0.64±0.1	1.31±0.3	0.46±0.1	1.3±0.3	34.8±4.0	2.3±0.3	12.2±4.0	6.62±2.2	19±2.1	1.7±0.2	0.07±0.0	1.4±0.1
Anti-ICAM/TfR / ASM NCs	7.7±0.4	0.93±0.1	2.26±0.2	0.76±0.1	4.3±0.5	13.2±2.0	28±4.4	3.21±0.3	9.84±1.0	6.4±1.4	5.4±1.2	0.12±0.0	3.1±0.2
AntiICAM/TfR/ ASM NCs (+LPS)	5.0±0.7	1.31±0.1	3.16±0.3	0.92±0.2	5.3±0.9	15.2±2.8	46±8.3	11.5±1.8	43.7±7.0	13±4.1	23±7.3	0.17±0.0	3.2±0.4

Data are Mean±S.E.M. %ID = percentage of injected dose; LR = localization ratio; SI = specificity Index; Ab = antibody; NC = nanocarrier. Antibody clones were YN1 for anti-ICAM and R1727 (R17, used for Dual) or 8D3 for anti-TfR.

4.2.6. Biodistribution of antibody-coated nanocarriers targeted to ICAM-1 and TfR

Next we tested the biodistribution of anti-ICAM/TfR NCs. In accord with greater targeting of nanocarriers to ICAM-1 in cell cultures,[208] anti-ICAM NCs had greater accumulation and targeting specificity than anti-TfR NCs in the brain and lungs, with similar liver uptake (Figure 18 and Table 6). Anti-ICAM/TfR NCs displayed lung accumulation and specificity which was intermediate of parental formulations, similar to the outcome observed in cell culture. This may be due to reduced valency of dually-targeted nanocarriers toward anti-ICAM, since control anti-ICAM/IgG nanocarriers had a similarly reduced pulmonary uptake and reduced targeting in cell culture (Figures 15 and 18). However, although lower, pulmonary accumulation of anti-TfR NCs was not affected by decreasing valency of this component (compare anti-TfR NCs and anti-TfR/IgG NCs in Figure 18). This suggests a stronger dependency on antibody surface-density for ICAM-1 vs. TfR targeting, in agreement with our finding showing that multivalency associated with nanocarriers vs. naked antibodies enhances specific targeting and endocytosis toward ICAM-1, while an opposite effect is observed for TfR (Figure 18).[208]

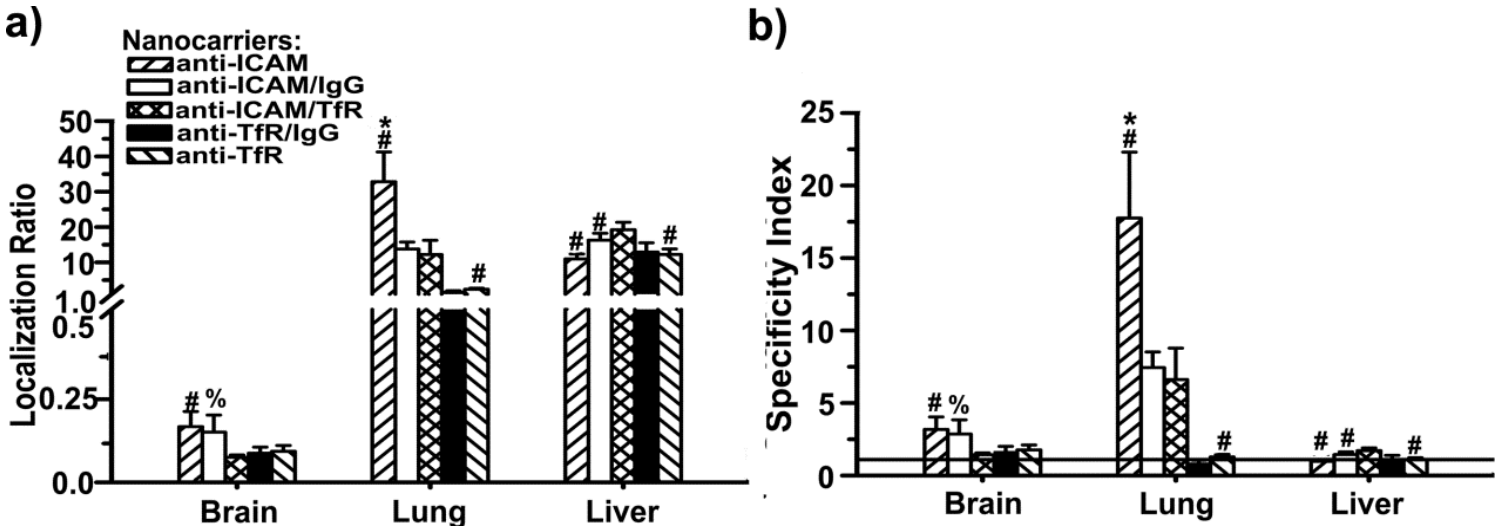

Figure 18. Biodistribution of nanocarriers coated with anti-ICAM-1 and anti-TfR in mice. Localization ratio (LR) and specificity index (SI) of brain, lungs, and liver are shown in (a) and (b), respectively. Data are mean ± S.E.M. * Compares anti-TfR NCs to anti-ICAM NCs; # compares dual-coated nanocarriers (either Ab/IgG or Ab1/Ab2) to their respective single-targeted nanocarriers; % compares anti-ICAM/TfR NCs to control Ab/IgG NCs. *,#,% represents $p < 0.05$ by Student's *t*-test.

Interestingly, brain accumulation and specificity of dually-targeted anti-ICAM/TfR NCs were comparable to anti-TfR NCs and lower than anti-ICAM NCs (Figure 18). This was independent of valency changes toward anti-ICAM or anti-TfR, since brain uptake of anti-ICAM/IgG NCs or anti-TfR/IgG NCs was similar to their single-targeted counterparts. For anti-ICAM/TfR NCs, anti-TfR (not anti-ICAM) ruled brain targeting despite the fact that anti-ICAM NCs accumulate in brain better. This also agrees with the observed reduction in endocytosis of nanocarriers via TfR compared to *naked* antibodies, while the opposite scenario arises for ICAM-1 targeting (Figure 18).[208] Therefore, it is possible that binding of anti-ICAM/TfR NCs to TfR reduces or delays uptake by cells despite the presence of anti-ICAM, lowering brain accumulation. This was not observed in lungs, likely due to relatively high ICAM-1 expression in this organ vs. the brain.[134,204] Liver uptake of anti-ICAM/TfR NCs behaved differently, which was slightly greater compared to single-targeted formulations. This may be due to reduced accumulation of these particles in the lungs and may also possibly represent increased targeting since liver displays both specific accumulation (due to ICAM-1 and TfR expression) as well as non-specific clearance.

4.2.7 Biodistribution of a therapeutic cargo single- or dual-targeted nanocarriers

These data support that exploiting different expression, valency requirements, and mechanistic patterns associated with distinct cell-surface receptors, as well as their combination targeting, holds potential to modify the biodistribution of drug delivery systems. We examined the impact of this approach on the delivery of ASM as a model cargo, which as mentioned in the previous section is deficient in Niemann Pick

disease types A-B. Then, combination targeting to ICAM-1 and TfR was tested. ASM was injected i.v. and targeted via anti-ICAM NCs, anti-TfR NCs, or anti-ICAM/TfR NCs compared to naked ASM (as in clinical applications).

Using similar doses of ^{125}I-ASM, coupling to anti-ICAM NCs or anti-TfR NCs significantly lowered blood levels of the circulating enzyme by 30 min post-injection, i.e. from 29.8±3.8% ID for naked enzyme to 4.1±0.4% ID and 9.8±0.5% ID for anti-ICAM/ASM NCs or anti-TfR/ASM NCs, respectively (Figure 19a and Table 6), suggesting greater removal from circulation and delivery to organs. ASM accumulation was enhanced in RES organs, non-RES peripheral organs, and also brain for ICAM-1- and TfR-targeted nanocarriers vs. naked counterparts, with greater benefit from ICAM-1 targeting. For instance, anti-ICAM/ASM NCs vs. anti-TfR/ASM NCs displayed liver SI 14.5±2.1 vs 4.8±0.4, lung SI 195.2±36.0 vs. 2.4±0.1, and brain SI 7.24±3.1 vs. 2.9±0.5, respectively.

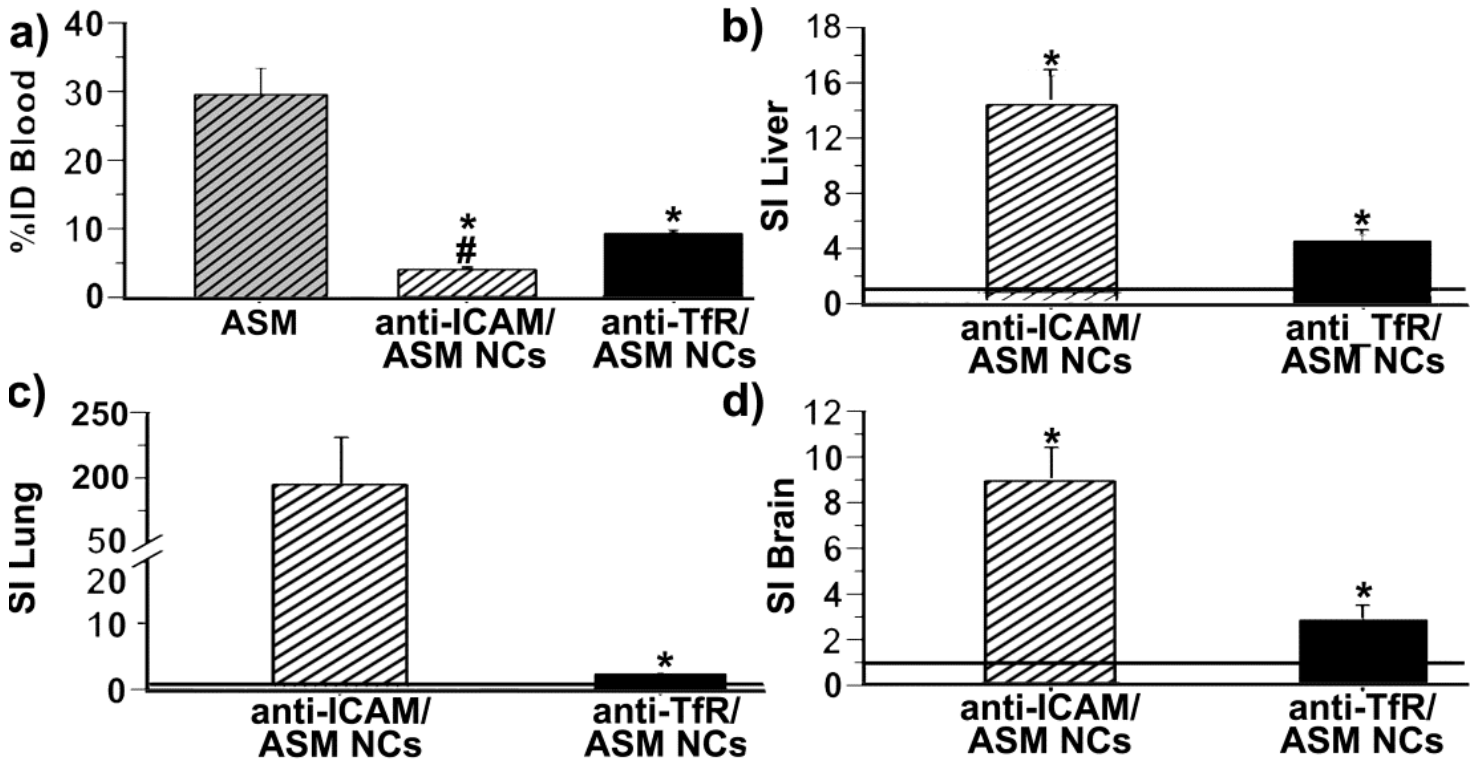

Figure 19. Lysosomal enzyme delivery in control mice by ICAM-1- vs. TfR-targeted nanocarriers. (a) Blood levels of ^{125}I-acid sphingomyelinase (^{125}I-ASM) injected i.v. in mice as a naked counterpart or coupled to ~250 nm anti-ICAM NCsvs. anti-TfR NCs, measured at 30 min after injection and expressed as the percentage of the injected dose (%ID). **(**b-d) Specific tissue accumulation of anti-ICAM/ASM NCs vs. anti-TfR/ASM NCs compared to naked ASM, calculated as the specificity index (SI). Data are mean ± S.E.M. * Compares naked enzyme vs carrier-coupled enzyme for each target and # compares targeting to ICAM-1 vs. TfR. *,# represents $p \leq 0.05$ by Student's *t*-test.

A similar result was observed when LPS was administered via intraperitoneal injection prior to the start of the experiment (Figure 20 and Table 6). In this model, ASM delivery using ICAM-1 or TfR-targeted nanocarriers again resulted in enhanced clearance from the circulation relative to naked ASM, and also greatly increased accumulation in brain lungs and liver (Figure 20). In liver, ASM delivery with TfR-targeted nanocarriers appeared more similar to ICAM-1-targeted nanocarriers, yet appeared less effective in lungs and brain (Figure 20). Therefore, targeting ICAM-1 or TfR may be valuable for lysosomal enzyme delivery, as previously shown, yet ICAM-1 targeting may offer advantages in the case of multivalent carriers.

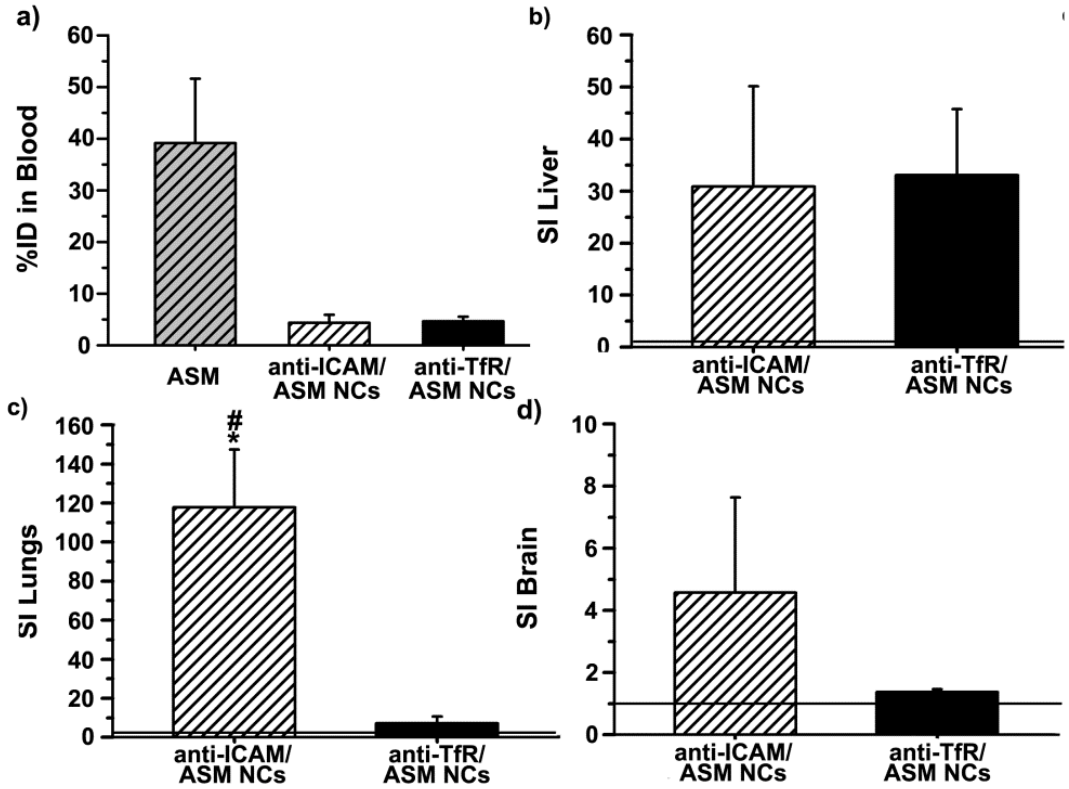

Figure 20. Lysosomal enzyme delivery in disease model mice by ICAM-1- vs. TfR-targeted nanocarriers. (a) Blood levels of ^{125}I-acid sphingomyelinase (^{125}I-ASM) injected i.v. in LPS-treated mice as a naked counterpart or coupled to ~250 nm anti-ICAM NCs vs. anti-TfR NCs measured at 30 min after injection and expressed as the percentage of the injected dose (%ID). (b-d) Specific tissue accumulation of anti-ICAM/ASM NCs vs. anti-TfR/ASM NCs compared to naked ASM, calculated as the specificity index (SI). Data are mean ± S.E.M. * Compares naked enzyme vs carrier-coupled enzyme for each target and # compares targeting to ICAM-1 vs. TfR. *,# represents $p < 0.05$ by Student's *t*-test.

Dually-targeted anti-ICAM/TfR NCs resulted in enhanced ASM accumulation and specificity in all three organs compared to naked enzyme (Figure 21). In comparison to single-targeted counterparts, this formulation displayed intermediate values of ASM accumulation and specificity in the lungs, and values more similar to those corresponding to ASM delivery by anti-TfR NCs in the brain and liver. This is similar to the result observed when tracing anti-ICAM/TfR NCs (Figure 18), showing paired co-distribution of the carrier targeting counterpart and cargo. As a consequence, combined-targeting resulted in a more homogenous, yet still specific and enhanced, delivery of ASM through different tissues (Figure 21b), which is preferred in diseases affecting multiple organs, such as Niemann-Pick disease A-B.

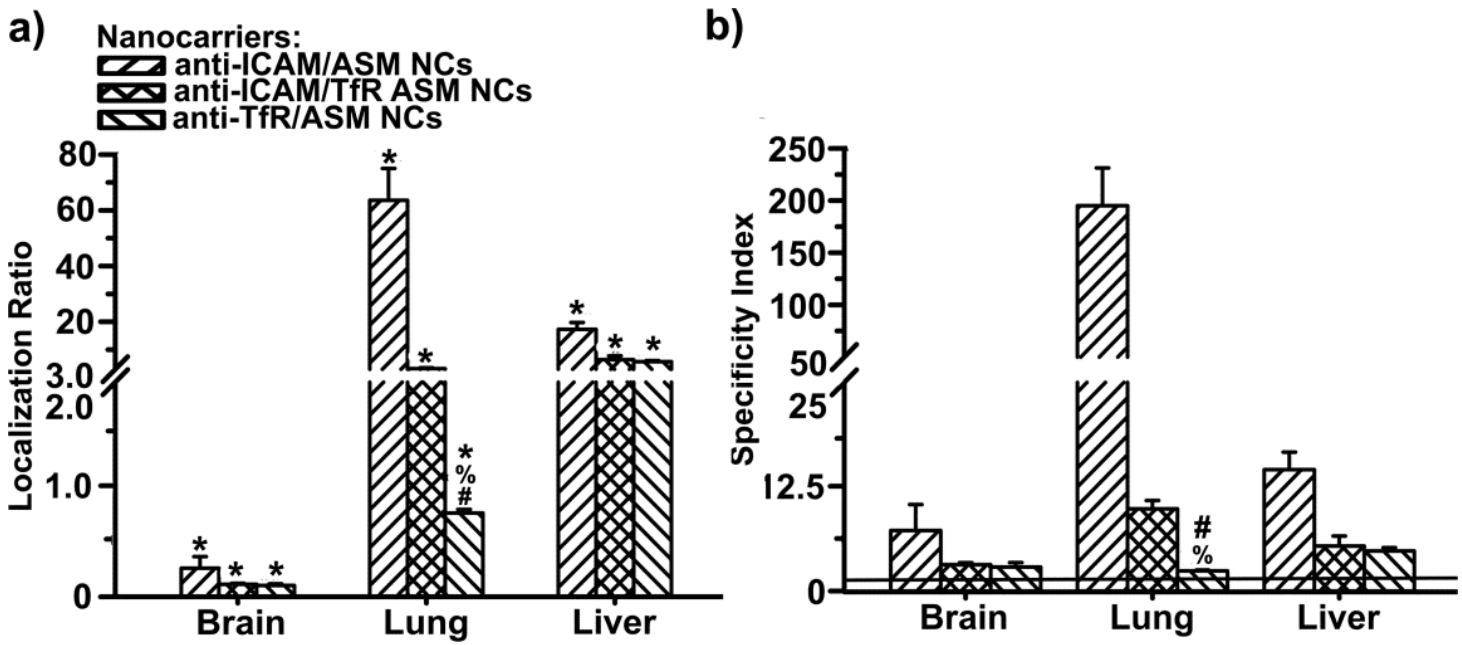

Figure 21. Delivery of ASM by nanocarriers dual-targeted to ICAM-1 and TfR in control mice. Localization ratio (LR) and specificity index (SI) of brain, liver, and lungs are shown in (a) and (b), respectively. Data are mean ± S.E.M. * Compares enzyme vs nanocarrier-coupled enzyme for each target; # compares targeting between single-targeted nanocarriers; % compares targeting of dually-targeted nanocarriers vs. single-targeted counterparts. *,#,% represents $p < 0.05$ by Student's *t*-test.

Furthermore, in mice challenged with LPS, in order to induce inflammation typically associated with Niemann-Pick A-B disease and other maladies, dually-targeted anti-ICAM/TfR NCs improved further ASM accumulation compared to a control situation (Figure 22). This pairs well with the fact that ICAM-1 is overexpressed under inflammatory conditions and, hence, dual-targeted nanocarriers retained the ability to respond to ICAM-1 overexpression.[154] Interestingly, this phenomenon was observed to a much lesser extent in the case of the brain (e.g. comparing the localization ratio and specificity index in Figure 22). This result is in accord with our previous observation indicating that TfR targeting seems to rule brain addressing (as opposed to the case of lungs) of dually-targeted anti-ICAM/TfR NCs (Figure 20). Interestingly, this is despite the expected increase in expression of ICAM-1, not TfR, in the brain under inflammatory conditions.[213] Hence, the resulting biodistribution of dual-targeted nanocarriers cannot be simply explained by their reduced valency to each individual receptor (as reported in the previous section), nor it corresponds to the combined biodistribution of their respective targeting moieties.

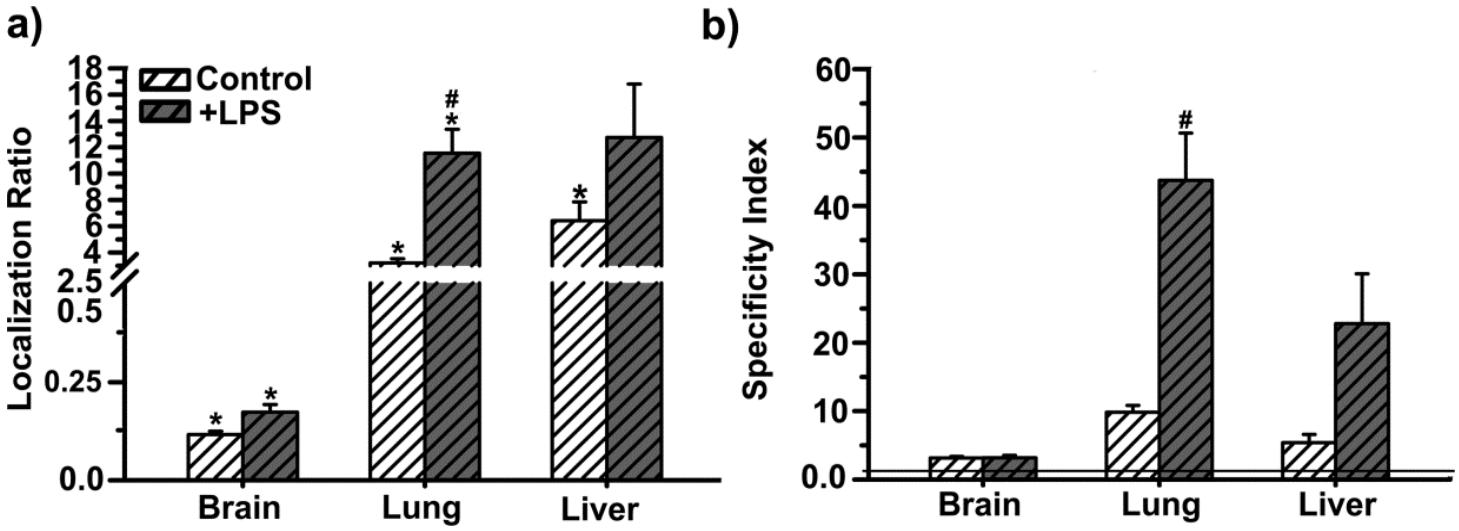

Figure 22. Delivery of ASM by nanocarriers dual-targeted to ICAM-1 and TfR in control versus inflammatory model mice. Localization ratio (LR) and specificity index (SI) of brain, lungs, and liver are shown in (a) and (b), respectively. Data are mean ± S.E.M. * Compares naked enzyme vs enzyme coupled to nanocarriers coated with both anti-ICAM and anti-TfR; # compares control mice vs mice pre-treated with LPS. *,# represents $p < 0.05$ by Student's *t*-test.

While we used a 1:1 ratio of two targeting antibodies on the nanocarrier surface, it is likely that further tuning of this parameter may improve organ selectivity. For example, selectivity for cancerous versus non-cancerous cells was enhanced by optimizing the ratio of folic acid and anti-EGFR antibody coupled to liposomes.[14] However, as in the case of nanocarriers targeted to multiple receptors with similar function, such optimization cannot be predicted, as numerous factors relative to both design parameter and physiological features may influence combined targeting strategies.

4.2.8. Conclusions

ICAM-1 and TfR have different attributes including function, response to pathology, and endocytic activity which has an apparent affect on their use for drug delivery. Targeting TfR versus ICAM-1 produced similar results with regard to binding of antibodies, yet antibody internalization was clearly favored in the case of TfR-targeting. On the other hand, ICAM-1 targeting demonstrated certain advantages, including binding to cells in inflammatory-like conditions and with relatively larger, multivalent NCs, and also in terms of nanocarrier internalization, perhaps due to restrictive size of clathrin-coated pits. Differences were also apparent *in vivo*, as naked anti-TfR targeted brain efficiently, yet worsened in the case of NCs, whereas ICAM-1 targeting improved when targeted with NCs and appeared best overall for targeting brain and lungs. This type of targeting is useful for therapy of lysosomal storage disorders, such as Niemann Pick disease types A-B, where brain delivery along with multi-organ delivery is needed, and we demonstrated the relative efficacy of ICAM-1 and TfR targeted NCs over naked enzyme, the current gold standard

therapy. Therefore, while both TfR and ICAM-1 are beneficial for drug delivery, TfR may be more suitable for delivery applications involving small, monovalent drug conjugates, whereas ICAM-1 appears preferable for delivery with larger, multivalent nanocarriers.

Regarding dual targeting of ICAM-1 and TfR, specific binding to cells was modified with respect to single-targeting of either receptor, yet was lower than dual-targeted CAMs from the previous chapter. Thus, targeting multiple receptors with similar function may help enhance binding, while either strategy can be used for modification. Endocytosis of anti-ICAM/TfR NCs was enhanced with respect to single-targeted formulations and this was also observed with PECAM-1/VCAM-1 targeted nanocarriers. Both ICAM-1/TfR and PECAM-1/VCAM-1 combinations exploit CAM- and clathrin-mediated endocytosis, yet different behaviors may be observed when other pathways are combined. ICAM-1 and TfR dual-targeting improved accumulation in brain, lungs, and liver *in vivo*. Accumulation in lungs paralleled ICAM-1 targeting, while in brain appeared more similar to TfR-targeted nanocarriers, suggesting that dual targeting of ICAM-1 and TfR modified the biodistribution relative to single-targeting of either receptor. Delivery of therapeutic ASM via ICAM/TfR targeted nanocarriers produced similar results with apparent improvement in inflammatory context, suggesting selectivity of this formulation for sites of disease as was observed in the case of particular multi-CAM-targeted combinations. Therefore, these findings provide new insights which support that targeting multiple receptors of different functions with nanocarriers appears a viable strategy to modify the binding, endocytosis, and biodistribution of nanocarriers.

4.3. Combination Targeting to Multiple Epitopes of the Same Receptor

4.3.1. Introduction

Directing nanocarriers to multiple epitopes of the same receptor is an intriguing strategy which has never been tested previously. In theory this approach may modulate parameters of drug targeting, such as binding to cells, internalization, and biodistribution tested in the previous section. For example, binding to one or multiple receptor epitopes may alter the conformation of the receptor and consequently affect nanocarrier avidity. Alternatively, targeting multiple epitopes may enable binding to multiple regions of a single receptor which may also enhance avidity and/or result in higher saturation levels by binding fewer receptors per nanocarrier. Empirical observations from the literature provide some support for this approach. For example, it is known that stimulation of a receptor at one epitope is known to alter activity at another epitope. Such is the case for stimulation *in vivo* of PECAM-1 with an antibody, which subsequently enhanced lung accumulation of a second antibody or fusion conjugate. In addition, binding, endocytosis, and lysosomal transport of PECAM-1-targeted nanocarriers were shown to depend on the epitope targeted.[179] Epitope selection is important for lung accumulation and induced cleavage of anti-angiotensin converting enzyme,[131,196] and brain selectivity of anti- TfR.[132]

Therefore, we hypothesized that targeting nanocarriers to multiple epitopes of the same receptor can be used as a strategy to modify binding to cells in culture and distribution in organs *in vivo*. To investigate this strategy, we selected the TfR as a target receptor due in part to availability of antibodies which are known to have

differential targeting *in vivo*.[132] Additionally, as described in the previous section, the TfR is widely studied as a receptor for drug delivery applications in the context of brain delivery and in cancer.[6,132,235]

4.3.2. Binding of antibodies vs. antibody-coated nanocarriers targeted to different TfR epitopes

Two monoclonal antibodies were selected to investigate combination targeting to multiple epitopes of the same receptor. These antibodies were rat anti-mouse TfR clones 8D3 (anti-TfR-8D3) and R17217 (anti-TfR-R17) which have been investigated previously in the literature and display distinct biodistribution patterns when administered *in vivo*.[132]

We first tested binding of these antibodies in cell culture to verify specific targeting over control IgG and to compare the binding toward different TfR epitopes. Both anti-TfR-8D3 and anti-TfR-R17 bound ECs specifically as compared to control IgG (3.4-fold versus 2.3-fold enhancement, Figure 23a,b), with anti-TfR-8D3 displaying comparatively greater binding than anti-TfR-R17 (1.5-fold, Figure 23b). This verifies that targeting TfR at these respective epitopes results in specific and differential binding to ECs.

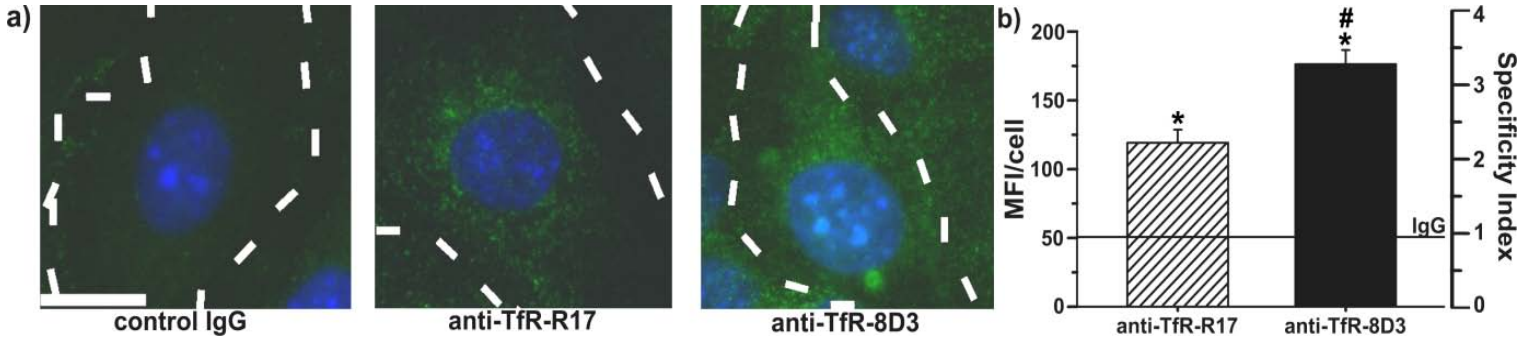

Figure 23. Binding of anti-TfR-8D3 versus anti-TfR-R17 to ECs. (a,b) Binding was tested by immunofluorescence after incubation for 1 h at 37°C in control H5V cells, and analyzed by fluorescence microscopy to assess the mean fluorescent intensity (MFI) and specificity index (SI, see methods) for each antibody. Phase contrast images were used to delimit cell borders (dashed white lines). Scale bar is ~10μm. Line in graph is shown as binding of control IgG. Data are mean ± S.E.M. *Compares with control IgG, # compares ant-TfR-R17 vs anti-TfR-8D3. *,# represents $p < 0.05$ by Student's *t*-test.

Since multivalency and size of targeted nanocarriers differ from that of naked antibodies, we next assessed the binding of antibody-coated nanocarriers targeted via anti-TfR-8D3 or anti-TfR-R17. Nanocarriers coated with anti-TfR-R17 or anti-TfR-8D3 had similar characteristics, with size ranging between ~235-265 nm, zeta potential from -14.5 to -16 mV, and coating density of 185-220 antibody molecules per particle (Table 7). Literature values of the affinity of antibodies directed to TfR epitopes 8D3 or R17 ranged from 0.5-2.3 nm.[234,236]

Table 7. Characterization of nanocarriers single- or dual-targeted to TfR epitopes

Nanocarrier coating	Size (nm)	PDI	Zeta potential (mv)	Coating Valency Ab/NC	
Single:					
Anti-TfR-8D3 NCs	265±28	0.29±0.04	-14.5±3.4	185±2.4	
Anti-TfR-8D3/IgG NCs	255±40	0.25±0.09	-12.9±3.9	8D3: 98.5±4.0	IgG: 152±9.7
Anti-TfR-R17 NCs	235±15	0.18±0.04	-15.9±1.6	220±6.27	
Anti-TfR-R17/IgG NCs	251±13	0.19±0.01	-9.50±0.3	R17: 154±0.9	IgG: 136±0.3
Dual:					
Anti-TfR-R17/8D3 NCs	258±12	0.25±0.02	-14.5±3.7	8D3: 115±0.9	R17: 140±7.2

Data are Mean ± S.E.M. Ab = antibody; NC = Nanocarrier; PDI = polydispersity. Anti-TfR-8D3 was clone 8d3 and anti-TfR-R17 was clone R17217.

When each antibody was coated onto nanocarriers and tested under the same conditions as for naked antibodies, binding of nanocarriers targeted to the 8D3 epitope of TfR was again higher than nanocarriers targeted to the R17 epitope (Figure 24 a-c). Indeed, targeting the 8D3 epitope of the TfR enhanced binding over the R17 epitope considerably more for nanocarriers than for naked antibodies (8.5-fold versus 1.5-fold, Figure 24b versus 23b), indicating that epitope 8D3 is more amenable to binding with relatively larger and multivalently targeted NCs.

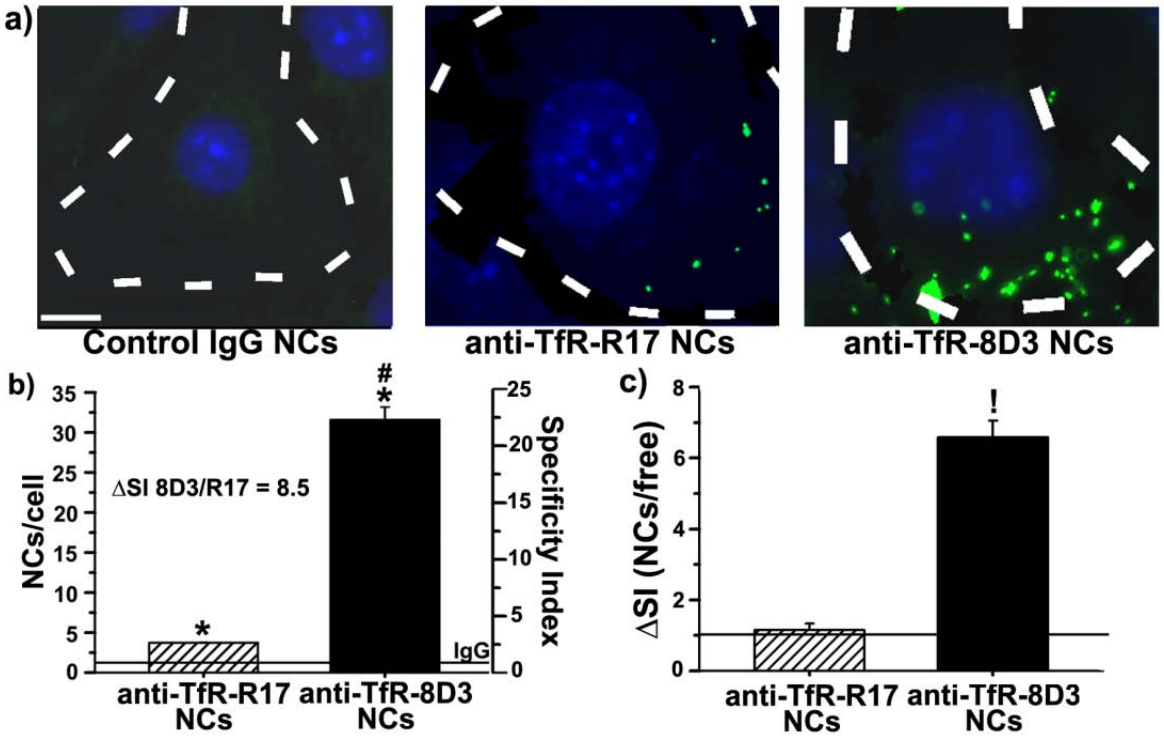

Figure 24. Binding of antibody-coated nanocarriers targeted to TfR epitope 8D3 versus R17. (a-c) Binding was tested after incubation for 1 h at 37 °C in control H5V cells, and analyzed by fluorescence microscopy to assess the mean nanocarriers per cell (NCs/cell) and specificity index (SI, see methods) for each formulation. Phase contrast images were used to delimit cell borders (dashed white lines). Scale bar is ~10μm. Binding of control IgG is shown as a line in b. Data are mean ± S.E.M. *Compares with control IgG, # compares ant-TfR-R17 NCs vs anti-TfR-8D3 NCs, ! compares nanocarriers versus corresponding naked antibody. *,#,! represents $p < 0.05$ by Student's *t*-test.

Binding at the R17 epitope was similarly efficient whether used as a naked targeting moiety or reformatted into a multivalent NCs, while anti-TfR-8D3 was more efficient in the NC format (Figure 24c).

4.3.3. Binding of antibody-coated nanocarriers targeted to multiple TfR epitopes

We next tested binding of nanocarriers dually targeted to TfR epitopes R17 and 8D3. This is, to the best of our understanding, the first time that dual-targeting to different epitopes on the same receptor is examined. Nanocarriers were coated with a 1:1 ratio of anti-TfR-R17 and anti-TfR-8D3. To control for the difference in valency relative to parental carriers, binding of anti-TfR R17/8D3 NCs was compared to nanocarriers coated with a 1:1 ratio of R17 or 8D3 and control IgG. These nanocarriers (anti-TfR-R17/IgG NCs and anti-TfR-8D3/IgG NCs, respectively) displayed similar size, zeta potential, and total antibody surface-coating to anti-TfR-R17/8D3 NCs (Table 7).

Lowering targeting valency to ~ 50% that of parental nanocarriers had opposite effects on binding for nanocarriers targeted to epitopes R17 versus 8D3. Binding of anti-TfR-R17/IgG NCs was enhanced with respect to fully-coated anti-TfR-R17 NCs, whereas binding of anti-TfR-8D3 NCs worsened with lower valency (Figure 25). As a result, lowering valency nearly doubled binding of nanocarriers targeted to the R17 epitope, whereas binding of nanocarriers targeting the 8D3 epitope was lowered by half. The behavior observed for the 8D3 epitope is intuitive, since lowering valency reduces the avidity of NCs for the target epitope. This was similar to the behavior of anti-ICAM valency in the previous chapter, where binding

was reduced 3-fold as a result of halving the anti-ICAM valency. Yet, the behavior of anti-TfR-R17 NCs with valency is also plausible, as increasing valency past a certain threshold has been shown to lead to suboptimal binding for certain receptors.[130] In terms of binding, lowering valency may cause NCs to occupy fewer receptors per cell, allowing for a larger total number of NCs to bind the given receptor pool.[130]

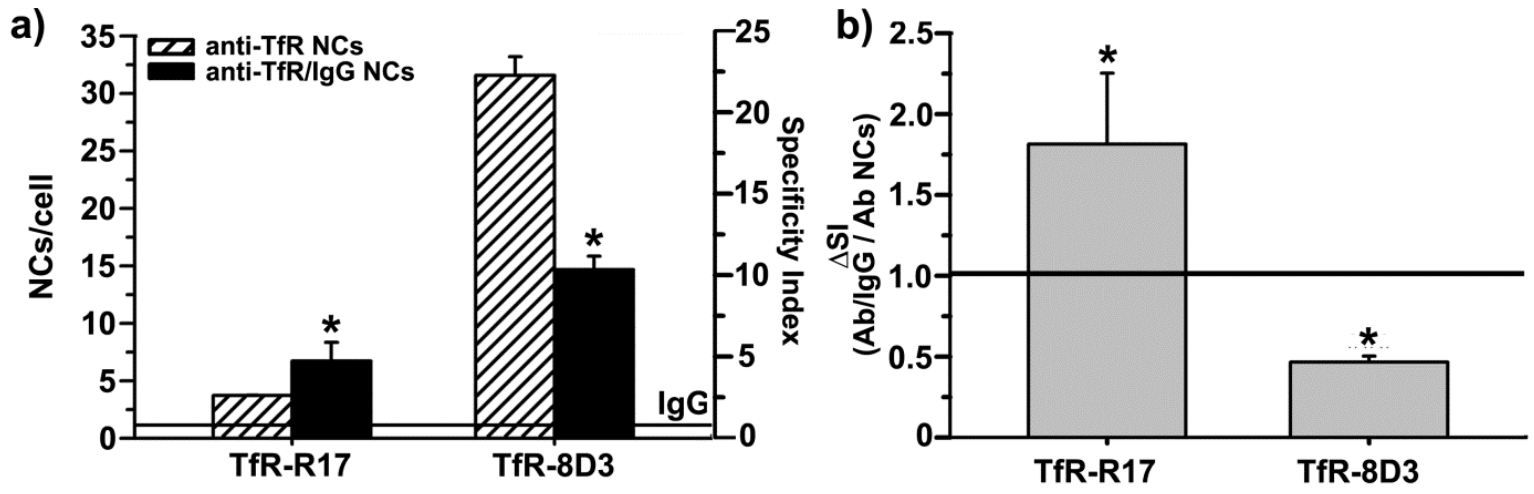

Figure 25. Effect of antibody valency on binding of antibody-coated nanocarriers targeted to TfR epitope 8D3 versus R17. (a-b) Binding was tested after incubation for 1 h at 37 °C in control H5V cells and analyzed by fluorescence microscopy to assess the mean number of nanocarriers per cell (NCs/cell) and specificity index (SI) for each formulation. Line in (a,b) indicates binding of control IgG. Data are mean ± S.E.M. *Compares nanocarriers coated with anti-TfR to nanocarriers coated with a 1:1 ratio of anti-TfR/IgG (1:1 coating of anti-TfR and control IgG). * represents $p < 0.05$ by Student's *t*-test.

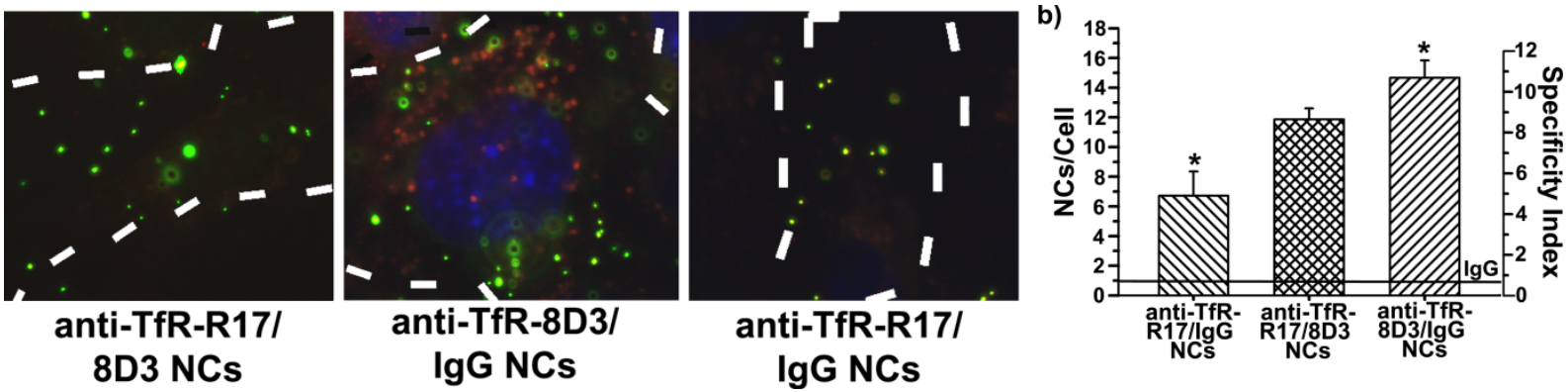

Figure 26. Binding of antibody-coated nanocarriers dually targeted TfR epitopes 8D3 and R17. (a-b) Binding was tested after incubation for 1 h at 37 °C in control H5V cells and analyzed by fluorescence microscopy to assess the number of nanocarriers per cell (NCs/cell) and specificity index (SI) for each formulation. Phase contrast images were used to delimit cell borders (dashed white lines). Scale bar is ~10μm. Line in (b) indicates binding of control IgG. Data are mean ± S.E.M. *Compares with anti-TfR R17/8D3 NCs. * represents $p < 0.05$ by Student's *t*-test.

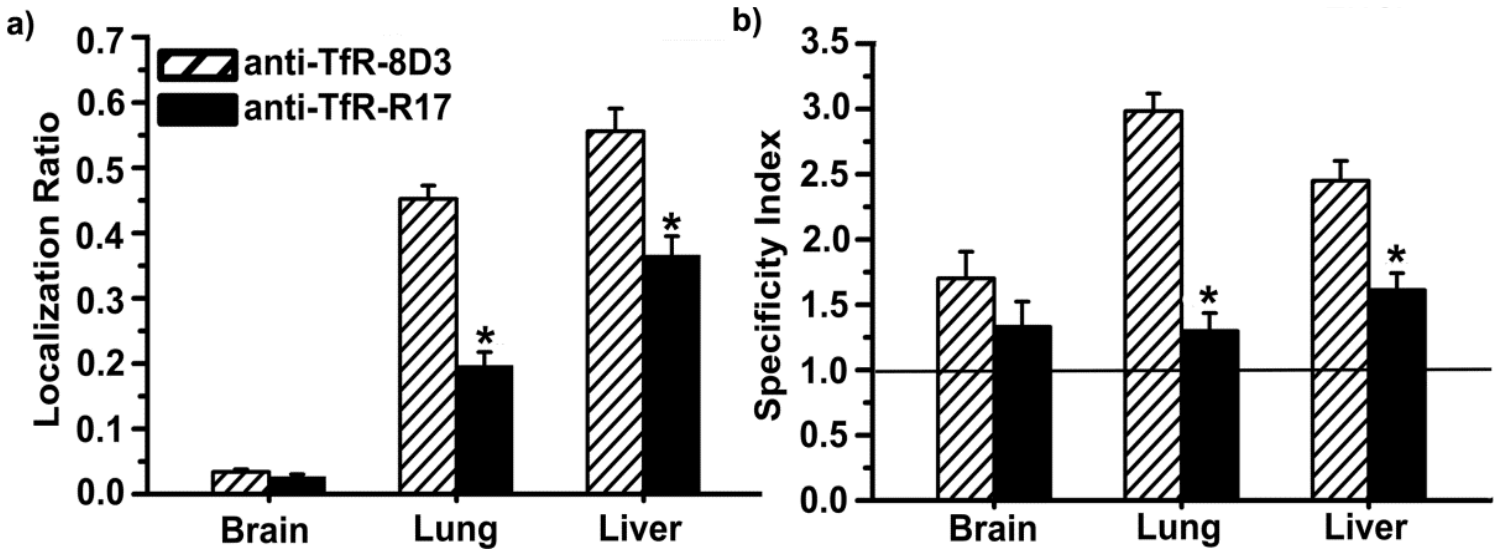

Figure 27. Biodistribution of anti-TfR-8D3 versus anti-TfR-R17 in mice. The localization ratio or LR (a) and specificity index orI (b) in brain, lungs, and liver were calculated as described (see Methods). Data are mean ± S.E.M. * Compares anti-TfR-8D3 vs. anti-TfR-R17. * represents $p < 0.05$ by Student's *t*-test.

Binding of anti-TfR-8D3/R17 NCs was intermediate of anti-TfR-R17/IgG NCs and anti-TfR-8D3/IgG NCs, respectively (Figure 26). Dual targeting of TfR epitopes R17 and 8D3 with nanocarriers, therefore, modulated cellular binding independently of nanocarrier valency. This suggests, for the first time, that targeting nanocarriers to multiple epitopes of the same receptor can be utilized as a strategy to modify nanocarrier binding, highlighting the rather overlooked relevance of precise epitope targeting and its implications in designing effective targeted drug delivery systems.

4.3.4. Biodistribution of antibodies vs. antibody-coated nanocarriers targeted to different TfR epitopes

We next tested the biodistribution of anti-TfR-8D3 versus anti-TfR-R17 *in vivo*. These antibodies were injected i.v. as naked ^{125}I-labeled counterparts in mice followed by organ analysis after euthanasia. As in previous cases, we focused on the brain, lungs, and liver as examples of central nervous system, peripheral, and clearance organs, respectively, yet additional data on kidneys, heart, and spleen are also provided in accompanying Table 8. As shown in Figure 27, both anti-TfR-8D3 and anti-TfR-R17 resulted in comparable (Figure 27a) and specific (SI value above 1) accumulation in brain (Figure 27b). Yet, they also accumulated considerably and specifically in other organs.

Anti-TfR-8D3 targeted TfR throughout the body more efficiently than anti-TfR-R17, yet the specificity of this antibody in peripheral organs exceeded its brain specificity, which was not observed in the case of anti-TfR-R17. This is despite the

fact that both antibodies have been reported to display similar affinity[234,236] and in agreement with greater targeting of anti-TfR-8D3 in cell culture (Figure 23). This result is also consistent with previous work showing the different biodistribution patterns of these antibodies *in vivo,*[132] which may be due to differential accessibility of their respective epitope targets, or different presence throughout the body of receptor isoforms predominantly exposing these particular epitopes. Indeed, previous works have shown differences in reactivity of anti-TfR antibodies to different cell lines or tissues *in vivo,*[237,238] and two TfR isoforms displaying distinct post-translational glycosylations have been reported in mice.[239]

Next, we assessed targeting of nanocarriers coated with anti-TfR-8D3 or anti-TfR-R17. Nanocarriers coated with anti-TfR-R17 or anti-TfR-8D3 both displayed increased accumulation in brain, lungs, and liver in comparison to their naked antibody counterparts (Figures 28a and 29a). This result pairs well with enhanced avidity of nanocarriers vs naked antibodies due to high valency and also indicates a different biodistribution pattern, as in the case of naked antibodies. Although brain still showed specific uptake for both types of nanocarriers (SI > 1), surprisingly, the targeting specificity of anti-TfR-8D3 NCs over control IgG NCs was decreased in lungs, liver, and slightly in brain in comparison to that of naked anti-TfR-8D3 (Figure 28b). This was in contrast to anti TfR-R17 NCs, which displayed only decreased specificity toward the liver, but not the brain or lungs (Figure 29b).

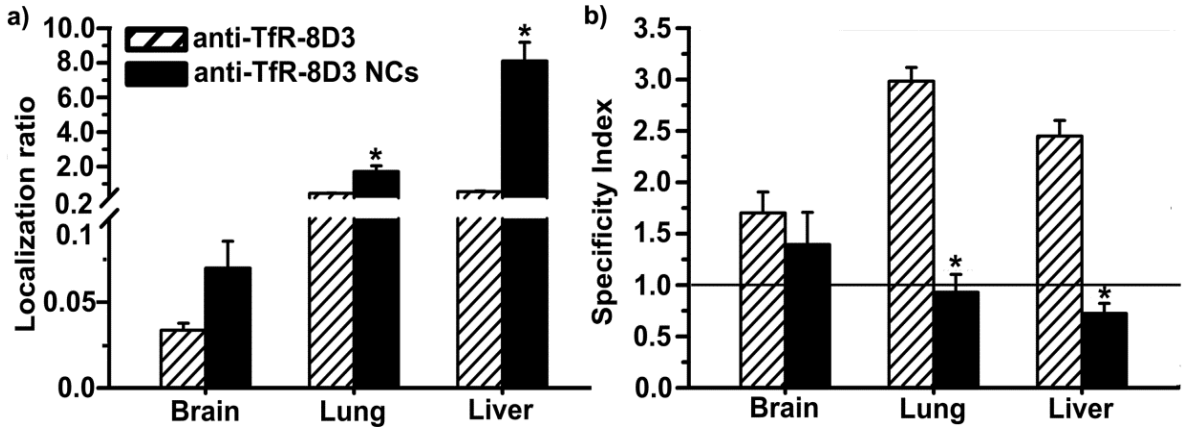

Figure 28. Biodistribution of anti-TfR-8D3 vs. nanocarriers coated with anti-TfR-8D3. Localization ratio (LR) and specificity index (SI) of brain, lungs, and liver are shown in (a) and (b), respectively. * Compares anti-TfR-8D3 vs. anti-TfR-8D3 NCs. Data are mean ± S.E.M. * represents $p < 0.05$ by Student's *t*-test.

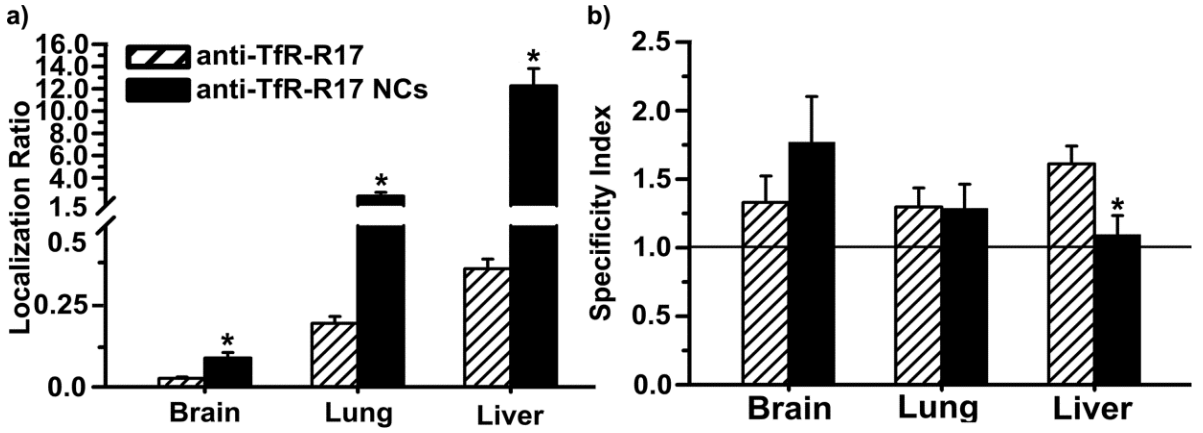

Figure 29. Biodistribution of anti-TfR-R17 vs. nanocarriers coated with anti-TfR-R17. (a) Localization ratio (LR) and (b) specificity index (SI) of brain, lungs, and liver. Data are mean ± S.E.M. * Compares anti-TfR-R17 vs. anti-TfR-R17 NCs. * represents $p < 0.05$ by Student's *t*-test.

Table 8. Biodistribution of antibodies and antibody-coated NCs targeted to different TfR epitopes.

Ab or NC	Blood	Kidney		Spleen		Heart		Lungs		Liver		Brain	
Antibody:	%ID	LR	SI	LR	SI	LR	SI	LR	SI	LR	SI	LR	SI
Anti-TfR-R17	57±9.7	0.1±0.00	0.5±0.1	0.1±0.00	0.7±0.1	1.1±0.4	7.2±2.8	0.2±0.0	1.3±0.1	0.4±0.0	1.6±0.1	0.03±0.00	1.3±0.2
Anti-TfR-8D3	42±1.3	0.6±0.00	2.3±0.1	0.1±0.00	1.2±0.1	0.6±0.1	4.2±0.4	0.5±0.0	3.0±0.1	0.6±0.0	2.5±0.2	0.03±0.00	1.7±0.2
Single:													
Anti-TfR-R17 NCs	6.8±0.7	0.6±0.00	1.1±0.1	0.5±0.06	1.2±0.2	23±3.9	1.5±0.3	2.4±0.3	1.3±0.2	12±1.6	1.1±0.1	0.09±0.02	1.8±0.3
Anti-TfR-8D3 NCs	7.8±1.2	0.3±0.00	0.7±0.1	0.3±0.00	0.8±0.1	38±6.4	2.5±0.4	1.7±0.3	0.9±0.2	8.1±1.1	0.7±0.1	0.07±0.02	1.4±0.3
Anti-TfR-R17/IgG NCs	5.3±0.4	0.5±0.08	1.0±0.1	0.4±0.04	1.0±0.1	18±1.1	1.2±0.1	1.6±0.4	0.9±0.2	13±2.6	1.2±0.2	0.08±0.02	1.7±0.4
Anti-TfR-8D3/IgG NCs	15±1.3	0.3±0.03	0.7±0.1	0.3±0.05	0.8±0.2	25±5.0	1.6±0.3	0.6±0.0	0.3±0.0	4.0±0.6	0.4±0.1	0.05±0.01	1.0±0.2
Dual:													
Anti-TfR-R17/8D3 NCs	11±1.3	0.3±0.03	0.7±0.1	0.3±0.04	0.8±0.1	28±4.4	1.8±0.3	1.3±0.4	0.7±0.2	7.6±1.2	0.7±0.1	0.03±0.00	0.7±0.1

Data are Mean±S.E.M.; %ID = percentage of injected dose; LR = Localization Ratio; SI = Specificity Index; Ab = antibody; NC = Nanocarrier. Anti-TfR-8D3 was clone 8D3 and anti-TfR-R17 was clone R17217.

Therefore, it appears that enhanced organ uptake of nanocarriers may be in part due to non-specific accumulation. This is in accord with results presented in the previous section showing that, despite enhanced valency, anti-TfR NCs pose steric hindrances leading to poor binding and suboptimal induction of endocytosis as compared to naked antibodies, according to TfR length and natural size restrictions of clathrin-coated pits.[208] In this situation, it is possible that anti-TfR NCs may bind non-specifically to Fc receptors in tissues, resulting in low specificity. Also, this effect seems to depend on the precise epitope targeted and, consequently, its different location and accessibility.

In general, anti-TfR-R17 NCs displayed more robust targeting versus anti-TfR-8D3 counterparts, as opposed to antibodies. A similar outcome has been observed for nanocarriers addressed to different epitopes of PECAM-1, where targeting to membrane proximal epitopes resulted in lack of nanocarrier targeting.[179] Greater targeting by anti-TfR-R17 NCs *in vivo* is opposite to greater targeting by anti-TfR-8D3 NCs in cell culture, also emphasizing differences in the presence/accessibility of their epitopes in different cell types and tissues.[132,237-239]

4.3.5. Biodistribution of antibody-coated carriers targeted to multiple TfR epitopes

We next examined the biodistribution of anti-TfR-R17/8D3 NCs. Interestingly, specific accumulation in organs depended more on the epitope targeted by anti-TfR-8D3 vs anti-TfR-R17 (Figure 30a). For instance, 50% reduction in valency did not impact targeting or specificity by anti-TfR-R17, while a similar reduction negatively impacted both parameters in the case of anti-TfR-8D3 (Figure 30a).

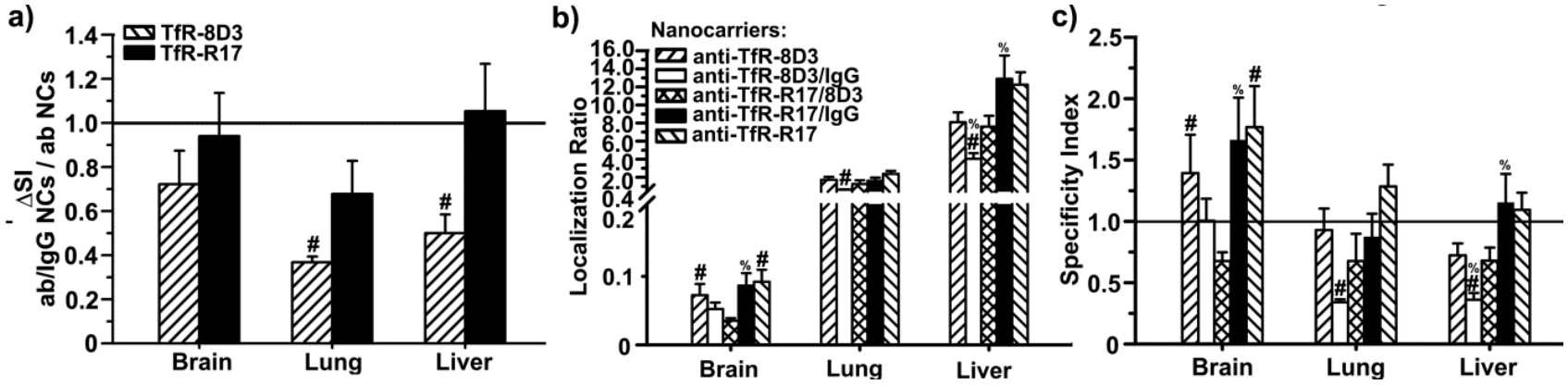

Figure 30. Biodistribution of antibody-coated nanocarriers dual targeted to TfR epitopes 8D3 and R17. (a) LR and (b) SI of brain, lungs, and liver are shown in (a) and (b), respectively. Data are mean ± S.E.M. * compares anti-TfR-R17 NCs to anti-TfR-8D3 NCs; # compares dual-coated NCs (either Ab/IgG or Ab1/Ab2) to their respective parental, single-targeted NCs; % compares anti-TfR-R17/8D3 NCs to control Ab/IgG NCs. *,#,% represents $p < 0.05$ by Student's *t*-test.

A 50% reduction in valency also decreased targeting to the anti-TfR 8D3 epitope in cell culture, while targeting to the anti-TfR-R17 epitope showed a modest, yet statistically significant, improvement. As compared to either parent nanocarrier, dually-targeted anti-TfR-R17/8D3 counterparts displayed reduced accumulation in brain and comparable pulmonary levels, while liver accumulation was similar to that of anti-TfR-8D3 NCs and lower than for anti-TfR-R17 counterparts (Figure 30b). In addition, anti-TfR-R17/8D3 NCs lost targeting specificity for all three organs, as their SI value fell below 1 (Figure 30c). These effects could in theory be explained by reduced overall avidity of dually-targeted nanocarriers toward each independent epitope on TfR. Indeed, the specificity of anti-TfR-R17/8D3 in liver and lung had an intermediate value compared to that of single-targeted nanocarriers coated at similar valencies (anti-TfR-R17/IgG and anti-TfR-8D3/IgG; Figure 30c). However, this was not the case for brain, where dually-targeted nanocarriers accumulated below the level of both anti-TfR/IgG counterparts. It is possible that binding to two TfR epitopes may modify the conformation of the receptor so that exposure and, hence, binding to these epitopes may become impaired, displacing the antigen–antibody equilibrium toward the unbound form. Conceivable, this phenomenon could impact firm binding of dually-targeted nanocarriers at different extents in tissues expressing different receptor isoforms,[237,238] such as those displaying different post-translational glycosylations.[239] However, at present, the distribution of these TfR glycoforms in brain vs. other organs remains uncharacterized.

4.3.6. Conclusion

Combination targeting to multiple epitopes of the same receptor may aid in enhancing or controlling the delivery of nanocarriers, but this hypothesis remained unexplored to this point. Selection of anti-TfR 8D3 versus R17 antibodies resulted in differential binding to cells and biodistribution *in vivo* when examined as free antibodies, differential response to formatting as targeted nanocarriers versus free antibodies, and differential binding when formatted as targeted nanocarries, thus demonstrating the importance of epitope selection for optimizing targeting to TfR. Targeting multiple TfR epitopes with a single nanocarrier modified binding in cell cultures and biodistribution *in vivo*, and this constitutes the first evidence that this approach can be utilized to control the distribution of nanomedicines. Importantly, modification was independent of ligand valency, affirming that the strategy itself accounted for the observed binding and biodistribution modifications. Collectively, these results highlight the role of precise epitope targeting in drug delivery, the dependency on cell and tissue type (apart from other factors), and the unpredictability of these outcomes, yet indicating for the first time that combined targeting to multiple epitopes of a single cell-surface receptor may help modify the biodistribution of nanomedicines.

Section 5. Overall conclusions

5.1 Summary.

Despite concerted efforts over the past few decades, precise delivery of pharmaceutical agents remains a complex, yet important challenge. Indeed, many diseases (common or rare, morbid or mortal, chronic or acute, local or systemic) could be treated more effectively by addressing this problem. A promising approach in this regard is the development of targeted drug delivery systems which enhance accumulation at the intended site and reduce delivery to off-target areas. Yet, targeting single cell-surface molecules presents certain limitations such as improved but still suboptimal accumulation in many organs/tissues (e.g accumulation in tumors, brain, kidneys, heart), due to lack of selective and heterogeneous (spatially and temporally) expression of the target molecule at the intended site. Intracellular delivery can also be challenging using nanocarriers targeted to single receptors, as valency and size requirements of nanocarriers can limit their efficiency. Combination-targeting has recently arisen as a strategy to address these issues, yet it remains a nascent field with few systematic studies examining effects of this approach in general terms, both in cell cultures and *in vivo*.

This dissertation provides significant evidence validating the overall hypothesis that combination targeting can enhance and/or modify the binding, endocytosis, and biodistribution of polymer nanocarriers in different contexts and to different extents. With regard to targeting polymer nanocarriers to multiple Ig-like CAMs, the binding level and selectivity of multi-CAM targeted nanocarriers for

diseased vs. control cells can be modified using different combinations of CAMs or by the multiplicity of affinity moieties utilized. Internalization of multi-CAM-targeted nanocarriers appears enhanced by targeting receptors associated with different endocytic pathways (CAM- and clathrin-mediated endocytosis), rather than targeting multiple receptors associated with the same endocytic pathway (CAM-endocytosis). Yet, the rate of internalization is efficent regardless of the combination or multiplicity of affinity moieties utilized. Multi-CAM-targeted can also modify *in vivo* performance. Dual targeted combinations enhance specificity for organs, but triple-targeting provides the best performance *in vivo* of the combinations tested, enabling relatively higher specifity in control and particularly diseased tissues of nanocarriers and associated therapeutic cargo.

In the case of multiple receptors with different functions, exemplified by ICAM-1 and TFR in this work, combination targeting also appears useful for modifying binding, internalization, or biodistribution of polymer nanocarriers. The different biological attributes (e.g. function, response to pathology, and endocytic activity) of ICAM-1 and TfR affected their drug delivery performance. Whereas binding to ICAM or TfR with antibodies is fairly similar, internalization is favored in the case of TfR-targeting. However ICAM-1 targeting was favored in terms of binding to cells in inflammatory-like conditions, with relatively larger and multivalent NCs, and in terms of nanocarrier internalization. Performance *in vivo* indicated that both TfR- and ICAM-1 targeting enhanced accumulation in organs where TfR-targeting appeared more effective with free antibodies than targeted

nanocarriers, and ICAM-1 targeting improved when targeted with NCs and appeared best overall. Dual-targeting of TfR and ICAM-1 modified binding of nanocarriers to cells, yet was lower than nanocarriers dual-targeted to CAMs. This affirms that targeting receptors of the same or different functions are both viable approaches to control nanocarrier binding. Dual-targeting of ICAM-1 and TfR enhanced nanocarrier internalization compared with single-targeting of TfR and slightly (although not significantly) compared with single-targeting of ICAM-1, which, as observed with PECAM-1/VCAM-1 targeting, supports that targeting receptors associated with different endocytic pathways may improve nanocarrier internalization. *In vivo*, accumulation of dual-targeted nanocarriers in different organs was ruled by ICAM-1 (lungs) or TfR (brain), suggesting that targeting multiple receptors with different functions and endocytic activity modified the biodistribution and delivery of associated therapeutic cargo.

Finally, we demonstrated for the first time that targeting polymer nanocarriers to multiple epitopes of the same receptor may also aid in modulating the delivery of nanocarriers. Differential binding of nanocarriers observed when addressed to distinct TfR epitopes also occurs with dual targeting of nanocarriers targeted toward TfR epitopes with a single nanocarrier and independently of ligand valency. A similar result can also be attained *in vivo*, where differential accumulation and specificity for tissues of nanocarriers addressed to distinct TfR epitopes was also demonstrated when targeting multiple TfR epitopes, suggesting that combined targeting to multiple

epitopes of a single cell-surface receptor may help modify the binding and biodistribution of nanomedicines.

Overall, whether nanocarriers are directed to multiple receptors of similar or different functions, or to multiple epitopes of the same receptor, combination targeting enhances, decreases, or results in a similar level of targeting to cells and in vivo accumulation in organs depending on the combination of receptors or epitopes targeted, physiological versus pathological status, and also on the particular target organ. Consequently, combination targeting can be utilized to modulate targeting performance. Combination targeting also allows modulation of nanocarrier internalization whether targeting receptors of similar or different functions, and targeting receptors associated with different pathways (CAM- and clathrin-mediated endocytosis) seems more favorable than targeting receptors associated with the same pathway. In all contexts examined, the modulatory behavior could not be predicted, which indicates the necessity of exploring strategies for combination targeting experimentally.

5.2. Future Directions

Although these studies provided relevant insight and affirm that combination targeting using the three strategies described may be utilized to modify the binding, internalization, and/or biodistribution of nanocarriers, several questions are relevant to supplementing and expanding this work. Future studies should examine in more depth the effects of combination targeting to receptors with the same versus different

physiological functions. For example, competition studies could verify whether multi-targeted formulations bind to more than one of their targets, and to what extent. This will provide insight into the relative contribution of each of the targets to binding, and also on the binding behavior (synergistic vs. additive). Such a study can be performed in cell culture by evaluating nanocarrier binding in the presence of free ligands to provide competition for the target receptor. This type of study is also possible *in vivo*, but would likely be more costly due to need for larger amounts of ligand (e.g. antibody, which is expensive).

Another useful experiment would be to evaluate which pathways are induced during endocytosis of multi-targeted nanocarriers. Presumably, targeting multiple receptors induces the pathways associated with each receptor, yet this is unknown. Also, the extent of endocytic activation, uptake kinetics, intracellular route and fate may differ when multiple pathways (or a single pathway via multiple receptors) are stimulated. In addition, this type of stimulation may induce novel uncharacterized mechanisms of uptake. This study can be done by performing internalization experiments in the presence of pharmacological agents or siRNA to inhibit particular mechanisms of endocytosis. *In vivo*, it may be possible to perform such a study by employing knockout mouse models which lack proteins critical to particular mechanisms of endocytosis, although some of these may not be available due to pre-mature lethality as a result of the phenotype.

The effect of nanocarrier (size, shape, composition) and ligand (size, valency, stiffness) characteristics should also be evaluated to gain more detailed insight in the performance of these systems and how they may be optimized for particular applications. This type of characterization would be valuable for designing combination targeting strategies for particular applications, and it is difficult to predict *a priori* how these parameters will affect the overall delivery performance because varying a single parameter can have multiple and opposing effects. For example, increasing the valency of ligands on the nanocarrier surface does not necessarily increase avidity for the target receptor (see Background on the role of size and valency on nanocarrier performance). This can be examined by titrating these parameters in cell cultures or *in vivo.* In addition, studies examining the cellular localization of combined-targeted nanocarriers *in vivo* would be particulary helpful to determine presence in particular tissues and define the application accordingly. This could be examined using immunohistochemistry or by energy-dispersive X-ray spectroscopy of nanocarriers loaded with an iron core.

Transport of multi-targeted nanocarriers across cellular barriers remains a virtually untouched area in the literature, and could be explored by varying the coating ratios of ligands systematically to examine whether the fraction of internalized carriers which are transported across cells can be modulated. This may be examined using cells cultured on transwell filters, or *in vivo* using fractionation techniques (e.g. capillary depletion) to differentiate accumulation in the vasculature vs. the tissue parenchyma. Combination targeting along with more precise control of

ligand display on the particular surface by adding ligands to particular "patches" or domains may allow for greater control over modulation of targeting performance, and as a result more precise adaptation of nanocarriers for particular applications.[197,198] Although much remains to be learned with respect to combination targeting, the promise of this approach is considerable as it allows the drug delivery system to be endowed with targeting capability by combining properties of existing targets which can be optimized, rather than having to discover new targets.

5.3. Publications

As a result of this dissertation, the following publications have been produced. A review paper summarizing the field with insights for future research is planned:

-**Papademetriou I**, Muro S. Combination-targeting to multiple endothelial cell adhesion molecules modulates binding, endocytosis, and in vivo biodistribution of drug nanocarriers and their therapeutic cargoes (Submitted).

-Ansar M, Bhowmick T, **Papademetriou I**, Serrano D, Muro S. Biological functionalization of drug delivery carriers to bypass size restrictions of receptor-mediated endocytosis independently from receptor-targeting (Under revision, ACS Nano).

-**Papademetriou I**, Garnacho C, Muro S. (2013) In vivo performance of nanocarriers dually-targeted to epitopes of the same versus different receptors. Biomaterials. 34(13):3459-66.

-**Papademetriou J**, Garnacho C, Serrano D, Bhowmick T, Schuchman EH, Muro S. (2013) Comparative binding, endocytosis, and biodistribution of antibodies and antibody-coated carriers for targeted delivery of lysosomal enzymes to ICAM-1 versus transferrin receptor. J Inherit Metab Dis. 36(3):467-77.

References

1.Torchilin VP. Drug targeting. *Eur J Pharm Sci* 2000;**11 Suppl 2**:S81-91.

2.Langer R. Drug delivery and targeting. *Nature* 1998;**392**:5-10.

3.Muro S. Challenges in design and characterization of ligand-targeted drug delivery systems. *J Control Release* 2012;**164**:125-37.

4.Bae YH, Park K. Targeted drug delivery to tumors: myths, reality and possibility. *J Control Release* 2011;**153**:198-205.

5.Muro S. New biotechnological and nanomedicine strategies for treatment of lysosomal storage disorders. *Wiley Interdiscip Rev Nanomed Nanobiotechnol* 2010;**2**:189-204.

6.Pardridge WM. Biopharmaceutical drug targeting to the brain. *J Drug Target* 2010;**18**:157-67.

7.Veeranarayanan S, Poulose AC, Mohamed MS, Varghese SH, Nagaoka Y, Yoshida Y, et al. Synergistic Targeting of Cancer and Associated Angiogenesis Using Triple-Targeted Dual-Drug Silica Nanoformulations for Theragnostics. *Small* 2012;**8**:3476-89.

8.Muzykantov VR, Radhakrishnan R, Eckmann DM. Dynamic factors controlling targeting nanocarriers to vascular endothelium. *Curr Drug Metab* 2012;**13**:70-81.

9.Kamaly N, Xiao Z, Valencia PM, Radovic-Moreno AF, Farokhzad OC. Targeted polymeric therapeutic nanoparticles: design, development and clinical translation. *Chem Soc Rev* 2012;**41**:2971-3010.

10.Grove J, Marsh M. The cell biology of receptor-mediated virus entry. *J Cell Biol* 2011;**195**:1071-82.

11.Smith CW. 3. Adhesion molecules and receptors. *J Allergy Clin Immunol* 2008;**121**:S375-9; quiz S414.

12.McAteer MA, Schneider JE, Ali ZA, Warrick N, Bursill CA, von zur Muhlen C, et al. Magnetic resonance imaging of endothelial adhesion molecules in mouse atherosclerosis using dual-targeted microparticles of iron oxide. *Arterioscler Thromb Vasc Biol* 2008;**28**:77-83.

13.Zhang Y, Zhu C, Pardridge WM. Antisense gene therapy of brain cancer with an artificial virus gene delivery system. *Mol Ther* 2002;**6**:67-72.

14.Saul JM, Annapragada AV, Bellamkonda RV. A dual-ligand approach for enhancing targeting selectivity of therapeutic nanocarriers. *J Control Release* 2006;**114**:277-87.

15.Chacko A-M, Nayak M, Greineder CF, Delisser HM, Muzykantov VR. Collaborative Enhancement of Antibody Binding to Distinct PECAM-1 Epitopes Modulates Endothelial Targeting. *PloS one* 2012;**7**:e34958.

16.Han J, Zern BJ, Shuvaev VV, Davies PF, Muro S, Muzykantov V. Acute and chronic shear stress differently regulate endothelial internalization of nanocarriers targeted to platelet-endothelial cell adhesion molecule-1. *ACS Nano* 2012;**6**:8824-36.

17.Bhowmick T, Berk E, Cui X, Muzykantov VR, Muro S. Effect of flow on endothelial endocytosis of nanocarriers targeted to ICAM-1. *J Control Release* 2012;**157**:485-92.

18.Moghimi SM, Hunter AC, Murray JC. Long-circulating and target-specific nanoparticles: theory to practice. *Pharmacol Rev* 2001;**53**:283-318.

19.Ghaffarian R, Bhowmick T, Muro S. Transport of nanocarriers across gastrointestinal epithelial cells by a new transcellular route induced by targeting ICAM-1. *J Control Release* 2012;**163**:25-33.

20.Duncan R, Richardson SC. Endocytosis and intracellular trafficking as gateways for nanomedicine delivery: opportunities and challenges. *Mol Pharm* 2012;**9**:2380-402.

21.Serrano D, Muro S. Endothelial Cell Adhesion Molecules and Drug Delivery Applications. In: Aranda-Espinoza H, editor. Mechanobiology of the Endothelium. Maryland: Science Publishers; 2014.

22.Dienst A, Grunow A, Unruh M, Rabausch B, Nor JE, Fries JW, et al. Specific occlusion of murine and human tumor vasculature by VCAM-1-targeted recombinant fusion proteins. *J Natl Cancer Inst* 2005;**97**:733-47.

23.Ferrante EA, Pickard JE, Rychak J, Klibanov A, Ley K. Dual targeting improves microbubble contrast agent adhesion to VCAM-1 and P-selectin under flow. *J Control Release* 2009;**140**:100-7.

24.Serres S, Mardiguian S, Campbell SJ, McAteer MA, Akhtar A, Krapitchev A, et al. VCAM-1-targeted magnetic resonance imaging reveals subclinical disease in a mouse model of multiple sclerosis. *FASEB J* 2011;**25**:4415-22.

25.Kozower BD, Christofidou-Solomidou M, Sweitzer TD, Muro S, Buerk DG, Solomides CC, et al. Immunotargeting of catalase to the pulmonary endothelium alleviates oxidative stress and reduces acute lung transplantation injury. *Nat Biotechnol* 2003;**21**:392-8.

26.Dziubla TD, Shuvaev VV, Hong NK, Hawkins BJ, Madesh M, Takano H, et al. Endothelial targeting of semi-permeable polymer nanocarriers for enzyme therapies. *Biomaterials* 2008;**29**:215-27.

27.Ding BS, Hong N, Christofidou-Solomidou M, Gottstein C, Albelda SM, Cines DB, et al. Anchoring Fusion Thrombomodulin to the Endothelial Lumen Protects against Injury-induced Lung Thrombosis and Inflammation. *Am J Respir Crit Care Med* 2009;**180**:247-56.

28.Murciano J-C, Muro S, Koniaris L, Christofidou-Solomidou M, Harshaw DW, Albelda SM, et al. ICAM-directed vascular immunotargeting of antithrombotic agents to the endothelial luminal surface. *Blood* 2003;**101**:3977-84.

29.Hamilton AJ, Huang SL, Warnick D, Rabbat M, Kane B, Nagaraj A, et al. Intravascular ultrasound molecular imaging of atheroma components in vivo. *J Am Coll Cardiol* 2004;**43**:453-60.

30.Weller GE, Villanueva FS, Tom EM, Wagner WR. Targeted ultrasound contrast agents: in vitro assessment of endothelial dysfunction and multi-targeting to ICAM-1 and sialyl Lewisx. *Biotechnol Bioeng* 2005;**92**:780-8.

31.Choi KS, Kim SH, Cai QY, Kim SY, Kim HO, Lee HJ, et al. Inflammation-specific T1 imaging using anti-intercellular adhesion molecule 1 antibody-conjugated gadolinium diethylenetriaminepentaacetic acid. *Mol Imaging* 2007;**6**:75-84.

32.Kim K, Huang SW, Ashkenazi S, O'Donnell M, Agarwal A, Kotov NA, et al. Photoacoustic imaging of early inflammatory response using gold nanorods. *Applied Physics Letters* 2007;**90**:223901.

33.Zhang N, Chittasupho C, Duangrat C, Siahaan TJ, Berkland C. PLGA nanoparticle--peptide conjugate effectively targets intercellular cell-adhesion molecule-1. *Bioconjug Chem* 2008;**19**:145-52.

34.Gunawan RC, Auguste DT. Immunoliposomes That Target Endothelium In Vitro Are Dependent on Lipid Raft Formation. *Mol Pharm* 2010;**7**:1569-75.

35.Park S, Kang S, Veach AJ, Vedvyas Y, Zarnegar R, Kim JY, et al. Self-assembled nanoplatform for targeted delivery of chemotherapy agents via affinity-regulated molecular interactions. *Biomaterials* 2010;**31**:7766-75.

36.Shao X, Zhang H, Rajian JR, Chamberland DL, Sherman PS, Quesada CA, et al. 125I-labeled gold nanorods for targeted imaging of inflammation. *ACS Nano* 2011;**5**:8967-73.

37.Garnacho C, Serrano D, Muro S. A fibrinogen-derived peptide provides intercellular adhesion molecule-1-specific targeting and intraendothelial transport of polymer nanocarriers in human cell cultures and mice. *J Pharmacol Exp Ther* 2012;**340**:638-47.

38.Hsu J, Northrup L, Bhowmick T, Muro S. Enhanced delivery of alpha-glucosidase for Pompe disease by ICAM-1-targeted nanocarriers: comparative performance of a strategy for three distinct lysosomal storage disorders. *Nanomedicine* 2012;**8**:731-9.

39.Ding B-S, Hong N, Murciano J-C, Ganguly K, Gottstein C, Christofidou-Solomidou M, et al. Prophylactic thrombolysis by thrombin-activated latent prourokinase targeted to PECAM-1 in the pulmonary vasculature. *Blood* 2008;**111**:1999-2006.

40.Wu D, Pardridge WM. Neuroprotection with noninvasive neurotrophin delivery to the brain. *Proc Natl Acad Sci U S A* 1999;**96**:254-9.

41.Zhang Y, Pardridge WM. Neuroprotection in transient focal brain ischemia after delayed intravenous administration of brain-derived neurotrophic factor conjugated to a blood-brain barrier drug targeting system. *Stroke* 2001;**32**:1378-84.

42.Zhang Y, Pardridge WM. Conjugation of brain-derived neurotrophic factor to a blood-brain barrier drug targeting system enables neuroprotection in regional brain ischemia following intravenous injection of the neurotrophin. *Brain Res* 2001;**889**:49-56.

43.Song BW, Vinters HV, Wu D, Pardridge WM. Enhanced neuroprotective effects of basic fibroblast growth factor in regional brain ischemia after conjugation to a blood-brain barrier delivery vector. *J Pharmacol Exp Ther* 2002;**301**:605-10.

44.Lee HJ, Zhang Y, Zhu C, Duff K, Pardridge WM. Imaging brain amyloid of Alzheimer disease in vivo in transgenic mice with an Abeta peptide radiopharmaceutical. *J Cereb Blood Flow Metab* 2002;**22**:223-31.

45.Kurihara A, Pardridge WM. Imaging brain tumors by targeting peptide radiopharmaceuticals through the blood-brain barrier. *Cancer Res* 1999;**59**:6159-63.

46.Suzuki T, Wu D, Schlachetzki F, Li JY, Boado RJ, Pardridge WM. Imaging endogenous gene expression in brain cancer in vivo with 111In-peptide nucleic acid antisense radiopharmaceuticals and brain drug-targeting technology. *J Nucl Med* 2004;**45**:1766-75.

47.Wu D, Pardridge WM. Central nervous system pharmacologic effect in conscious rats after intravenous injection of a biotinylated vasoactive intestinal peptide analog coupled to a blood-brain barrier drug delivery system. *J Pharmacol Exp Ther* 1996;**279**:77-83.

48.Leavy O. Therapeutic antibodies: past, present and future. *Nat Rev Immunol* 2010;**10**:297.

49.Vellard M. The enzyme as drug: application of enzymes as pharmaceuticals. *Curr Opin Biotechnol* 2003;**14**:444-50.

50.Bouchard PR, Hutabarat RM, Thompson KM. Discovery and development of therapeutic aptamers. *Annu Rev Pharmacol Toxicol* 2010;**50**:237-57.

51.de Fougerolles A, Vornlocher HP, Maraganore J, Lieberman J. Interfering with disease: a progress report on siRNA-based therapeutics. *Nat Rev Drug Discov* 2007;**6**:443-53.

52.Taniyama Y, Azuma J, Kunugiza Y, Iekushi K, Rakugi H, Morishita R. Therapeutic option of plasmid-DNA based gene transfer. *Curr Top Med Chem* 2012;**12**:1630-7.

53.Guy B. Adjuvants for Protein- and Carbohydrate-Based Vaccines In: Guo Z, Boons G-J, editors. Carbohydrate-Based Vaccines and Immunotherapies. Hoboken: John Wiley & Sons; 2008. p. 89-115.

54.Rosenberg SA, Yang JC, Restifo NP. Cancer immunotherapy: moving beyond current vaccines. *Nat Med* 2004;**10**:909-15.

55.Pan D, Caruthers SD, Senpan A, Schmieder AH, Wickline SA, Lanza GM. Revisiting an old friend: manganese-based MRI contrast agents. *Wiley Interdiscip Rev Nanomed Nanobiotechnol* 2010;**3**:162-73.

56.Sheets NC, Wang A. Radioisotopes and Nanomedicine. In: Singh PN, editor. Radioisotopes - Applications in Bio-Medical Science. Rijeka: InTech; 2011. p. 47-66.

57.Luo S, Zhang E, Su Y, Cheng T, Shi C. A review of NIR dyes in cancer targeting and imaging. *Biomaterials* 2011;**32**:7127-38.

58.Weissleder R, Pittet MJ. Imaging in the era of molecular oncology. *Nature* 2008;**452**:580-9.

59.Stride E, Saffari N. Microbubble ultrasound contrast agents: a review. *Proc Inst Mech Eng H* 2003;**217**:429-47.

60.Musacchio T, Torchilin VP. siRNA delivery: from basics to therapeutic applications. *Front Biosci* 2013;**18**:58-79.

61.Craparo EF, Bondi ML. Application of polymeric nanoparticles in immunotherapy. *Curr Opin Allergy Clin Immunol* 2012;**12**:658-64.

62.Ruiz-Garcia A, Bermejo M, Moss A, Casabo VG. Pharmacokinetics in drug discovery. *J Pharm Sci* 2008;**97**:654-90.

63.Dingemanse J, Appel-Dingemanse S. Integrated pharmacokinetics and pharmacodynamics in drug development. *Clin Pharmacokinet* 2007;**46**:713-37.

64.Williams HD, Trevaskis NL, Charman SA, Shanker RM, Charman WN, Pouton CW, et al. Strategies to address low drug solubility in discovery and development. *Pharmacol Rev* 2013;**65**:315-499.

65.Owens DE, 3rd, Peppas NA. Opsonization, biodistribution, and pharmacokinetics of polymeric nanoparticles. *Int J Pharm* 2006;**307**:93-102.

66.Ishida T, Atobe K, Wang X, Kiwada H. Accelerated blood clearance of PEGylated liposomes upon repeated injections: effect of doxorubicin-encapsulation and high-dose first injection. *J Control Release* 2006;**115**:251-8.

67.Pardridge WM. Drug transport across the blood-brain barrier. *J Cereb Blood Flow Metab* 2012;**32**:1959-72.

68.Matsumura Y, Maeda H. A new concept for macromolecular therapeutics in cancer chemotherapy: mechanism of tumoritropic accumulation of proteins and the antitumor agent smancs. *Cancer Res* 1986;**46**:6387-92.

69.Gabor F, Fillafer C, Neutsch L, Ratzinger G, Wirth M. Improving oral delivery. *Handb Exp Pharmacol* 2010;345-98.

70.Prow TW, Grice JE, Lin LL, Faye R, Butler M, Becker W, et al. Nanoparticles and microparticles for skin drug delivery. *Adv Drug Deliv Rev* 2011;**63**:470-91.

71.Cryan SA, Sivadas N, Garcia-Contreras L. In vivo animal models for drug delivery across the lung mucosal barrier. *Adv Drug Deliv Rev* 2007;**59**:1133-51.

72.Lai SK, Wang YY, Hanes J. Mucus-penetrating nanoparticles for drug and gene delivery to mucosal tissues. *Adv Drug Deliv Rev* 2009;**61**:158-71.

73.Bareford LM, Swaan PW. Endocytic mechanisms for targeted drug delivery. *Adv Drug Deliv Rev* 2007;**59**:748-58.

74.Vicent MJ, Duncan R. Polymer conjugates: nanosized medicines for treating cancer. *Trends Biotechnol* 2006;**24**:39-47.

75.Caldwell J, Gardner I, Swales N. An introduction to drug disposition: the basic principles of absorption, distribution, metabolism, and excretion. *Toxicol Pathol* 1995;**23**:102-14.

76.Lin JH, Lu AY. Role of pharmacokinetics and metabolism in drug discovery and development. *Pharmacol Rev* 1997;**49**:403-49.

77.Uhrich KE, Cannizzaro SM, Langer RS, Shakesheff KM. Polymeric systems for controlled drug release. *Chem Rev* 1999;**99**:3181-98.

78.Allen TM, Cullis PR. Drug delivery systems: entering the mainstream. *Science* 2004;**303**:1818-22.

79.Baumann A. Early development of therapeutic biologics--pharmacokinetics. *Curr Drug Metab* 2006;**7**:15-21.

80.Bendayan R, Lee G, Bendayan M. Functional expression and localization of P-glycoprotein at the blood brain barrier. *Microsc Res Tech* 2002;**57**:365-80.

81.LaVan DA, McGuire T, Langer R. Small-scale systems for in vivo drug delivery. *Nat Biotechnol* 2003;**21**:1184-91.

82.Duncan R. The dawning era of polymer therapeutics. *Nat Rev Drug Discov* 2003;**2**:347-60.

83.Torchilin VP. Multifunctional nanocarriers. *Adv Drug Deliv Rev* 2006;**58**:1532-55.

84.Bangham AD, Standish MM, Watkins JC. Diffusion of univalent ions across the lamellae of swollen phospholipids. *J Mol Biol* 1965;**13**:238-52.

85.Torchilin VP. Liposomes as targetable drug carriers. *Crit Rev Ther Drug Carrier Syst* 1985;**2**:65-115.

86.Gregoriadis G. Overview of liposomes. *J Antimicrob Chemother* 1991;**28 Suppl B**:39-48.

87.Immordino ML, Dosio F, Cattel L. Stealth liposomes: review of the basic science, rationale, and clinical applications, existing and potential. *Int J Nanomedicine* 2006;**1**:297-315.

88.Gregoriadis G, Senior J. The phospholipid component of small unilamellar liposomes controls the rate of clearance of entrapped solutes from the circulation. *FEBS Lett* 1980;**119**:43-6.

89.Torchilin VP. Recent advances with liposomes as pharmaceutical carriers. *Nat Rev Drug Discov* 2005;**4**:145-60.

90.Pai SS, Tilton RD, Przybycien TM. Poly(ethylene glycol)-modified proteins: implications for poly(lactide-co-glycolide)-based microsphere delivery. *AAPS J* 2009;**11**:88-98.

91.Danhier F, Ansorena E, Silva JM, Coco R, Le Breton A, Preat V. PLGA-based nanoparticles: an overview of biomedical applications. *J Control Release* 2012;**161**:505-22.

92.Bernkop-Schnurch A, Dunnhaupt S. Chitosan-based drug delivery systems. *Eur J Pharm Biopharm* 2012;**81**:463-9.

93.Matricardi P, Meo CD, Coviello T, Alhaique F. Recent advances and perspectives on coated alginate microspheres for modified drug delivery. *Expert Opin Drug Deliv* 2008;**5**:417-25.

94.Park K. Albumin: a versatile carrier for drug delivery. *J Control Release* 2012;**157**:3.

95.Champion JA, Katare YK, Mitragotri S. Particle shape: a new design parameter for micro- and nanoscale drug delivery carriers. *J Control Release* 2007;**121**:3-9.

96.Hsu J, Muro, S. Nanomedicine and drug delivery strategies for treatment of genetic diseases. In: Plaseska-Karanfilska D, editor. Human genetic diseases. Rijeka, Croatia: InTech.; 2011. p. 241-66.

97.Parveen S, Misra R, Sahoo SK. Nanoparticles: a boon to drug delivery, therapeutics, diagnostics and imaging. *Nanomedicine* 2012;**8**:147-66.

98.Beija M, Salvayre R, Lauth-de Viguerie N, Marty JD. Colloidal systems for drug delivery: from design to therapy. *Trends Biotechnol* 2012;**30**:485-96.

99.Discher BM, Won YY, Ege DS, Lee JC, Bates FS, Discher DE, et al. Polymersomes: tough vesicles made from diblock copolymers. *Science* 1999;**284**:1143-6.

100.Medina SH, El-Sayed ME. Dendrimers as carriers for delivery of chemotherapeutic agents. *Chem Rev* 2009;**109**:3141-57.

101.Lee CC, MacKay JA, Frechet JM, Szoka FC. Designing dendrimers for biological applications. *Nat Biotechnol* 2005;**23**:1517-26.

102.Jansen JF, de Brabander-van den Berg EM, Meijer EW. Encapsulation of guest molecules into a dendritic box. *Science* 1994;**266**:1226-9.

103.Sadekar S, Ghandehari H. Transepithelial transport and toxicity of PAMAM dendrimers: implications for oral drug delivery. *Adv Drug Deliv Rev* 2012;**64**:571-88.

104.Torchilin VP. Micellar nanocarriers: pharmaceutical perspectives. *Pharm Res* 2007;**24**:1-16.

105.Brodin A, Nyqvist-Mayer A. In vitro release studies on lidocaine aqueous solutions, micellar solutions, and o/w emulsions. *Acta Pharm Suec* 1982;**19**:267-84.

106.Azeem A, Anwer MK, Talegaonkar S. Niosomes in sustained and targeted drug delivery: some recent advances. *J Drug Target* 2009;**17**:671-89.

107.Heister E, Brunner EW, Dieckmann GR, Jurewicz I, Dalton AB. Are carbon nanotubes a natural solution? Applications in biology and medicine. *ACS Appl Mater Interfaces* 2013;**5**:1870-91.

108.Choi HS, Frangioni JV. Nanoparticles for biomedical imaging: fundamentals of clinical translation. *Mol Imaging* 2010;**9**:291-310.

109.Chan WC, Maxwell DJ, Gao X, Bailey RE, Han M, Nie S. Luminescent quantum dots for multiplexed biological detection and imaging. *Curr Opin Biotechnol* 2002;**13**:40-6.

110.Reddy LH, Arias JL, Nicolas J, Couvreur P. Magnetic nanoparticles: design and characterization, toxicity and biocompatibility, pharmaceutical and biomedical applications. *Chem Rev* 2012;**112**:5818-78.

111.Kamaly N, Miller AD. Paramagnetic liposome nanoparticles for cellular and tumour imaging. *Int J Mol Sci* 2010;**11**:1759-76.

112.McAteer MA, Mankia K, Ruparelia N, Jefferson A, Nugent HB, Stork LA, et al. A leukocyte-mimetic magnetic resonance imaging contrast agent homes rapidly to activated endothelium and tracks with atherosclerotic lesion macrophage content. *Arterioscler Thromb Vasc Biol* 2012;**32**:1427-35.

113.Nacev A, Beni C, Bruno O, Shapiro B. Magnetic nanoparticle transport within flowing blood and into surrounding tissue. *Nanomedicine (Lond)* 2010;**5**:1459-66.

114.Higashi N, Kawahara J, Niwa M. Preparation of helical peptide monolayer-coated gold nanoparticles. *J Colloid Interface Sci* 2005;**288**:83-7.

115.Tang F, Li L, Chen D. Mesoporous silica nanoparticles: synthesis, biocompatibility and drug delivery. *Adv Mater* 2012;**24**:1504-34.

116.Xu L, Yang BF, Ai J. MicroRNA transport: a new way in cell communication. *J Cell Physiol* 2013;**228**:1713-9.

117.Manz B, Matrosovich M, Bovin N, Schwemmle M. A polymorphism in the hemagglutinin of the human isolate of a highly pathogenic H5N1 influenza virus determines organ tropism in mice. *J Virol* 2010;**84**:8316-21.

118.MacLaren R, Cui W, Cianflone K. Adipokines and the immune system: an adipocentric view. *Adv Exp Med Biol* 2008;**632**:1-21.

119.Snoeys J, Mertens G, Lievens J, van Berkel T, Collen D, Biessen EA, et al. Lipid emulsions potently increase transgene expression in hepatocytes after adenoviral transfer. *Mol Ther* 2006;**13**:98-107.

120.Vitetta ES, Krolick KA, Miyama-Inaba M, Cushley W, Uhr JW. Immunotoxins: a new approach to cancer therapy. *Science* 1983;**219**:644-50.

121.Budker V, Gurevich V, Hagstrom JE, Bortzov F, Wolff JA. pH-sensitive, cationic liposomes: a new synthetic virus-like vector. *Nat Biotechnol* 1996;**14**:760-4.

122.Meyer DE, Shin BC, Kong GA, Dewhirst MW, Chilkoti A. Drug targeting using thermally responsive polymers and local hyperthermia. *J Control Release* 2001;**74**:213-24.

123.Weinstein JN, Magin RL, Yatvin MB, Zaharko DS. Liposomes and local hyperthermia: selective delivery of methotrexate to heated tumors. *Science* 1979;**204**:188-91.

124.Torchilin VP. Passive and active drug targeting: drug delivery to tumors as an example. *Handb Exp Pharmacol* 2010;**197**:3-53.

125.Suk JS, Suh J, Choy K, Lai SK, Fu J, Hanes J. Gene delivery to differentiated neurotypic cells with RGD and HIV Tat peptide functionalized polymeric nanoparticles. *Biomaterials* 2006;**27**:5143-50.

126.Sawant R, Torchilin V. Intracellular transduction using cell-penetrating peptides. *Mol Biosyst* 2010;**6**:628-40.

127.Gooding M, Browne LP, Quinteiro FM, Selwood DL. siRNA delivery: from lipids to cell-penetrating peptides and their mimics. *Chem Biol Drug Des* 2012;**80**:787-809.

128.MacEwan SR, Chilkoti A. Harnessing the power of cell-penetrating peptides: activatable carriers for targeting systemic delivery of cancer therapeutics and imaging agents. *Wiley Interdiscip Rev Nanomed Nanobiotechnol* 2013;**5**:31-48.

129.Calderon AJ, Bhowmick T, Leferovich J, Burman B, Pichette B, Muzykantov V, et al. Optimizing endothelial targeting by modulating the antibody density and particle concentration of anti-ICAM coated carriers. *J Control Release* 2011;**150**:37-44.

130.Schaffer DV, Lauffenburger DA. Optimization of cell surface binding enhances efficiency and specificity of molecular conjugate gene delivery. *J Biol Chem* 1998;**273**:28004-9.

131.Balyasnikova IV, Karran EH, Albrecht RF, 2nd, Danilov SM. Epitope-specific antibody-induced cleavage of angiotensin-converting enzyme from the cell surface. *Biochem J* 2002;**362**:585-95.

132.Lee HJ, Engelhardt B, Lesley J, Bickel U, Pardridge WM. Targeting rat anti-mouse transferrin receptor monoclonal antibodies through blood-brain barrier in mouse. *J Pharmacol Exp Ther* 2000;**292**:1048-52.

133.Muro S, Schuchman EH, Muzykantov VR. Lysosomal enzyme delivery by ICAM-1-targeted nanocarriers bypassing glycosylation- and clathrin-dependent endocytosis. *Mol Ther* 2006;**13**:135-41.

134.Hsu J, Serrano D, Bhowmick T, Kumar K, Shen Y, Kuo YC, et al. Enhanced endothelial delivery and biochemical effects of alpha-galactosidase by ICAM-1-targeted nanocarriers for Fabry disease. *J Control Release* 2011;**149**:323-31.

135.Mistry PK, Wraight EP, Cox TM. Therapeutic delivery of proteins to macrophages: implications for treatment of Gaucher's disease. *Lancet* 1996;**348**:1555-9.

136.LeBowitz JH, Grubb JH, Maga JA, Schmiel DH, Vogler C, Sly WS. Glycosylation-independent targeting enhances enzyme delivery to lysosomes and decreases storage in mucopolysaccharidosis type VII mice. *Proc Natl Acad Sci U S A* 2004;**101**:3083-8.

137.Prince WS, McCormick LM, Wendt DJ, Fitzpatrick PA, Schwartz KL, Aguilera AI, et al. Lipoprotein receptor binding, cellular uptake, and lysosomal delivery of fusions between the receptor-associated protein (RAP) and alpha-L-iduronidase or acid alpha-glucosidase. *J Biol Chem* 2004;**279**:35037-46.

138.Chen CH, Dellamaggiore KR, Ouellette CP, Sedano CD, Lizadjohry M, Chernis GA, et al. Aptamer-based endocytosis of a lysosomal enzyme. *Proc Natl Acad Sci U S A* 2008;**105**:15908-13.

139.Osborn MJ, McElmurry RT, Peacock B, Tolar J, Blazar BR. Targeting of the CNS in MPS-IH using a nonviral transferrin-alpha-L-iduronidase fusion gene product. *Mol Ther* 2008;**16**:1459-66.

140.Armstrong JS. Mitochondrial medicine: pharmacological targeting of mitochondria in disease. *Br J Pharmacol* 2007;**151**:1154-65.

141.Boddapati SV, Tongcharoensirikul P, Hanson RN, D'Souza GG, Torchilin VP, Weissig V. Mitochondriotropic liposomes. *J Liposome Res* 2005;**15**:49-58.

142.Flierl A, Jackson C, Cottrell B, Murdock D, Seibel P, Wallace DC. Targeted delivery of DNA to the mitochondrial compartment via import sequence-conjugated peptide nucleic acid. *Mol Ther* 2003;**7**:550-7.

143.Muratovska A, Lightowlers RN, Taylor RW, Wilce JA, Murphy MP. Targeting large molecules to mitochondria. *Adv Drug Deliv Rev* 2001;**49**:189-98.

144.Chan CK, Jans DA. Using nuclear targeting signals to enhance non-viral gene transfer. *Immunol Cell Biol* 2002;**80**:119-30.

145.Rajendran L, Knolker HJ, Simons K. Subcellular targeting strategies for drug design and delivery. *Nat Rev Drug Discov* 2010;**9**:29-42.

146.Pardridge WM. Blood-brain barrier drug targeting: the future of brain drug development. *Mol Interv* 2003;**3**:90-105, 51.

147.Gadsby DC. Ion channels versus ion pumps: the principal difference, in principle. *Nat Rev Mol Cell Biol* 2009;**10**:344-52.

148.Ambudkar SV, Kim IW, Sauna ZE. The power of the pump: mechanisms of action of P-glycoprotein (ABCB1). *Eur J Pharm Sci* 2006;**27**:392-400.

149.Scherer F, Anton M, Schillinger U, Henke J, Bergemann C, Kruger A, et al. Magnetofection: enhancing and targeting gene delivery by magnetic force in vitro and in vivo. *Gene Ther* 2002;**9**:102-9.

150.Zhang G, Gao X, Song YK, Vollmer R, Stolz DB, Gasiorowski JZ, et al. Hydroporation as the mechanism of hydrodynamic delivery. *Gene Ther* 2004;**11**:675-82.

151.Neumann E, Schaefer-Ridder M, Wang Y, Hofschneider PH. Gene transfer into mouse lyoma cells by electroporation in high electric fields. *EMBO J* 1982;**1**:841-5.

152.Anwer K, Kao G, Proctor B, Anscombe I, Florack V, Earls R, et al. Ultrasound enhancement of cationic lipid-mediated gene transfer to primary tumors following systemic administration. *Gene Ther* 2000;**7**:1833-9.

153.Zeira E, Manevitch A, Khatchatouriants A, Pappo O, Hyam E, Darash-Yahana M, et al. Femtosecond infrared laser-an efficient and safe in vivo gene delivery system for prolonged expression. *Mol Ther* 2003;**8**:342-50.

154.Chuang YC, Chou AK, Wu PC, Chiang PH, Yu TJ, Yang LC, et al. Gene therapy for bladder pain with gene gun particle encoding pro-opiomelanocortin cDNA. *J Urol* 2003;**170**:2044-8.

155.Frankel AD, Pabo CO. Cellular uptake of the tat protein from human immunodeficiency virus. *Cell* 1988;**55**:1189-93.

156.Joliot A, Pernelle C, Deagostini-Bazin H, Prochiantz A. Antennapedia homeobox peptide regulates neural morphogenesis. *Proc Natl Acad Sci U S A* 1991;**88**:1864-8.

157.Joliot A, Prochiantz A. Transduction peptides: from technology to physiology. *Nat Cell Biol* 2004;**6**:189-96.

158.Aderem A, Underhill DM. Mechanisms of phagocytosis in macrophages. *Annu Rev Immunol* 1999;**17**:593-623.

159.Champion JA, Mitragotri S. Role of target geometry in phagocytosis. *Proc Natl Acad Sci USA* 2006;**103**:4930-4.

160.Mercer J, Helenius A. Virus entry by macropinocytosis. *Nat Cell Biol* 2009;**11**:510-20.

161.Sahay G, Alakhova DY, Kabanov AV. Endocytosis of nanomedicines. *J Control Release* 2010;**145**:182-95.

162.Hillaireau H, Couvreur P. Nanocarriers' entry into the cell: relevance to drug delivery. *Cell Mol Life Sci* 2009;**66**:2873-96.

163.Pardridge WM, Buciak JL, Friden PM. Selective transport of an anti-transferrin receptor antibody through the blood-brain barrier in vivo. *J Pharmacol Exp Ther* 1991;**259**:66-70.

164.Pardridge WM, Eisenberg J, Yang J. Human blood-brain barrier transferrin receptor. *Metabolism* 1987;**36**:892-5.

165.Parton RG, Joggerst B, Simons K. Regulated internalization of caveolae. *J Cell Biol* 1994;**127**:1199-215.

166.Kirkham M, Parton RG. Clathrin-independent endocytosis: new insights into caveolae and non-caveolar lipid raft carriers. *Biochim Biophys Acta* 2005;**1746**:349-63.

167.McIntosh DP, Tan XY, Oh P, Schnitzer JE. Targeting endothelium and its dynamic caveolae for tissue-specific transcytosis in vivo: a pathway to overcome cell barriers to drug and gene delivery. *Proc Natl Acad Sci U S A* 2002;**99**:1996-2001.

168.Muro S, Wiewrodt R, Thomas A, Koniaris L, Albelda SM, Muzykantov VR, et al. A novel endocytic pathway induced by clustering endothelial ICAM-1 or PECAM-1. *J Cell Sci* 2003;**116**:1599-609.

169.Muro S, Cui X, Gajewski C, Murciano J-C, Muzykantov VR, Koval M. Slow intracellular trafficking of catalase nanoparticles targeted to ICAM-1 protects endothelial cells from oxidative stress. *Am J Physiol, Cell Physiol* 2003;**285**:C1339-47.

170.Muro S, Gajewski C, Koval M, Muzykantov VR. ICAM-1 recycling in endothelial cells: a novel pathway for sustained intracellular delivery and prolonged effects of drugs. *Blood* 2005;**105**:650-8.

171.Muro S, Mateescu M, Gajewski C, Robinson M, Muzykantov VR, Koval M. Control of intracellular trafficking of ICAM-1-targeted nanocarriers by endothelial Na+/H+ exchanger proteins. *Am J Physiol Lung Cell Mol Physiol* 2006;**290**:L809-17.

172.Garnacho C, Shuvaev V, Thomas A, McKenna L, Sun J, Koval M, et al. RhoA activation and actin reorganization involved in endothelial CAM-mediated endocytosis of anti-PECAM carriers: critical role for tyrosine 686 in the cytoplasmic tail of PECAM-1. *Blood* 2008;**111**:3024-33.

173.Serrano D, Bhowmick T, Chadha R, Garnacho C, Muro S. Intercellular adhesion molecule 1 engagement modulates sphingomyelinase and ceramide, supporting uptake of drug carriers by the vascular endothelium. *Arterioscler Thromb Vasc Biol* 2012;**32**:1178-85.

174.Tuma P, Hubbard AL. Transcytosis: crossing cellular barriers. *Physiol Rev* 2003;**83**:871-932.

175.Muro S, Garnacho C, Champion JA, Leferovich J, Gajewski C, Schuchman EH, et al. Control of endothelial targeting and intracellular delivery of therapeutic enzymes by modulating the size and shape of ICAM-1-targeted carriers. *Mol Ther* 2008;**16**:1450-8.

176.Derksen JT, Morselt HW, Kalicharan D, Hulstaert CE, Scherphof GL. Interaction of immunoglobulin-coupled liposomes with rat liver macrophages in vitro. *Exp Cell Res* 1987;**168**:105-15.

177.Marsh EW, Leopold PL, Jones NL, Maxfield FR. Oligomerized transferrin receptors are selectively retained by a lumenal sorting signal in a long-lived endocytic recycling compartment. *J Cell Biol* 1995;**129**:1509-22.

178.Vyas SP, Sihorkar V. Endogenous carriers and ligands in non-immunogenic site-specific drug delivery. *Adv Drug Deliv Rev* 2000;**43**:101-64.

179.Garnacho C, Albelda SM, Muzykantov VR, Muro S. Differential intra-endothelial delivery of polymer nanocarriers targeted to distinct PECAM-1 epitopes. *J Control Release* 2008;**130**:226-33.

180.Oh P, Borgstrom P, Witkiewicz H, Li Y, Borgstrom BJ, Chrastina A, et al. Live dynamic imaging of caveolae pumping targeted antibody rapidly and specifically across endothelium in the lung. *Nat Biotechnol* 2007;**25**:327-37.

181.Eniola AO, Hammer DA. In vitro characterization of leukocyte mimetic for targeting therapeutics to the endothelium using two receptors. *Biomaterials* 2005;**26**:7136-44.

182.Sun D, Nakao S, Xie F, Zandi S, Schering A, Hafezi-Moghadam A. Superior sensitivity of novel molecular imaging probe: simultaneously targeting two types of endothelial injury markers. *FASEB J* 2010;**24**:1532-40.

183.Eniola AO, Willcox PJ, Hammer DA. Interplay between rolling and firm adhesion elucidated with a cell-free system engineered with two distinct receptor-ligand pairs. *Biophys J* 2003;**85**:2720-31.

184.Gunawan RC, Auguste DT. The role of antibody synergy and membrane fluidity in the vascular targeting of immunoliposomes. *Biomaterials* 2009;**31**:900-7.

185.Gunawan RC, Almeda D, Auguste DT. Complementary targeting of liposomes to IL-1alpha and TNF-alpha activated endothelial cells via the transient expression of VCAM1 and E-selectin. *Biomaterials* 2011;**32**:9848-53.

186.Robbins GP, Saunders RL, Haun JB, Rawson J, Therien MJ, Hammer DA. Tunable Leuko-polymersomes That Adhere Specifically to Inflammatory Markers. *Langmuir* 2010;**26**:14089-96.

187.Ha SH, Carson A, Agarwal A, Kotov NA, Kim K. Detection and monitoring of the multiple inflammatory responses by photoacoustic molecular imaging using selectively targeted gold nanorods. *Biomedical Optics Express* 2011;**2**:645-57.

188.Aird WC. Endothelium in health and disease. *Pharmacol Rep* 2008;**60**:139-43.

189.Ricard I, Payet MD, Dupuis G. VCAM-1 is internalized by a clathrin-related pathway in human endothelial cells but its alpha(4)beta(1) integrin counter-receptor remains associated with the plasma membrane in human T lymphocytes. *Eur J Immunol* 1998;**28**:1708-18.

190.Vestweber D, Blanks JE. Mechanisms that regulate the function of the selectins and their ligands. *Physiol Rev* 1999;**79**:181-213.

191.Kneuer C, Ehrhardt C, Radomski MW, Bakowsky U. Selectins - potential pharmacological targets? *Drug Discov Today* 2006;**11**:1034-40.

192.Setiadi H, Sedgewick G, Erlandsen SL, McEver RP. Interactions of the cytoplasmic domain of P-selectin with clathrin-coated pits enhance leukocyte adhesion under flow. *J Cell Biol* 1998;**142**:859-71.

193.Voinea M, Manduteanu I, Dragomir E, Capraru M, Simionescu M. Immunoliposomes directed toward VCAM-1 interact specifically with activated endothelial cells - A potential tool for specific drug delivery. *Pharmaceutical Research* 2005;**22**:1906-17.

194.Ying X, Wen H, Lu WL, Du J, Guo J, Tian W, et al. Dual-targeting daunorubicin liposomes improve the therapeutic efficacy of brain glioma in animals. *J Control Release* 2010;**141**:183-92.

195.Markoutsa E, Papadia K, Clemente C, Flores O, Antimisiaris SG. Anti-Abeta-MAb and dually decorated nanoliposomes: effect of Abeta1-42 peptides on interaction with hCMEC/D3 cells. *Eur J Pharm Biopharm* 2012;**81**:49-56.

196.Balyasnikova IV, Metzger R, Visintine DJ, Dimasius V, Sun ZL, Berestetskaya YV, et al. Selective rat lung endothelial targeting with a new set of monoclonal antibodies to angiotensin I-converting enzyme. *Pulm Pharmacol Ther* 2005;**18**:251-67.

197.Kaewsaneha C, Tangboriboonrat P, Polpanich D, Eissa M, Elaissari A. Janus colloidal particles: preparation, properties, and biomedical applications. *ACS Appl Mater Interfaces* 2013;**5**:1857-69.

198.Jones MR, Mirkin CA. Materials science: Self-assembly gets new direction. *Nature* 2012;**491**:42-3.

199.Kissel K, Hamm S, Schulz M, Vecchi A, Garlanda C, Engelhardt B. Immunohistochemical localization of the murine transferrin receptor (TfR) on blood-tissue barriers using a novel anti-TfR monoclonal antibody. *Histochem Cell Biol* 1998;**110**:63-72.

200.Marlin SD, Springer TA. Purified intercellular adhesion molecule-1 (ICAM-1) is a ligand for lymphocyte function-associated antigen 1 (LFA-1). *Cell* 1987;**51**:813-9.

201.Jevnikar AM, Wuthrich RP, Takei F, Xu HW, Brennan DC, Glimcher LH, et al. Differing regulation and function of ICAM-1 and class II antigens on renal tubular cells. *Kidney Int* 1990;**38**:417-25.

202.Altieri DC, Duperray A, Plescia J, Thornton GB, Languino LR. Structural recognition of a novel fibrinogen gamma chain sequence (117-133) by intercellular adhesion molecule-1 mediates leukocyte-endothelium interaction. *J Biol Chem* 1995;**270**:696-9.

203.He X, Miranda SR, Xiong X, Dagan A, Gatt S, Schuchman EH. Characterization of human acid sphingomyelinase purified from the media of overexpressing Chinese hamster ovary cells. *Biochim Biophys Acta* 1999;**1432**:251-64.

204.Garnacho C, Dhami R, Simone E, Dziubla T, Leferovich J, Schuchman EH, et al. Delivery of acid sphingomyelinase in normal and niemann-pick disease mice using intercellular adhesion molecule-1-targeted polymer nanocarriers. *J Pharmacol Exp Ther* 2008;**325**:400-8.

205.Muro S, Dziubla T, Qiu W, Leferovich J, Cui X, Berk E, et al. Endothelial targeting of high-affinity multivalent polymer nanocarriers directed to intercellular adhesion molecule 1. *J Pharmacol Exp Ther* 2006;**317**:1161-9.

206.Papademetriou IT, Garnacho C, Schuchman EH, Muro S. In vivo performance of polymer nanocarriers dually-targeted to epitopes of the same or different receptors. *Biomaterials* 2013;**34**:3459–66.

207.Garlanda C, Parravicini C, Sironi M, De Rossi M, Wainstok de Calmanovici R, Carozzi F, et al. Progressive growth in immunodeficient mice and host cell recruitment by mouse endothelial cells transformed by polyoma middle-sized T antigen: implications for the pathogenesis of opportunistic vascular tumors. *Proc Natl Acad Sci U S A* 1994;**91**:7291-5.

208.Papademetriou J, Garnacho C, Serrano D, Bhowmick T, Schuchman EH, Muro S. Comparative binding, endocytosis, and biodistribution of antibodies and antibody-coated carriers for targeted delivery of lysosomal enzymes to ICAM-1 versus transferrin receptor. *J Inherit Metab Dis* 2013;**36**:467-77.

209.Muro S. Intercellular Adhesion Molecule-1 and Vascular Cell Adhesion Molecule-1. In: Aird WC, editor. Endothelial biomedicine. 1 ed. New York: Cambridge University Press; 2007. p. 1058-70.

210.Couty JP, Rampon C, Leveque M, Laran-Chich MP, Bourdoulous S, Greenwood J, et al. PECAM-1 engagement counteracts ICAM-1-induced signaling in brain vascular endothelial cells. *J Neurochem* 2007;**103**:793-801.

211.Carlos TM, Harlan JM. Leukocyte-endothelial adhesion molecules. *Blood* 1994;**84**:2068-101.

212.Warram JM, Sorace AG, Saini R, Umphrey HR, Zinn KR, Hoyt K. A triple-targeted ultrasound contrast agent provides improved localization to tumor vasculature. *J Ultrasound Med* 2011;**30**:921-31.

213.Henninger DD, Panes J, Eppihimer M, Russell J, Gerritsen M, Anderson DC, et al. Cytokine-induced VCAM-1 and ICAM-1 expression in different organs of the mouse. *J Immunol* 1997;**158**:1825-32.

214.Romer LH, McLean NV, Yan HC, Daise M, Sun J, DeLisser HM. IFN-gamma and TNF-alpha induce redistribution of PECAM-1 (CD31) on human endothelial cells. *J Immunol* 1995;**154**:6582-92.

215.Schuchman EH, Desnick RJ. Niemann-Pick Disease Types A and B: Acid Sphingomyelinase Deficiencies. In: Scriver C, Beaudet A, Sly W, Valle D, Childs B, Kinzler K, et al., editors. The Metabolic and Molecular Bases of Inherited Disease. 8th ed. New York: McGraw-Hill; 2001. p. 3589-610.

216.Grill J, Van Beusechem VW, Van Der Valk P, Dirven CM, Leonhart A, Pherai DS, et al. Combined targeting of adenoviruses to integrins and epidermal growth factor receptors increases gene transfer into primary glioma cells and spheroids. *Clin Cancer Res* 2001;**7**:641-50.

217.Li X, Zhou H, Yang L, Du G, Pai-Panandiker AS, Huang X, et al. Enhancement of cell recognition in vitro by dual-ligand cancer targeting gold nanoparticles. *Biomaterials* 2011;**32**:2540-5.

218.Jefferies WA, Brandon MR, Hunt SV, Williams AF, Gatter KC, Mason DY. Transferrin receptor on endothelium of brain capillaries. *Nature* 1984;**312**:162-3.

219.Fishman JB, Rubin JB, Handrahan JV, Connor JR, Fine RE. Receptor-mediated transcytosis of transferrin across the blood-brain barrier. *J Neurosci Res* 1987;**18**:299-304.

220.Dautry-Varsat A. Receptor-mediated endocytosis: the intracellular journey of transferrin and its receptor. *Biochimie* 1986;**68**:375-81.

221.Conrad ME, Umbreit JN. Iron absorption and transport-an update. *Am J Hematol* 2000;**64**:287-98.

222.Rothlein R, Dustin ML, Marlin SD, Springer TA. A human intercellular adhesion molecule (ICAM-1) distinct from LFA-1. *J Immunol* 1986;**137**:1270-4.

223.Rothlein R, Wegner C. Role of intercellular adhesion molecule-1 in the inflammatory response. *Kidney Int* 1992;**41**:617-9.

224.Fuchs H, Lucken U, Tauber R, Engel A, Gessner R. Structural model of phospholipid-reconstituted human transferrin receptor derived by electron microscopy. *Structure* 1998;**6**:1235-43.

225.Jun CD, Carman CV, Redick SD, Shimaoka M, Erickson HP, Springer TA. Ultrastructure and function of dimeric, soluble intercellular adhesion molecule-1 (ICAM-1). *J Biol Chem* 2001;**276**:29019-27.

226.Lossinsky AS, Mossakowski MJ, Pluta R, Wisniewski HM. Intercellular adhesion molecule-1 (ICAM-1) upregulation in human brain tumors as an expression of increased blood-brain barrier permeability. *Brain Pathol* 1995;**5**:339-44.

227.Carpén O, Pallai P, Staunton DE, Springer TA. Association of intercellular adhesion molecule-1 (ICAM-1) with actin-containing cytoskeleton and alpha-actinin. *The Journal of Cell Biology* 1992;**118**:1223-34.

228.Frey A, Giannasca KT, Weltzin R, Giannasca PJ, Reggio H, Lencer WI, et al. Role of the glycocalyx in regulating access of microparticles to apical plasma membranes of intestinal epithelial cells: implications for microbial attachment and oral vaccine targeting. *J Exp Med* 1996;**184**:1045-59.

229.DeGraba T, Azhar S, Dignat-George F, Brown E, Boutiere B, Altarescu G, et al. Profile of endothelial and leukocyte activation in Fabry patients. *Ann Neurol* 2000;**47**:229-33.

230.Shen JS, Meng XL, Moore DF, Quirk JM, Shayman JA, Schiffmann R, et al. Globotriaosylceramide induces oxidative stress and up-regulates cell adhesion molecule expression in Fabry disease endothelial cells. *Mol Genet Metab* 2008;**95**:163-8.

231.Nanami M, Ookawara T, Otaki Y, Ito K, Moriguchi R, Miyagawa K, et al. Tumor necrosis factor-alpha-induced iron sequestration and oxidative stress in human endothelial cells. *Arterioscler Thromb Vasc Biol* 2005;**25**:2495-501.

232.Visser CC, Voorwinden LH, Crommelin DJ, Danhof M, de Boer AG. Characterization and modulation of the transferrin receptor on brain capillary endothelial cells. *Pharm Res* 2004;**21**:761-9.

233.Pardridge WM, Boado RJ. Reengineering biopharmaceuticals for targeted delivery across the blood-brain barrier. *Methods Enzymol* 2012;**503**:269-92.

234.Bjorn MJ, Groetsema G. Immunotoxins to the murine transferrin receptor: intracavitary therapy of mice bearing syngeneic peritoneal tumors. *Cancer Res* 1987;**47**:6639-45.

235.Daniels TR, Bernabeu E, Rodriguez JA, Patel S, Kozman M, Chiappetta DA, et al. The transferrin receptor and the targeted delivery of therapeutic agents against cancer. *Biochim Biophys Acta* 2012;**1820**:291-317.

236.Boado RJ, Zhang Y, Wang Y, Pardridge WM. Engineering and expression of a chimeric transferrin receptor monoclonal antibody for blood-brain barrier delivery in the mouse. *Biotechnol Bioeng* 2009;**102**:1251-8.

237.Panaccio M, Zalcberg JR, Thompson CH, Leyden MJ, Sullivan JR, Lichtenstein M, et al. Heterogeneity of the human transferrin receptor and use of anti-transferrin receptor antibodies to detect tumours in vivo. *Immunol Cell Biol* 1987;**65 (Pt 6)**:461-72.

238.Takahashi S, Esserman L, Levy R. An epitope on the transferrin receptor preferentially exposed during tumor progression in human lymphoma is close to the ligand binding site. *Blood* 1991;**77**:826-32.

239.van Driel IR, Goding JW. Heterogeneous glycosylation of murine transferrin receptor subunits. *Eur J Biochem* 1985;**149**:543-8.